CRANFIELD INSTITUTE OF TECHNOLOGY

DEPARTMENT OF MATHEMATICS

PhD THESIS

Academic Year 1983 - 84

J L PARRY

Mathematical Modelling and Computer Simulation of Heat and Mass Transfer in Agricultural Grain Drying

Supervisor: N Laws

November 1983

SUMMARY

Mathematical modelling and computer simulation of grain drying are now widely used in agricultural engineering research. Several models have been proposed to describe the heat and mass transfer processes in the basic types of convective grain drier. Most of these models, however, have been derived under assumptions which are not explicitly stated and which restrict their applications from the outset. Furthermore, the differences which exist between various models are not always clarified in the literature. It is important with an ever-increasing demand for the accurate modelling of drying systems, for the researcher to understand the basic assumptions inherent in a particular model and hence to be aware of its limitations. In addition, the problems of obtaining satisfactory solutions for particular models have generally been given only a cursory treatment.

The purpose of this work is, firstly, to provide a general framework from which mathematical models for any type of drier may be derived under suitable assumptions. The use of this framework is illustrated by the formulation of models for the four basic types of convective grain drier, namely fixed bed, concurrent flow, counterflow and crossflow. Previous work is then discussed in the context of these models. The resulting systems of differential equations for each of the models obtained are non-linear and have, in general, no analytical solution. The analytical/semi-analytical solutions to particular problems associated with the above cases are pursued as far as possible. However, as is evident from this investigation, purely numerical techniques provide the only practicable means of obtaining an accurate solution to any grain drying problem of current interest. Therefore, suitable computational techniques were devised and implemented for the solution of the three distinct cases, namely the fixed bed, steady-state concurrent flow and steady-state counterflow problems. These techniques are described together with appropriate validation cases.

CONTENTS

FIGURES

TABLES

NOTATION

The following symbols are used with the given meaning throughout. The meaning of other symbols will be made clear in the context in which they occur.

		Units
c_α	specific heat of constituent α	J $kg^{-1}{}^0C^{-1}$
h_{fg}	latent heat of vaporisation of water	J kg^{-1}
*{h	volumetric heat transfer coefficient	J $m^{-3}s^{-1}{}^0C^{-1}$
*{k	drying rate coefficient	s^{-1}
ρ_α	density of constituent α	kg m^{-3}
ε	void ratio	dim'less
V_a, V_p	speeds of moist air and moist grain respectively, related to mass flow rates G_a, G_p by $G_a = \varepsilon \rho_a V_a$ and $G_p = p_p V_p$	m s^{-1}
H	specific humidity of dry air	dim'less
T	drying air temperature	°C
M	moisture content of product - decimal dry basis (d.b.)	dim'less
θ	grain temperature	°C
ϕ	relative humidity, $0.0 \leqq \phi \leqq 1.0$	dim'less
T	absolute temperature	°K
M_e	equilibrium moisture content	dim'less
MR	moisture ratio = $(M - M_e)/(M_o - M_e)$	dim'less
x	independent space variable	m
t	independent time variable	s
L	depth of drying chamber	m
m	net density of vapour formed/unit time	kg $m^{-3}s^{-1}$
ψ	net rate of energy transferred from grain to air/unit volume	J $m^{-3}s^{-1}$
θ_v	'mean' evaporation temperature $\theta \leqq \theta_v \leqq T$, for $T \geqq \theta$	°C

* also used to denote numerical integration step-size.

Suffices

a	dry air	constituents
v	water vapour in the air	
p	product (grain)	
w	moisture in the grain	
o	initial value	
e	equilibrium value	

EQUATION NUMBERING CONVENTION

The following widely used convention is followed throughout. Equations are numbered consecutively within each section i.e. (1), (2), ... Within each section, equation k is cited as (k). Outside of the section containing the equation to be referenced, equation k, of section j, in chapter i is cited as (i.j-k). This convention also applies to other entities such as inequalities, conditions etc.

CHAPTER ONE: INTRODUCTION

1.1 Background to the Problem

Much of the drying and conditioning of agricultural crops is carried out by artificial means. Greater yields and the need for storage over long periods of time demand a high degree of control over various properties of the final product. Excess moisture content, for example, can encourage the growth of moulds and infestation by insects and hence cause damage to the stored crop. Grain is graded according to various physical properties such as moisture content, bulk density, germination and contamination. Its assessed quality is the basis for determining its subsequent usage and commercial value - for detailed discussion see Brooker et al (1974). Grain driers are widely used to ensure that at least some of these demands on the final product are met.

Various types of drier are used for the drying of granular materials. The type most commonly employed for the drying of agricultural grain makes use of the through circulation of air. The main mechanism for heat and moisture transfer in this type of drier is the bulk convection of the circulating air.

Convective grain driers fall into two natural categories, namely batch driers and continuous flow driers. Batch driers are characterised by the fact that grain is dried either with heated air in shallow layers of less than one metre thick or with near-ambient air in beds of several metres depth. In near-ambient, or low temperature, air driers, the drying may take place over many hours, days or even weeks. Continuous flow driers are usually classified according to the relative directions of flow of grain and air viz. crossflow, concurrent flow, counterflow. The fixed bed drier and the three types of continuous flow drier are illustrated schematically in Figure 1. In crossflow driers the bulk flow of air is perpendicular to the bulk flow of grain. In concurrent flow driers these flows are in the same direction whereas in counterflow driers the bulk flows are in opposite directions. All types of convective drier use a fan or some similar device to move the air through the drying chamber which contains the grain. There may also be some form of heating device to heat the circulating air.

In most continuous flow driers, grain flows through the drier under gravity. There are, of course, variations on the basic types of drier described. For example, the basic concurrent flow and counterflow configurations may be combined in a multistage/mixed flow drier with alternate heating and cooling sections.

The speed and efficiency of drying depend on the temperature and humidity of the drying air. Thus agricultural driers are often categorised according to whether the air temperature is low (up to 5°C above ambient temperature), medium (40-250°C) or high (up to 1000°C). At high temperatures one can get increased throughput of grain but this is often accompanied by a deterioration in the properties of the grain e.g. germination. It is therefore important to understand what happens to grain temperature and moisture content during the drying process in order that safe operating temperatures may be determined for a given type of drier, see Nellist (1978, 1981).

The use of simulation to provide a better understanding of the drying process is now firmly established. Clearly, suitably constructed models can be used to help with the design of new driers and to promote the more efficient use of existing driers.

1.2 Review of Previous Work

There is an extensive literature concerned with the general area of drying in the field of process engineering, and in particular in chemical engineering. However, much of this literature is concerned with 'equilibrium' exchange processes and not with the problems of obtaining a detailed description of the product state at all points throughout the drier over the duration of drying. Furthermore, predictions of the type required by agricultural engineers must take account of the particular properties of grain as a biological product. For these reasons most of the available models directly relevant to the current work are to be found in the agricultural engineering literature.

A number of different types of mathematical model have been developed to describe the heat and mass transfer processes in grain drying. The present work is primarily concerned with the description

of these processes in deep bed drying. However, for a complete description, it is necessary to prescribe constitutive equations defining the transfer rates locally in terms of the air and grain conditions. These rates may be approximately determined from studies of thin-layer, or single-kernel, drying.

The drying of biological materials in thin layers ventilated by through flow of air has been observed to take place in two or more distinct periods, see e.g. Sherwood (1936). In very wet material, there may be an initial constant rate drying period during which the material is fully saturated and has a surface covering of free water. The rate is then only dependent on the external conditions and is given approximately by (Brooker et al (1974) p.185)

$$\frac{dM}{dt} = \frac{h}{h_{fg}} (T - T_{wb}),$$

where T_{wb} represents the wet bulb temperature of the drying air. Following this constant rate period is a falling rate period during which the drying rate is initially approximately proportional to the remaining area of normally wetted surface. When all of this free moisture has been removed the hygroscopic limit is attained (Chen and Johnson (1969) call this the tertiary moisture content). At this point the capillary theory tells us that, in capillary-porous bodies, the vapour pressure lowering effect becomes significant, see e.g. Luikov (1966), and a second falling rate period begins. In this and any subsequent 'periods' the drying rate is dependent on the rate at which moisture, in both liquid and vapour form, is transported from the interior to the surface of the grain. For cereal grains most drying of interest usually takes place in the falling rate periods, see e.g. Simmonds et al (1953). Many theories have been proposed to explain the transport of moisture and heat in biological materials but it is now generally recognised that diffusion is the rate controlling mechanism in the drying of grain at moderate temperatures.

The work of Luikov (1966) on capillary-porous bodies has formed the basis for a number of recent models involving partial differential equations for the temperature and moisture content distributions within

the individual grain kernel. In particular, Husain et al (1973) solved a coupled heat and mass diffusion model as part of a simulation to predict the drying characteristics of rough rice. Since, however, in most applications, the thermal diffusivity is large compared to the moisture diffusivity, it is generally thought sufficiently accurate to solve the moisture diffusion equation alone for the moisture distribution within the kernel. This in turn leads to an estimate of the moisture loss from the individual kernel. Numerous workers have made use of this single equation model. For example, Ingram (1976a,b) incorporated the model in an overall fixed bed simulation. Representing the grain kernel by various geometric shapes, such as a sphere and a slab, he made use of series solutions to the diffusion equation given in appropriate form. His solution took account of the varying surface conditions of the kernel.

Unfortunately the time required for the numerical solution of diffusion type models is generally very large. Therefore, many workers prefer the use of empirical or semi-theoretical thin-layer models. In particular, Lewis (1921) proposed a model analogous to Newton's law of cooling. He suggested that the rate of drying be assumed to be directly proportional to the difference between the moisture content of the material being dried and its equilibrium moisture content (e.m.c.) - the e.m.c. of a material being the moisture content corresponding to vapour pressure equilibrium of the material with its environment. This may be expressed mathematically in the form

$$\frac{dM}{dt} = -k\ (M - M_e) \qquad (1),$$

where k is known as the drying constant. This model is based on the diffusion theory discussed above but assumes that the resistance to diffusion occurs mainly in a thin outer layer of the body. A number of workers have adapted the basic model (1) to represent thin-layer data more accurately over a wide range of temperature and moisture content. For example, Henderson and Pabis (1961) replaced the constant k by a drying rate coefficient in the form of an Arrhenius type relation involving temperature. A recent review of models for the falling rate drying of fully exposed biological materials has been given by Sharaf-Eldeen et al (1979).

In the thin-layer drying models discussed above the main mechanism of moisture and heat transport is that of diffusion. In convective grain driers, however, molar transport due to diffusion is generally considered negligible as compared to that due to convection. Now the equations describing the transport processes in an individual grain kernel and those describing the transport processes in a drier may be derived from the same physical laws of balance of mass, momentum and energy. However, in view of the different assumptions concerning the dominant transport mechanism in each case, the resulting systems of equations are distinctly different in nature.

Deep bed models are generally divided into three types, namely logarithmic or exponential, layer by layer or 'heat and mass balance', and partial differential equation models, see Morey et al (1978). There are, however, overlapping features in these models and the classification is therefore somewhat arbitrary.

The first model of logarithmic type was obtained by Hukill (1954) from a simplified analysis of deep bed drying. Assuming that the (time) rate of drying at some given depth x after time t is proportional to the (spatial) rate of decrease in air temperature at (x,t) he obtained

$$G_a c_a \frac{\partial T}{\partial x} = \rho_p h_{fg} \frac{\partial M}{\partial t} \qquad (2),$$

This is equivalent to assuming that the (sensible) heat energy lost by the air provides solely the latent heat of vaporisation required to dry the grain and neglects sensible heating of the grain. Further, assuming 'fully exposed' grain conditions at the air inlet point, and hence an empirical boundary condition of the form (1), with a similar form of initial condition for the temperature distribution throughout the bed, Hukill obtained the formula

$$MR = \frac{2^X}{(2^X + 2^\tau - 1)} \qquad (3),$$

where X and τ are respectively dimensionless depth and time variables. He found, however, that his model underestimated the time required to dry grain to a specified moisture content and suggested that this was due to inaccuracies in the thin-layer type grain boundary

condition. Barre et al (1971) obtained the analogous expression

$$MR = \frac{e^{X}}{(e^{X} + e^{\tau} - 1)},$$

and hence an expression for the drying time required to reach a given mean moisture content, of the form

$$\tau = \ell n \left\{ \frac{e - 1}{e^{\overline{MR}} - 1} \right\}.$$

They applied their model to crossflow drying. More recently, Young and Dickens (1975) used Hukill's model to estimate the costs of grain drying in fixed bed and crossflow systems and Sabbah et al (1979) used such a model to simulate solar drying of grain. Logarithmic models are useful because of their simplicity but are, at best, only acceptable in low airflow, low temperature applications.

Boyce (1965), taking into account the sensible heating of the grain during drying, presented a model for the layer by layer calculation of the temperatures and moisture contents of air and grain. He used his model to simulate the drying of remoistened barley but found, however, that the drying times predicted by his model were too long. Boyce (1966) obtained improved predictions with a modified model which included an empirical expression for his volumetric heat transfer coefficient as a function of temperature and mass airflow rate. Thompson et al (1968) presented a similar model which incorporated a procedure to adjust the predicted values of air temperature and humidity to ensure that the predicted relative humidity did not exceed 100%. They further indicated how the model might be used for the simulation of continuous flow driers. Henderson & Henderson (1968) also presented such a model and used it to perform a 'sensitivity' study of the effects on their predicted values of variations in empirical constants involved in their drying rate expression and of changes in the airflow rate. These models are all based on heat and mass balances taken over a thin layer of grain in which it is assumed that conditions are constant over a given increment in time. Heat and mass balance models have been used for different types of drier and in some cases have produced satisfactory

results for a variety of crops. The attainable accuracy of the predictions made using such models is, however, restricted by the assumptions usually made in their derivation.

Partial differential equation models are formulated according to the standard laws of heat and mass transfer and thus have a sound thermo-mechanical basis. Van Arsdel (1955) was among the first to produce such a model consisting of a system of four hyperbolic partial differential equations for simultaneous heat and mass transfer, which he presented in terms of dimensionless independent variables. Klapp (1963) presented equations for heat and mass transfer in a granular bed, for which, under simplifying assumptions, he obtained a perturbation solution in terms of modified Bessel functions. A number of other workers have made use of such solutions. In particular, Ngoddy et al (1966) used a solution of the pure heat transfer problem to simulate heat transfer in a deep bed of pea beans. Huang and Gunkel (1972) presented a model for the simulation of heating and surface drying in a deep bed of onions. Their model took conduction effects into account although these were neglected in order to obtain an analytical solution to the heat transfer problem. Work begun in 1966 at Michigan State University led to the development of a number of models which are summarised in Bakker-Arkema et al (1974) and Brooker et al (1974). These authors presented models for the fixed bed case and for each of the steady state cases for crossflow, concurrent flow and counterflow drier simulation. Other contributions have been made by Spencer (1969a, 1972), O'Callaghan et al (1971), Nellist (1974) and Ingram (1976a,b).

It was observed above that analytical solutions have been obtained for certain cases, under simplifying assumptions. Such solutions generally involve indefinite integrals of modified Bessel functions. However, little mention appears to have been made in the literature of the techniques used for the evaluation of such integrals.

Van Arsdel obtained numerical solutions to his model using (i) a predictor-corrector technique employing mid-point predictor and trapezoidal corrector formulae with simultaneous correction in all four dependent variables, and (ii) a simple finite difference approximation to a slightly modified form of his equations.

Bakker-Arkema et al (1974) presented FORTRAN programs for the numerical solution of each of their four models. For the fixed bed case they employed an explicit finite difference technique incorporating a time-step calculation dependent on a specified stability criterion. Their program does not, however, appear to contain any error control mechanism. For the crossflow case, they make use of the same numerical technique, although for this problem the termination criteria are slightly different. For the concurrent flow case they make use of a program developed by Lastman employing an Adams-Moulton technique to solve the resulting initial value problem. Such techniques are examples of implicit linear multistep methods and have strong stability properties but are not necessarily appropriate for the solution of stiff systems of differential equations, such as those which occur in concurrent flow drier models. For the counterflow case, which is a two-point boundary value problem, they used a search technique based on an algorithm due to Powell (1964), together with the Adams-Moulton routine, to obtain successive approximations to the solution by minimising a prescribed objective function of the predicted inlet air properties.

Spencer (1969a) used a centred-difference approximation space-wise and the fourth order Kutta-Merson technique to advance the solution to his fixed bed equations time-wise. His technique incorporates a time-step adjustment stratagem based on the truncation error estimate obtained at each step using the Kutta-Merson method, but maintains a constant space step, see Spencer (1969b) for a discussion.

Ingram (1976a) presented a FORTRAN program for the solution of his fixed bed equations. He makes use of an explicit finite difference technique with a single iterative correction, in effect a crude implicit method. The program contains a simple step stratagem for computation in the x-direction facilitating a local error check at each integration step. It does not, however, contain such a device for computations in the t-direction. His program also contains an option to use either an empirical drying rate expression, based on the Lewis' type expression (1), or a diffusion equation calculation for the determination of drying rate such as described above.

Nelson (1960) presented an 'analysis of batch grain-drier perf-

ormance' in which he obtained an equation for the 'average drying effect by air', E, in terms of three dimensionless variables. The quantity E is defined as the mass of moisture removed from the grain per unit mass of drying air circulated through it.

Nelson begins by presenting a list of 26 physical variables pertinent to this problem. As he points out, this list is by no means unique or exhaustive. Generally, however, such a list may be divided into the following three categories:

(i) linear dimensions of both the grain kernel (see section 3.3) and the drying chamber,
(ii) kinematic variables, such as the airflow rate, and kinetic characteristics, such as the air viscosity,
(iii) the moisture and thermal states of the drying air and grain.

In his analysis, Nelson made the assumption that all the variables could be expressed in terms of five independent dimensions, viz. length, mass, time, temperature and heat. This assumption means, in effect, that mechanical and thermal energies are not interconvertible. Since, in such cases, the amount of interconversion is very small, however, the assumption of an independent heat dimension would not appear unreasonable. He then appealed to the Buckingham Pi theorem (see Buckingham (1914)), to deduce that his 26 variables could be reduced to a set of 21 independent dimensionless variables. Most of these were disregarded, however, in view of their limited significance to the problems of drier design. His final equation for E, as defined above, may be written in terms of three other dimensionless parameters, in the form

$$E = f\left((M_o - M_e^o),\ \frac{T_o - T_{L_i}}{T_o},\ \frac{L}{V_a t}\right) \quad ,$$

where T_{L_i} represents "the 'ideal' leaving air temperature (dry-bulb) after constant wet-bulb process to equilibrium humidity for grain at initial moisture content", and M_e^o is the e.m.c. corresponding to the inlet air state. Making use of experimental data, Nelson then obtained an expression of the form

$$E = c_1 \left[\frac{(M_o - M_e^o)(T_o - T_{L_i})}{T_o}\right]^n \left[1 - \exp(-c_2 L/(V_a t))\right] ,$$

where c_1, c_2 and n are constants.

Chien, Matthes and Verma (1969) assumed a functional relationship for MR of the form

$$MR = f\left(\frac{V_a t}{L} , \frac{x}{L} , \frac{T_s}{T_o}\right) ,$$

where T_s represents the "pseudo-saturation temperature" of the air (see Boyce 1965)). Again, making use of experimental results, these authors arrived at an expression for MR of the form

$$MR = \exp\left[(a + bx/L)\frac{V_a t}{L} + (c + dx/L)\right] , \quad \text{for } MR \leqq 1 ,$$

where a,b,c, and d are functions of the dimensionless 'temperature ratio', $\frac{T_s}{T_o}$.

The type of approach described above is obviously of great value in reducing the work involved in finding appropriate constitutive relationships for heat and mass transfer. Clearly, however, much experimental work is still required to obtain the requisite 'semi-empirical' expressions involving the selected non-dimensional variables. Such work is beyond the scope of this thesis. Indeed, use is made of already established empirical relationships for this purpose (see section 3.3), even though the evidence suggests that such relationships are not suited to the simulation of all of the drying problems examined in the current work.

Finally, some authors have presented the heat and mass balance equations in their PDE models for the fixed bed case in terms of dimensionless independent and dependent variables. Some of these were mentioned earlier in this section, namely Van Arsdel, Klapp and Ngoddy et al. In order, however, to facilitate writing each of these models

in non-dimensional form, certain simplifying assumptions had to be made. For example, in Klapp (1963) it is assumed that the heat transfer coefficient is constant over the range of variables considered.

1.3 Criticisms and Aims

As far as can be determined, the available mathematical models for grain drier simulation have all been derived for one particular type of drier, usually the fixed bed drier. In some instances such models have then been modified for use in simulations of other types of drier, such as concurrent flow, crossflow or counterflow. Furthermore, as might be expected, this work is restricted to one-dimensional models. In view, however, of the increasing complexity of applications, it would appear that a general three-dimensional formulation is now required. Such an approach helps to focus on the assumptions inherent in the various models. In addition the general equations have some properties which are of interest in their own right. The mathematical problems associated with particular drier types have not always been posed in a precise and correct form and numerical techniques for their solution have generally been treated in an ad hoc fashion.

The initial aim of this thesis is to give a general framework for the derivation of mathematical models for grain drying. This aim is accomplished in chapter 2, wherein differential balance equations for a general mixture of ν constituents together with jump conditions which hold across surfaces of discontinuity within the mixture, are presented. This mixture theory is then applied to the binary mixture of moist air and moist grain and appropriate simplifying assumptions made to obtain a general system of differential equations for grain drying. It is shown that the general problem reduces to the consideration of a system of four partial differential equations representing balances of mass and energy within the grain and air.

In chapter 3, models for particular types of convective grain drier are deduced from the four general equations derived in chapter 2. Appropriate initial and boundary conditions for a properly posed mathematical problem are discussed for each of these cases. It is shown that, in the steady state, the systems of equations for the concurrent flow and counterflow driers each reduces to a set of three ordinary differential equations together with one linear algebraic equation.

The significance of the jump conditions for the grain drying equations is discussed with reference to the (time-dependent) concurrent flow model. The general topic of constitutive equations for mass and heat transfer rates is presented in the context of diffusion equation models while the choice of particular equations is deferred until the later discussions of validation cases.

The main concern of this work is with the detailed simulation of the grain drying process. However, in some fixed bed applications where the airflow rate and drying air temperature are both low, the air and grain can, for most purposes, be assumed to be instantaneously in thermal and moisture equilibrium. Under these conditions the four equation system is shown to be easily reduced to two equations for which the theory of simple waves may be used to obtain a solution. Such an 'equilibrium' model is deduced from the fixed bed model. For a detailed discussion of equilibrium models, however, see Sharp (1982). Finally, differences among various models in the literature are discussed in relation to the models presented herein. In particular, the energy balance equations for most of these models are shown to be thermodynamically inconsistent. Much of the basic material of chapters 2 and 3 has been published jointly with Professor N.Laws (Laws and Parry (1983)).

In the initial stages of concurrent flow drying, much of the sensible heat in the drying air is converted to latent heat of vaporisation. This means that near the inlet, where the rate of evaporation is greatest, the grain does not generally attain the inlet temperature of the drying air and relatively high temperatures may be used without damage to the grain. However, in order to predict safe drying air temperatures, suitably accurate techniques need to be used to solve the concurrent flow transfer equations.

There does not appear to be any work in the available literature, barring a few comments, which concentrates on the specific problems associated with solving equations representing heat and mass transfer in steady state concurrent flow drying. In Chapter 4, this case is firstly investigated semi-analytically. It is concluded, however, that at best, such an approach leads to a useful picture of the qualita-

tive behaviour of the solution. An accurate numerical algorithm, based on an established extrapolation technique, together with a brief outline of its computer implementation (see also Parry (1983a,b)), is then described. Results of simulations obtained using this technique are presented for the purposes of validating the model and of giving some indication of the performance of the algorithm used to solve it.

In fixed bed drying, a heating/cooling 'front' has been observed to progress through the grain fairly rapidly. This is then followed more slowly by a drying front, grain nearest the air inlet (bottom of the bed) drying much more rapidly than that near the air outlet (top of the bed). This behaviour is exemplified in Figures 12a-d. Much of the research effort on fixed bed drier simulation has, however, been concentrated on equilibrium exchange, while detailed simulation is required for an accurate prediction of heating/drying effects in the early stages of fixed bed drying.

In Chapter 5, a semi-analytical approach to solving the fixed bed drying equations is considered. Again, however, it is concluded that such an approach does not provide a practicable means to finding a useful solution. A numerical technique, developed for the solution of this problem, and incorporating a modification of the algorithm used for concurrent flow simulation, is described together with its computer implementation. Three validation cases are presented together with a cursory examination of factors affecting the accuracy and efficiency of the algorithm, as currently implemented.

In steady state drying with a counterflow drier, the exhausting air should attain both thermal and moisture equilibrium with the inlet grain. In addition, the outlet grain should attain a temperature close to that of the inlet air. This type of drier may, therefore, be efficient, but inlet drying air temperatures are limited, more severely than in a concurrent flow drier, by the maximum 'safe' grain temperature (see comment - section 1.1). For this reason, counterflow drying is most commonly used in grain cooling, or in the corresponding 'stage' of a mixed flow drier.

The two-point boundary value problem resulting from modelling

counterflow drying has been solved numerically by Bakker-Arkema et al (1974). Their algorithm uses a search technique (due to Powell (1964)) which finds a solution minimising an objective function of the form

$$F(H_o^{pred}, T_o^{pred}) = [(1 - T_o^{pred}/T_o)^2 + 1][(1 - H_o^{pred}/H_o)^2 + 1]. \quad (1)$$

As the authors point out, however, Powell's technique is for unconstrained optimisation problems and the resulting values of state variables may lead to infeasible state points. They make the further observation that the technique does not readily cope with driers in which an equilibrium state is approached and that short driers/coolers with high airflow rates are most easily facilitated.

In Chapter 6, the technique used to solve the counterflow model developed in Chapter 3, and which incorporates a NAG library subroutine, is described along with a brief outline of its computer implementation. A single validation model is then presented with a cursory analysis of the sensitivity of the algorithm to perturbations in the outlet conditions.

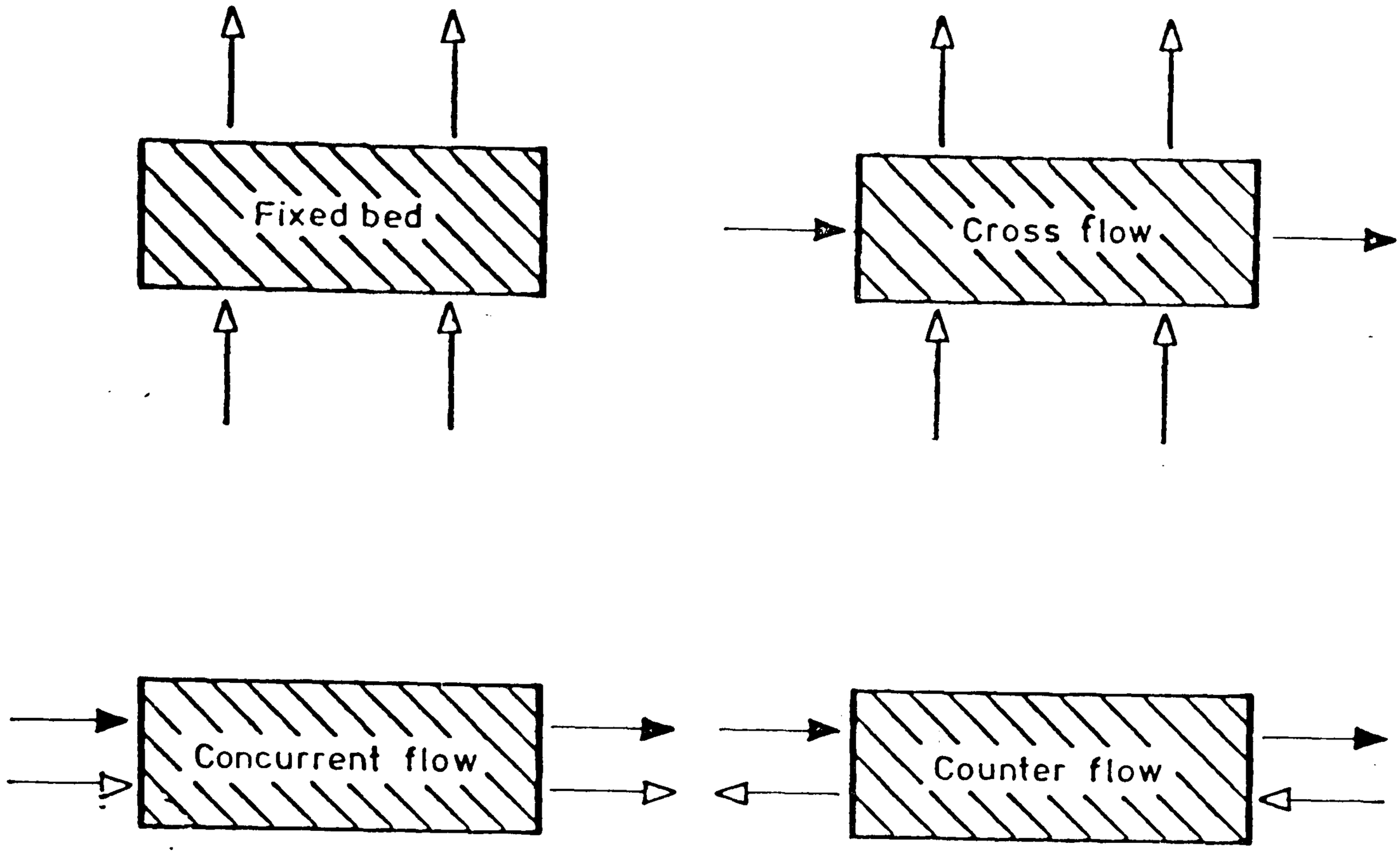

Figure 1. Schema for the four basic types of convective grain drier. (The directions of the flow of grain and air are respectively indicated by black and white arrows.)

CHAPTER TWO: A GENERAL MODEL FOR GRAIN DRYING

The purpose of this chapter is to present a general framework for the derivation of mathematical models of simultaneous heat and mass transfer in grain drying. In section 2.1 the standard continuum theory of mixtures is used to obtain the requisite theoretical framework. In section 2.2 appropriate assumptions are then made to derive a general model for deep bed grain drying. It is acknowledged that a specialist in the modern continuum theory of mixtures might find the approach somewhat pedestrian. In addition, an agricultural engineer might consider references to actual drying processes, at this stage, rather over-simplified. It is hoped, however, that this development will provide an interface between two disciplines and will have something to offer specialists in the respective fields.

2.1 The General Equations for a Mixture

For the general development, a mixture consisting of ν constituents is considered. These constituents may be solid or fluid and the primary interest lies in the interactions which may occur, for example chemical reactions, evaporation, condensation or heat transfer. Thus the basic balance laws of mass, momentum and energy for the individual phases need to take into account the various interactions. Furthermore, since there is no overall creation or destruction of mass, for example, there is a corresponding conservation law for the mixture as a whole. It is convenient to express all the required balance and conservation laws by considering an arbitrary fixed region R bounded by a fixed surface S. Here and subsequently the notation has been chosen to be compatible with that used in the review article by Atkin and Craine (1976). In particular the various constituents of the mixture are designated by Greek suffices so that $\mathscr{C}_\alpha$ represents the αth component of the mixture.

The balance of mass for each constituent of the mixture can be expressed as: the rate of increase of mass within R is equal to the net influx of mass across S per unit time plus the rate of mass production arising from the other constituents within R. Let ρ_α be the density of constituent $\mathscr{C}_\alpha$, $\underline{v}^\alpha$ the velocity and m_α the net density of mass production arising from all other constituents, then the corresponding mathematical statement is

$$\frac{\partial}{\partial t}\int_R \rho_\alpha dV = -\int_S \rho_\alpha \underline{v}^\alpha \cdot \underline{n} dS + \int_R m_\alpha dV, \qquad (1)$$

where $\underline{n}$ is the unit outward normal to the surface S. For reasonably smooth processes it follows from the arbitrariness of R, see for example Chadwick (1976), that (1) is equivalent to the differential equation

$$\frac{\partial \rho_\alpha}{\partial t} + \frac{\partial}{\partial x_k}\left(\rho_\alpha v_k^\alpha\right) = m_\alpha \quad . \qquad (2)$$

In (2) and subsequently, Cartesian tensor notation with respect to coordinates $x_i (1=1,2,3,)$ is employed. Latin indices are always used to denote tensor indices so that repeated Latin indices are summed over the appropriate range. Since Greek indices refer to the constituent under discussion, the summation convention does not apply. Summation over all constituents is specifically indicated as in (3) below.

Conservation of mass for the mixture as a whole requires that

$$\sum_{\alpha=1}^{\nu} m_\alpha = 0 \tag{3}$$

The balance of momentum for each constituent $\mathcal{C}_\alpha$ of the mixture can be expressed as follows: the rate of increase of linear momentum (of $\mathcal{C}_\alpha$) within R is equal to the net influx of linear momentum across S plus the resultant external body force plus the resultant surface force across S plus the interaction forces. Equivalently, this may be written

$$\frac{\partial}{\partial t} \int_R \rho_\alpha \underline{v}^\alpha dV = - \int_S \rho_\alpha \underline{v}^\alpha (\underline{v}^\alpha \cdot \underline{n}) dS + \int_R \rho_\alpha \underline{F}^\alpha dV + \int_S \underline{t}^\alpha dS + \int_R \underline{\phi}^\alpha dV, \tag{4}$$

where $\underline{F}^\alpha$ is the external body force and $\underline{\phi}^\alpha$ is the interaction, or diffusive, force. Also

$$t_i^\alpha = \sigma_{ji}^\alpha n_j \tag{5}$$

and σ_{ji}^α is called the partial stress tensor. Again, for smooth processes, it is easy to show that (4) is equivalent to the differential equation

$$\frac{\partial}{\partial t} (\rho_\alpha v_i^\alpha) + \frac{\partial}{\partial x_k} (\rho_\alpha v_k^\alpha) = \rho_\alpha F_i^\alpha + \frac{\partial \sigma_{ji}^\alpha}{\partial x_j} + \phi_i^\alpha \ . \tag{6}$$

Since the diffusive forces $\underline{\phi}^\alpha$ are purely internal forces it is clearly required that

$$\sum_{\alpha=1}^{\nu} \phi_i^\alpha = 0 \ . \tag{7}$$

In common with most applications, it is assumed that the partial stress tensors σ_{ij} are symmetric. This means that there are no internal couples within the mixture and that the equations of balance of moment of momentum are identically satisfied.

Finally the balance of energy for each constituent says that the rate of increase of internal energy and kinetic energy (of $\mathcal{C}_\alpha$) within R is equal to the net influx of energy across S per unit time plus the rate of working of the body forces, surface forces and interaction forces plus the rate of supply of heat from external sources plus the influx of heat across S per unit time plus the energy supplied by interactions. This balance may be expressed in the form

$$\frac{\partial}{\partial t}\int_R \rho_\alpha(E_\alpha + \tfrac{1}{2}\underline{v}^\alpha\cdot\underline{v}^\alpha)dV = -\int_S \rho_\alpha(E_\alpha + \tfrac{1}{2}\underline{v}^\alpha\cdot\underline{v}^\alpha)(\underline{v}^\alpha\cdot\underline{n})dS$$

$$+\int_R(\rho_\alpha\underline{F}^\alpha + \underline{\phi}^\alpha)\cdot\underline{v}^\alpha dV + \int_S \underline{t}^\alpha\cdot\underline{v}^\alpha dS$$

$$+\int_R \rho_\alpha r_\alpha dV - \int_S \underline{q}^\alpha\cdot\underline{n}dS + \int_R \psi_\alpha dV, \qquad (8)$$

where E_α is the internal energy and r_α the external heat supply per unit mass of $\mathcal{C}_\alpha$. Also $\underline{q}^\alpha$ is the heat flux carried by $\mathcal{C}_\alpha$. From (8) it is noted that the local rate of supply of energy to $\mathcal{C}_\alpha$ due to internal effects is

$$\psi_\alpha + \underline{\phi}^\alpha\cdot\underline{v}^\alpha .$$

Thus it may be seen that the net rate of supply of energy due to interactions consists of two parts. As far as can be determined, all previous models for drying ignore the contribution $\underline{\phi}^\alpha\cdot\underline{v}^\alpha$. It is significant that this application of the standard theory of mixtures clearly shows the necessity of including this term. The differential equation equivalent to (8) is

$$\frac{\partial}{\partial t}(\rho_\alpha E_\alpha) + \frac{\partial}{\partial x_k}(\rho_\alpha E_\alpha v_k^\alpha) = \tfrac{1}{2}m_\alpha v_i^\alpha v_i^\alpha + \sigma_{ik}^\alpha d_{ik}^\alpha + \rho_\alpha r_\alpha - \frac{\partial q^\alpha{}_k}{\partial x_k} + \psi_\alpha, \qquad (9)$$

where the rate of deformation tensor d^{α}_{ik} is defined by

$$d^{\alpha}_{ik} = \tfrac{1}{2}\left(\frac{\partial v^{\alpha}_{i}}{\partial x_k} + \frac{\partial v^{\alpha}_{k}}{\partial x_i} \right). \qquad (10)$$

Since the interactive energy supply terms are purely internal it is clearly required that

$$\sum_{\alpha=1}^{\nu} (\psi_{\alpha} + \underline{\phi}^{\alpha} \cdot \underline{v}^{\alpha}) = 0 \ . \qquad (11)$$

One of the features of the theory of mixtures, as presented here, is that each of the basic physical balance laws contains a source term due to interactions. From the physical standpoint it would be advantageous to be able to identify the term $\underline{\phi}^{\alpha}$ in (4), for example, with a definite mechanism. However, the dangers inherent in this approach are well known. For present purposes it is best to take the position of the mathematician and regard ϕ^{α} as an unknown which needs to be given a constitutive relation.

The analysis which leads to the partial differential equations (2), (6) and (9) demands that the considered thermomechanical process be smooth enough. In particular this means that discontinuities in the constituent densities are not allowed. However, discontinuous density fields often occur in practice - although it is more precise to speak of rapidly varying density fields which must be modelled mathematically by discontinuities. Thus the partial differential equations must be supplemented by the jump conditions which apply at a surface of discontinuity. The required conditions follow directly from (1), (4) and (8), see for example Chadwick (1976). Let U be the speed of the surface of discontinuity then

$$V^{\alpha} = U - \underline{v}^{\alpha} \cdot \underline{n} \qquad (12)$$

is the speed of propagation of the singular surface relative to the constituent $\mathcal{C}_{\alpha}$. With the help of the notation $[\Phi]$ to signify the jump in Φ across the singular surface, it may be shown that the

balances of mass, momentum and energy respectively yield

$$[\rho_\alpha V^\alpha] = 0, \tag{13}$$

$$[\rho_\alpha V^\alpha v_i^\alpha + t_i^\alpha] = 0, \tag{14}$$

$$[\rho_\alpha V^\alpha (E_\alpha + \tfrac{1}{2}\underline{v}^\alpha \cdot \underline{v}^\alpha) + \underline{t}^\alpha \cdot \underline{v}^\alpha - \underline{q}^\alpha \cdot \underline{n}] = 0. \tag{15}$$

The significance of the jump conditions (13) to (15) will become apparent in the next chapter when actual drying processes are discussed.

2.2 The General Equations for Grain Drying

In this section the general theory of mixtures outlined in the preceeding section is used to obtain the general equations for drying.

The first step is to decide upon the level of generality as far as the number of individual constituents is concerned. Clearly the moist air and moist grain consist of four separate phases. In practice, however, a four phase model is both too complicated and unnecessary. Thus one is led to a two phase model in which the moist air, i.e. dry air plus water vapour is regarded as one phase, which is denoted by $\mathscr{C}_1$. Similarly the moist grain, i.e. dry grain together with its water content, is assumed to be a single continuum, which is denoted by $\mathscr{C}_2$. One implication of this model is that at a particular point in the drier one is unable to distinguish between the velocity of the dry air and the velocity of the water vapour, but this does not appear to be a serious limitation. In addition, one is unable to distinguish between the respective temperatures of the air and the water vapour and between those of the grain and its moisture content.

Thus a model is formulated for grain drying on the basis of the application of the theory of binary mixtures. Let m be the net rate of mass transfer from the grain to the air i.e. the rate of evaporation of water, and let $\underline{\phi}$ be the interaction force on the moist air. Then it follows from (2.1 - 3) and (2.1 - 7) that

$$\left.\begin{aligned} m_1 &= -m_2 = m, \\ \underline{\phi}^1 &= -\underline{\phi}^2 = \underline{\phi}, \end{aligned}\right\} \tag{1}$$

In addition, with $\psi_2 = \psi$, (2.1-11) yields

$$\psi_1 = -\psi + \underline{\phi} \cdot (\underline{v}^2 - \underline{v}^1) \qquad (2)$$

It therefore follows that, while ψ is the energy supply to the grain $(-\psi)$ is <u>not</u> the net energy supply to the air. However, this point is not considered too important since, as is indicated later, the energetic significance of the interaction force $\underline{\phi}$ is minimal. Accordingly, for all practical purposes, $(-\psi)$ <u>is</u> the net energy supply to the air.

The density, ρ_1 of the moist air depends on the densities ρ_a and ρ_v of the dry air and water vapour respectively. In the same way the density, ρ_2, of the moist grain depends upon the densities ρ_p and ρ_w of the product and the water within the grain kernels. It is standard practice to measure ρ_p and ρ_w <u>per unit volume of the bed</u>. For practical purposes it is convenient to work with the <u>humidity ratio</u> $H = \rho_v/\rho_a$ and the <u>moisture content</u> (dry basis) $M = \rho_w/\rho_p$. Hence if ε is the void fraction*

$$\left.\begin{aligned} \rho_1 &= \varepsilon\rho_a(1 + H) \quad , \\ \rho_2 &= \rho_p(1 + M) \quad . \end{aligned}\right\} \qquad (3)$$

It should be noted that in the following development ρ_a, ρ_p and hence ε, will be assumed constant. These assumptions and their implications will be discussed in chapter 7.

Inspection of equations (2.1-2), (2.1-6) and (2.1-9) clearly indicates that a large number of constitutive relations is required for a fully determinate theory. A significant feature of the model proposed here is that the primary variables can be found from relatively few assumptions, as is now shown.

In heated air driers, the transfer of mass and energy is mainly due to the convective movement of the moist air through the moist grain. Thus a basic assumption, which parallels the usual assumption in gas

* Both ρ_1 and ρ_2 are measured per unit volume of the bed (i.e. mixture).

dynamics, is that there is no heat flux:

$$q_i^1 = q_i^2 = 0.$$

In solar drying there might be an external heat supply, but here it is assumed that

$$r_1 = r_2 = 0.$$

The internal energies of the moist air and grain are assumed to be given by the usual additive rule

$$\left.\begin{aligned} \rho_1 E_1 &= \varepsilon\rho_a E_a + \varepsilon\rho_v E_v , \\ \rho_2 E_2 &= \rho_p E_p + \rho_w E_w , \end{aligned}\right\} \tag{4}$$

with the obvious notation. With the help of (3) it may be shown that

$$E_1 = \frac{E_a + HE_V}{1 + H} , \tag{5}$$

$$E_2 = \frac{E_p + ME_w}{1 + M} , \tag{6}$$

Let T, θ denote the temperature of the moist air and grain respectively. Then the standard assumptions are that

$$E_a(T) = e_a + c_a T, \quad E_v(T) = e_v + c_v T, \tag{7}$$

$$E_w(\theta) = e_w + c_w \theta, \quad E_p(\theta) = e_p + c_p \theta, \tag{8}$$

where the base energies e and specific heats c are assumed constant. Clearly, the distance between the graphs of E_v and E_w as functions of temperature is the latent heat of evaporation of water.

Perhaps the most difficult and controversial aspect of the constitutive theory hinges on the specification of ψ and m. Different authors have different ways of arriving at an assumed form for the

net rate of supply of energy. Since this term includes the effect of temperature differences between the air and the grain and the energetic effect of mass transfer it is not surprising that there are differences of opinion.

As far as can be determined it is always assumed that ψ is some function of H, M, T and θ. It turns out that the basic properties of the system of partial differential equations which characterises the model herein are independent of the choice of the functional forms for ψ and m. Thus a discussion of detailed choices is postponed until section 3.3.

Next, it is always assumed that the dry air and the dry grain densities, ρ_a and ρ_p respectively, and the void ratio are constant. The problem of deciding upon constitutive relations for the partial stresses σ_{ij}^{α} remains. The usual practice in continuum mechanics would be to assume functional dependence on H, M, T, θ together with suitable kinematic variables. Ultimately the balance equations would then give the correct number of equations for the determination of the dependent variables. This procedure is not followed directly in this work. Rather a basic knowledge of the kinematics of existing driers is utilised in order to avoid making hypotheses which are not verifiable at the present time.

For all driers currently in use, the velocity fields of the air and the grain are approximately one dimensional and uniform. Let the air flow be in the x - direction with speed V_a and the flow of moist grain be in the y - direction with speed V_p. When convenient, as in a concurrent flow drier, x and y will be taken to be coincident. In this configuration the mass balance equations (2.1-2) become

$$\varepsilon\rho_a\left(\frac{\partial H}{\partial t} + V_a\frac{\partial H}{\partial x}\right) = m \quad , \tag{9}$$

$$\rho_p\left(\frac{\partial M}{\partial t} + V_p\frac{\partial M}{\partial y}\right) = -m \quad , \tag{10}$$

Since the velocity fields are respectively uniform, the energy balance equations reduce to

$$\varepsilon\rho_a(c_a + c_v H)\left(\frac{\partial T}{\partial t} + V_a \frac{\partial T}{\partial x}\right) = \frac{m}{2} V_a^2 - \psi + \underline{\phi}\cdot(\underline{v}^2 - \underline{v}^1) - mE_v(T), \qquad (11)$$

$$\rho_p(c_p + c_w M)\left(\frac{\partial \theta}{\partial t} + V_p \frac{\partial \theta}{\partial y}\right) = -\frac{m}{2} V_p^2 + \psi + mE_w(\theta). \qquad (12)$$

While there is no difficulty in proceeding from (11) and (12) with maximum generality, it is assumed here that the energetic significance of the kinetic energy and diffusive force terms is minimal. These assumptions are examined in the context of the numerical simulations presented in chapter 4. Thus (11) and (12) reduce to the approximate energy balance equations

$$\varepsilon\rho_a(c_a + c_v H)\left(\frac{\partial T}{\partial t} + V_a \frac{\partial T}{\partial x}\right) = -\psi - mE_v(T), \qquad (13)$$

$$\rho_p(c_p + c_w M)\left(\frac{\partial \theta}{\partial t} + V_p \frac{\partial \theta}{\partial y}\right) = \psi + mE_w(\theta). \qquad (14)$$

It might appear from (13) and (14) that the energy balance equations depend upon the base energies e_v and e_w. However, it is shown in section 3.3 that, once the constitutive relation for ψ is specified, this apparent dependence is no longer present.

Now (9), (10), (13) and (14) may be written in the matrix form

$$\frac{\partial \underline{u}}{\partial t} + A\frac{\partial \underline{u}}{\partial x} + B\frac{\partial \underline{u}}{\partial y} = \underline{b}, \qquad (15)$$

where $\underline{u} = [H, M, T, \theta]^T$, and where the matrices A and B are given by

$$A = \begin{bmatrix} V_a & 0 & 0 & 0 \\ 0 & 0 & 0 & 0 \\ 0 & 0 & V_a & 0 \\ 0 & 0 & 0 & 0 \end{bmatrix}, \qquad B = \begin{bmatrix} 0 & 0 & 0 & 0 \\ 0 & V_p & 0 & 0 \\ 0 & 0 & 0 & 0 \\ 0 & 0 & 0 & V_p \end{bmatrix}. \qquad (16)$$

Also

$$\underline{b} = \begin{bmatrix} b_1 \\ b_2 \\ b_3 \\ b_4 \end{bmatrix} = \begin{bmatrix} m/\varepsilon\rho_a \\ -m/\rho_p \\ \{-\psi - mE_v(T)\}/\{\varepsilon\rho_a(c_a + c_v H)\} \\ \{+\psi + mE_w(\theta)\}/\{\rho_p(c_p + c_w M)\} \end{bmatrix} . \qquad (17)$$

In practice V_a and V_p are known (and uniform) and thus can be regarded as given. Thus provided ψ and m are given only in terms of H, M, T and θ, the system of equations (15), provides four partial differential equations for the determination of the primary physical variables H, M, T and θ. There remains, however, the problem of deciding upon the role of the momentum equations (2.1-6).

The stated (approximate) kinematics of existing driers indicates that the motion of the grain and the air is that of two interpenetrating rigid bodies. Hence it suffices to idealise each phase as a rigid body. It then follows that the partial stresses are indeterminate (from the point of view of the constitutive relations). Further, it is clear from (2.1-6) that the equations of balance of momentum do not permit the determination of the individual components of the partial stress tensors. Rather, it is only possible to determine the resultant applied force on each phase in terms of the known velocity fields and the interaction force $\underline{\phi}$.

The system (2.2-15) provides (superficially at least) a determinate set of equations for H, M, T and θ. Once $\underline{\phi}$ has been given, (2.1-6) may be used to obtain the respective resultant applied forces on the two phases. At the present time these resultant forces are not quantities of interest, so from now on, the equations of balance of momentum will be disregarded. Correspondingly, it is asserted that the general equations of heat and mass transfer for driers are given by (9), (10), (13) and (14).

CHAPTER THREE: PARTICULAR MODELS

The purpose of this chapter is to obtain models for each of the four basic types of convective grain drier described in the Introduction using the mathematical framework developed in chapter 2. In section 3.1, models are given for the general, i.e. time-dependent, problems associated with each of these drier types, and, where applicable, the corresponding steady-state models are deduced from these. In section 3.2, the significance of the jump conditions, given in section 2.1, is discussed in relation to the concurrent flow model. In section 3.3, there is a general discussion of constitutive equations for the moisture and heat transfer rates. Particular choices adopted for use in the numerical investigations are given in appendices A and C. In section 3.4, an 'equilibrium' model, suitable for low airflow, low temperature drying, is deduced from the fixed bed model presented in section 3.1. Finally, in section 3.5 there is a discussion of other models in the light of the basic model presented herein. The purpose of this discussion is to examine the assumptions inherent in these models and, as far as possible, to illuminate the differences amongst these.

It is noted that, as far as can be determined, time-dependent models for each of the concurrent flow, counterflow and crossflow cases have not previously been presented or discussed in the literature.

3.1 Models for the Four Basic Types of Drier

In this section mathematical models are obtained for the four basic types of drier. An important part of this analysis is the discussion of suitable initial and boundary conditions demanded by engineering practice and the reconciliation of these conditions with the mathematical properties enjoyed by the model equations.

(a) Fixed Bed Model

It has already been stated that in a fixed bed drier, heated air passes through a deep bed of stationary grain. Prior to the air being forced through the bed, the temperature and moisture content of the grain will have experienced some equilibration due to natural heat and mass transfer within the bed. A typical application occurs in layer drying, in which fresh layers of grain are periodically added, without mixing, to the partially dried grain. Another application is ambient air drying during harvesting in which new moist grain is being continually added.

When a single batch of grain is to be dried, it is usual to assume that the moisture content and temperature of the grain are initially uniform throughout the bed. Clearly one would expect the model to cope with the general situation in which the initial moisture content and temperature of the grain varied arbitrarily with depth. Since the drying process is being driven by air which is forced into the bed, it is evident that the humidity and temperature of the incoming air should be known. It turns out that these conditions are precisely the conditions which should be expected for a properly posed problem for the mathematical model herein.

For a fixed bed drier $V_p = 0$, hence $B = 0$, and the system (2.2-15) reduces to

$$\frac{\partial \underline{u}}{\partial t} + A \frac{\partial \underline{u}}{\partial x} = \underline{b} \quad . \tag{1}$$

This system of semi-linear first order partial differential equations is hyperbolic, see e.g. Whitham (1974). There are two families of characteristics

$$\frac{dx}{dt} = V_a \qquad (C_1) \quad , \tag{2}$$

and

$$\frac{dx}{dt} = 0 \qquad (C_2) \quad , \tag{3}$$

and the system (1) reduces to

$$\left.\begin{aligned} \frac{dH}{dt} &= b_1 \\ \frac{dT}{dt} &= b_3 \end{aligned}\right\} \quad \text{along} \quad C \quad , \tag{4}$$

and

$$\left.\begin{aligned} \frac{dM}{dt} &= b_2 \\ \frac{d\theta}{dt} &= b_4 \end{aligned}\right\} \quad \text{along } C_2 \quad . \tag{5}$$

With reference to Figure 2, the initial characteristic OA represents the path of the moist air when the circulating fan is initially switched on. In the constant state region bounded by OA and Ox, the grain conditions are the initial conditions as discussed above. If now OA is regarded as the initial line, equations (4) may be solved along OA to obtain the initial air humidity and temperature throughout the bed as the first front of air moves through it. In view, therefore, of (4), it is not mathematically correct to prescribe initial air conditions since these would in general be different to those propagated by (4). Similarly, along Ot, the inlet air conditions may be prescribed but the grain conditions at this point are determined by (5) and hence cannot be prescribed.

Thus, for a bed of depth L, the appropriate initial and boundary conditions are respectively

$$\left.\begin{aligned} M(x,0) &= M_o(x) \\ \theta(x,0) &= \theta_o(x) \end{aligned}\right\} \quad 0 \leqq x \leqq L, \tag{6}$$

and

$$\left.\begin{aligned} H(0,t) &= H_o(t) \\ T(0,t) &= T_o(t) \end{aligned}\right\} \quad t > 0 \ . \tag{7}$$

Now any discontinuities in initial or boundary conditions are propagated along the appropriate characteristics. Thus a discontinuity in the initial grain conditions at some point in the bed, is propagated along the C_2 characteristic through that point and similarly any discontinuity in the inlet air conditions at any time is propagated along the C_1 characteristic through the corresponding point.

In view of the nature of the nonlinear vector function $\underline{b}(\underline{u})$, no analytical solution to either of the systems (1), or (4) and (5), is available, in general. Numerical solutions to either of these systems may, however, be obtained using numerical integration techniques. The system of equations (4) and (5) has the advantage over the system (1) that it may be solved by a wide class of well understood numerical methods. In addition any discontinuities in either initial or boundary conditions are clearly propagated along the characteristics.

(b) Crossflow Model

In a crossflow drier the air and grain flow in mutually perpendicular directions. Hence the crossflow drier is just the general drier described in section 2.2 and the required equations are (2.2-9, 10,13,14). The grain enters the drier along the line $y = 0$ and travels in the y-direction whereas the air enters along the line $x = 0$ and travels in the x-direction. The properties of the incoming grain are usually assumed to be spacewise uniform although they may vary in time. Similar properties are assumed for the incoming air. However, in prectice one is usually interested in a steady state problem so that the properties of both incoming grain and air are taken to be independent of time. In the steady state the differential equations

reduce to

$$A \frac{\partial \underline{u}}{\partial x} + B \frac{\partial \underline{u}}{\partial y} = \underline{b} \quad , \tag{8}$$

and, of course, $\underline{u}$ now depends only on x and y. The corresponding boundary conditions for a drier of width W and depth L are

$$\left.\begin{aligned} M(x,0) &= M_o \\ \theta(x,0) &= \theta_o \end{aligned}\right\} \quad 0 \leqq x \leqq W, \tag{9}$$

$$\left.\begin{aligned} H(0,y) &= H_o \\ T(0,y) &= T_o \end{aligned}\right\} \quad 0 \leqq y \leqq L. \tag{10}$$

Equations (8) are similar to the fixed bed equations (1). However, in this case the two families of characteristics are (see Figure 3)

$$\frac{dy}{dx} = 0 \qquad (C_1) \tag{11}$$

and

$$\frac{dx}{dy} = 0 \qquad (C_2) \tag{12}$$

and the system (8) reduces to

$$\left.\begin{aligned} V_a \frac{dH}{dx} &= b_1 \\ V_a \frac{dT}{dx} &= b_3 \end{aligned}\right\} \quad \text{along } C_1 \tag{13}$$

and

$$\left.\begin{aligned} V_p \frac{dM}{dy} &= b_2 \\ V_p \frac{d\theta}{dy} &= b_4 \end{aligned}\right\} \quad \text{along } C_2 \tag{14}$$

(c) Concurrent Flow Model

In a concurrent flow drier both air and grain flow in the same direction (but with different speeds). Thus x and y are taken to coincide so the general equations (2.2-15) reduce to

$$\frac{\partial \underline{u}}{\partial t} + C \frac{\partial \underline{u}}{\partial x} = \underline{b} \quad , \tag{15}$$

where

$$C = A + B \, . \tag{16}$$

Thus a variant of the fixed bed equations is again recovered. In this case the characteristics of (15) are the families of parallel lines

$$\frac{dx}{dt} = V_a \qquad (C_1) \quad , \tag{17}$$

$$\frac{dx}{dt} = V_p \qquad (C_2) \quad , \tag{18}$$

as shown in Figure 4. The system of equations (15) now reduces to

$$\left.\begin{aligned} \frac{dH}{dt} &= b_1 \\ \frac{dT}{dt} &= b_3 \end{aligned}\right\} \qquad \text{along } C_1 \quad , \tag{19}$$

together with

$$\left.\begin{aligned} \frac{dM}{dt} &= b_2 \\ \frac{d\theta}{dt} &= b_4 \end{aligned}\right\} \qquad \text{along } C_2 \quad . \tag{20}$$

The practical configuration of interest involves grain and air simultaneously entering the drier at $x = 0$, say. Thus the required initial conditions for a properly posed problem are

$$\left.\begin{aligned} M(0,t) &= M_o(t) \quad , \\ \theta(0,t) &= \theta_o(t) \quad , \\ H(o,t) &= H_o(t) \quad , \\ T(0,t) &= T_o(t) \quad . \end{aligned}\right\} \tag{21}$$

The steady state case here leads to a significant simplification because the governing equations are just ordinary differential equations.

There is another simplification because of the fact that b_2 is proportional to b_1. The reduced system of equations may be written as

$$\left.\begin{aligned} V_p \frac{dM}{dx} &= b_2 \quad , \\ V_a \frac{dT}{dx} &= b_3 \quad , \\ V_p \frac{d\theta}{dx} &= b_4 \quad , \end{aligned}\right\} \tag{22}$$

together with the algebraic equation

$$\varepsilon \rho_a V_a H + \rho_p V_p M = \text{constant}. \tag{23}$$

In this case the necessary initial conditions are given by (21) but with each of M_o, θ_o, H_o and T_o constant.

(d) Counterflow model

A counterflow drier involves the flow of air and grain in opposite directions. Let the grain flow in the positive x-direction with speed V_p and the air flow in the negative x-direction with speed V_a. Then the equations for this application reduce to the form (15) but with

$$C = B - A \quad . \tag{24}$$

The families of characteristics are shown in Figure 5. Since grain enters at one end of the drier (x = 0) and air enters at the other end (x = L) the required boundary conditions are

$$\left.\begin{aligned} M(0,t) &= M_o(t) \quad , \\ \theta(0,t) &= \theta_o(t) \quad , \end{aligned}\right\} \tag{25}$$

and

$$\left.\begin{aligned} H(L,t) &= H_o(t) \quad , \\ T(L,t) &= T_o(t) \quad . \end{aligned}\right\} \tag{26}$$

This represents a two point boundary value problem.

As before the main interest is in the steady state problem for which the governing differential equations are

$$\left.\begin{aligned} V_p \frac{dM}{dx} &= b_2 \quad , \\ V_a \frac{dT}{dx} &= -b_3 \quad , \\ V_p \frac{d\theta}{dx} &= b_4 \quad , \end{aligned}\right\} \tag{27}$$

together with

$$\varepsilon \rho_a V_a H - \rho_p V_p M = \text{constant}. \tag{28}$$

The boundary conditions for this special case are given in (25) and (26) with M_o, θ_o, H_o and T_o independent of time.

3.2 Significance of the Jump Conditions for the General Drying Equations

The significance of the jump conditions (2.1-13) to (2.1-15) for the general drying equations derived in section 2.1 is now examined. It suffices to discuss the jump conditions for the concurrent flow model. A similar analysis holds for the other three models.

The speeds of propagation of the singular surface relative to the air and the grain are respectively given by (2.1-12) as

$$V^1 = U - V_a \quad , \quad V^2 = U - V_p .$$

Since the flow is one-dimensional and the air and grain speeds are assumed constant, the jump conditions (2.1-13) to (2.1-15) yield

$$(U-V_a)[H] = 0, \quad (U-V_p)[M] = 0, \tag{1}$$

$$\varepsilon\rho_a(U-V_a)V_a[H] + [t_1^1] = 0, \quad \rho_p(U-V_p)V_p[M] + [t_1^2] = 0, \tag{2}$$

$$\varepsilon\rho_a(U-V_a)\{c_a[T] + [H(e_v + c_v T)]\} + V_a[t_1^1] = 0, \tag{3}$$

$$\rho_p(U-V)\{c_p[\theta] + [M(e_w + c_w\theta)]\} + V_p[t_1^2] = 0. \tag{4}$$

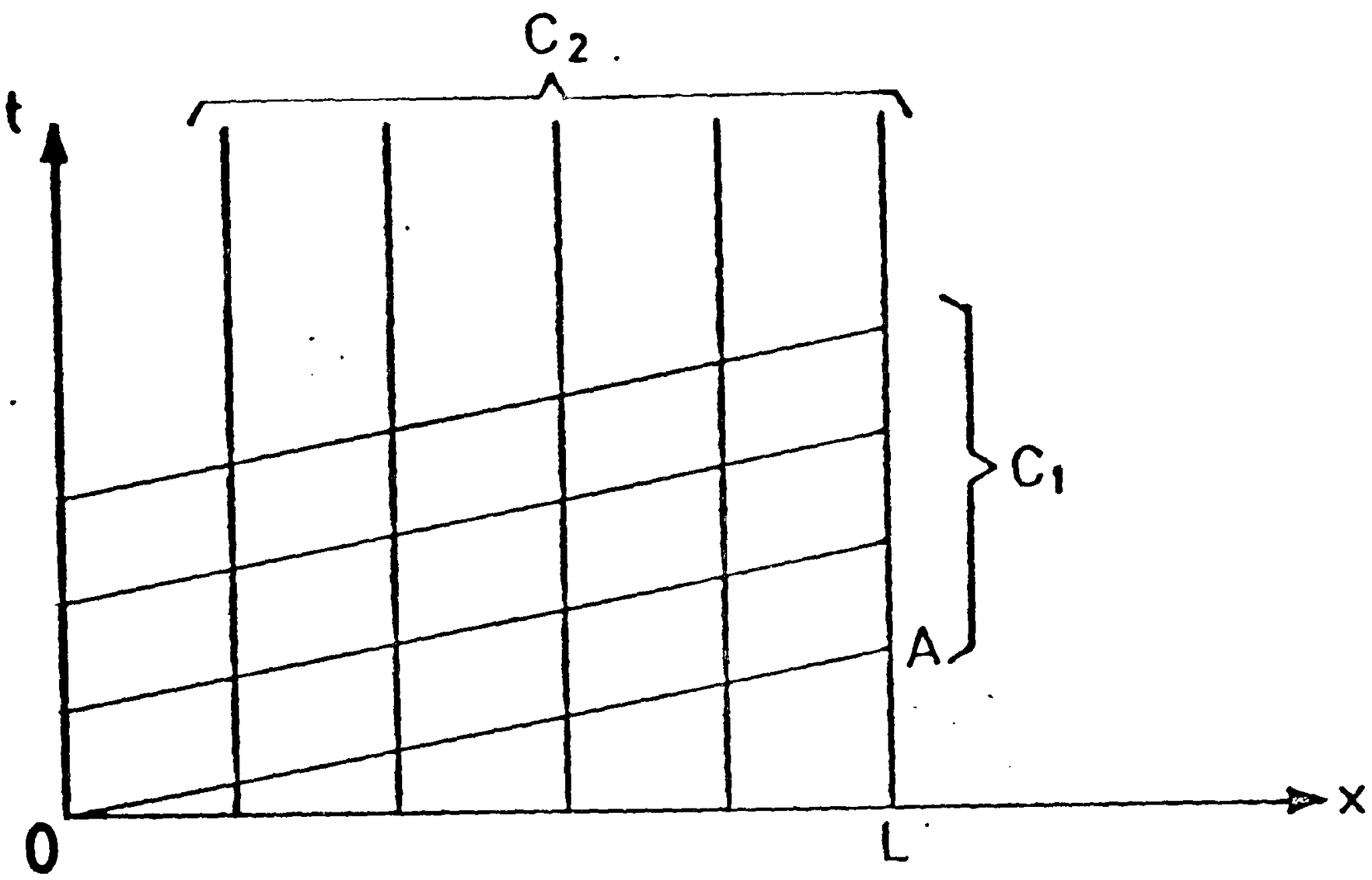

Figure 2. Families of characteristics for the fixed bed equations.

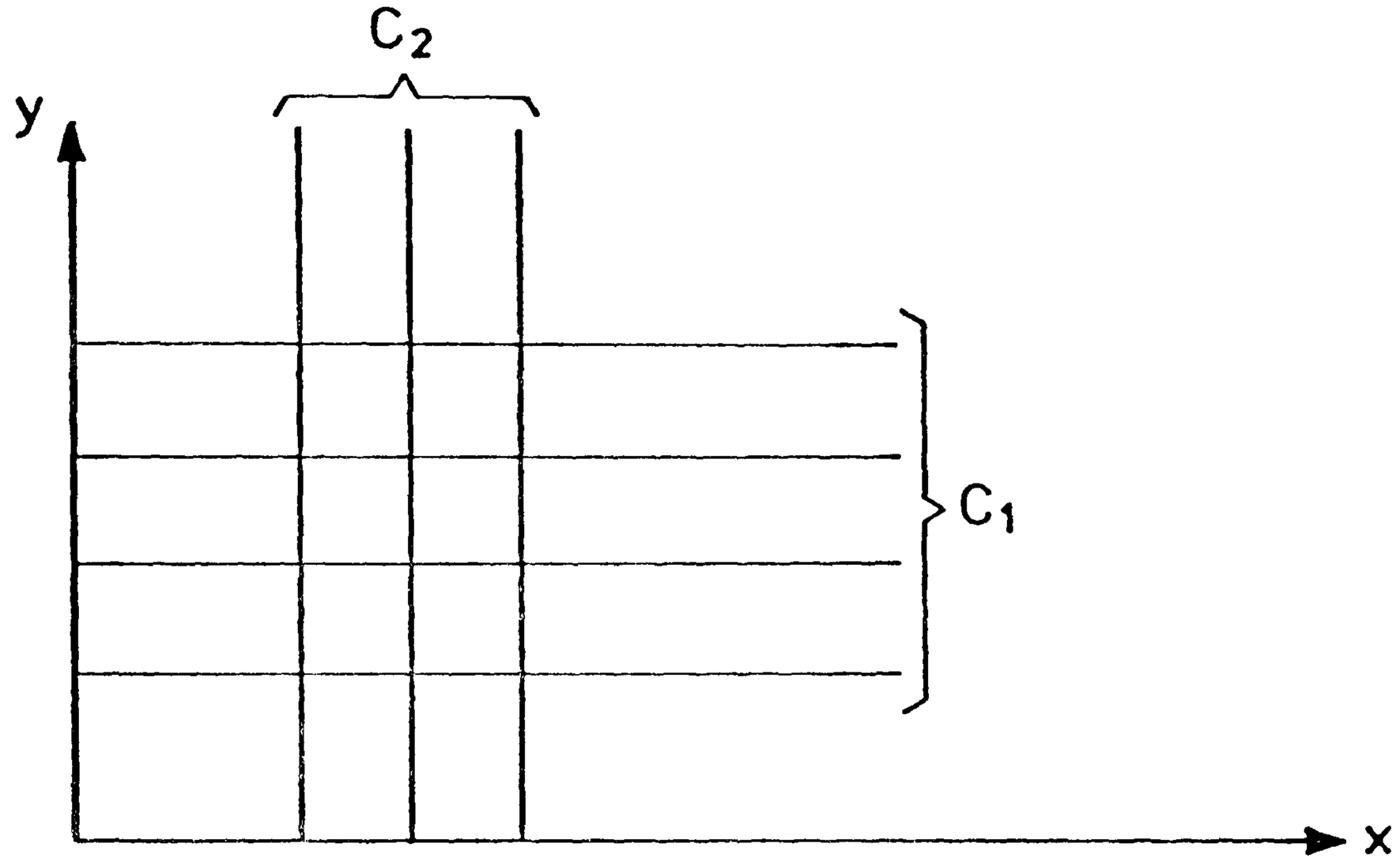

Figure 3. Families of characteristics for the steady state cross flow equations.

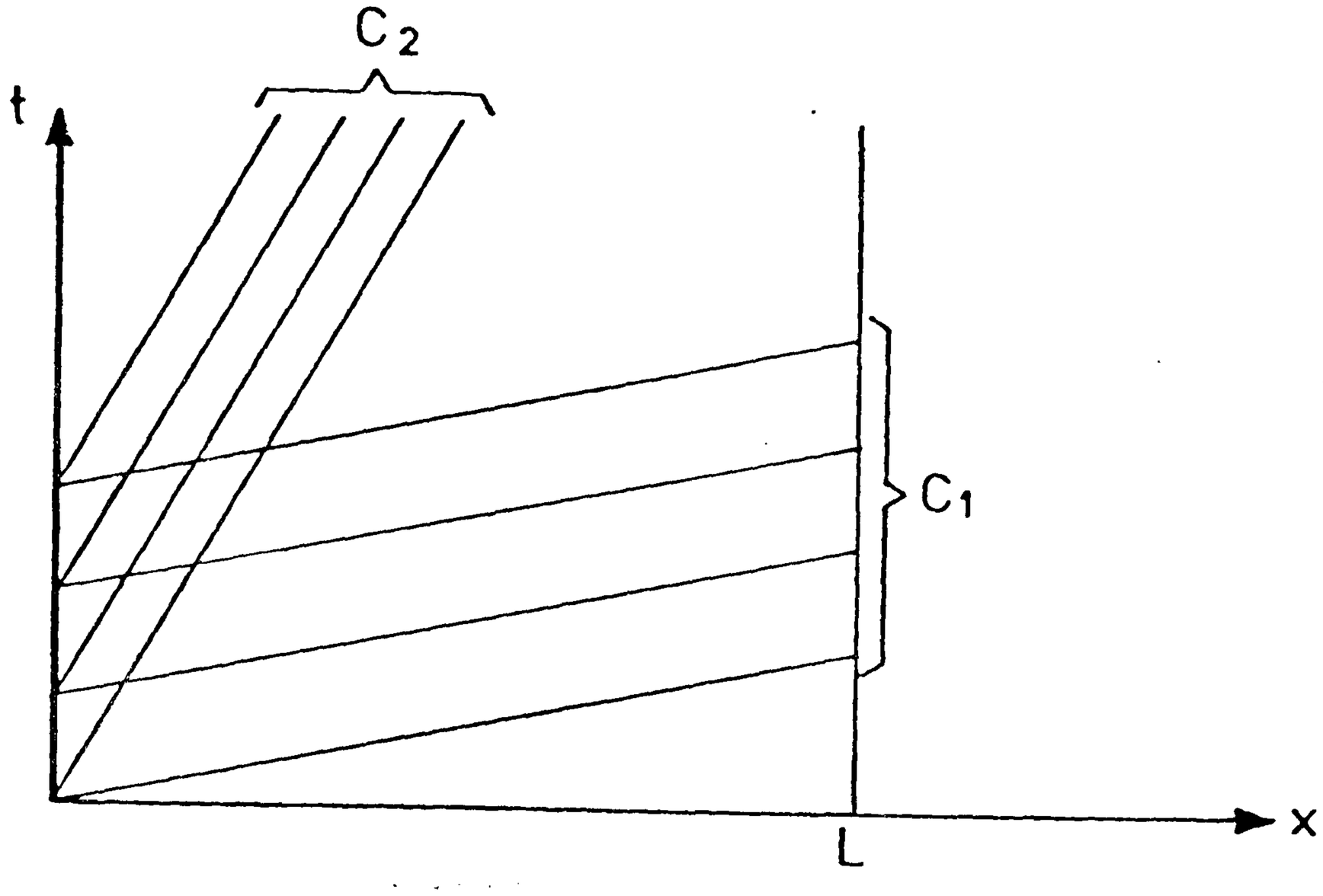

Figure 4. Families of characteristics for the concurrent flow equations.

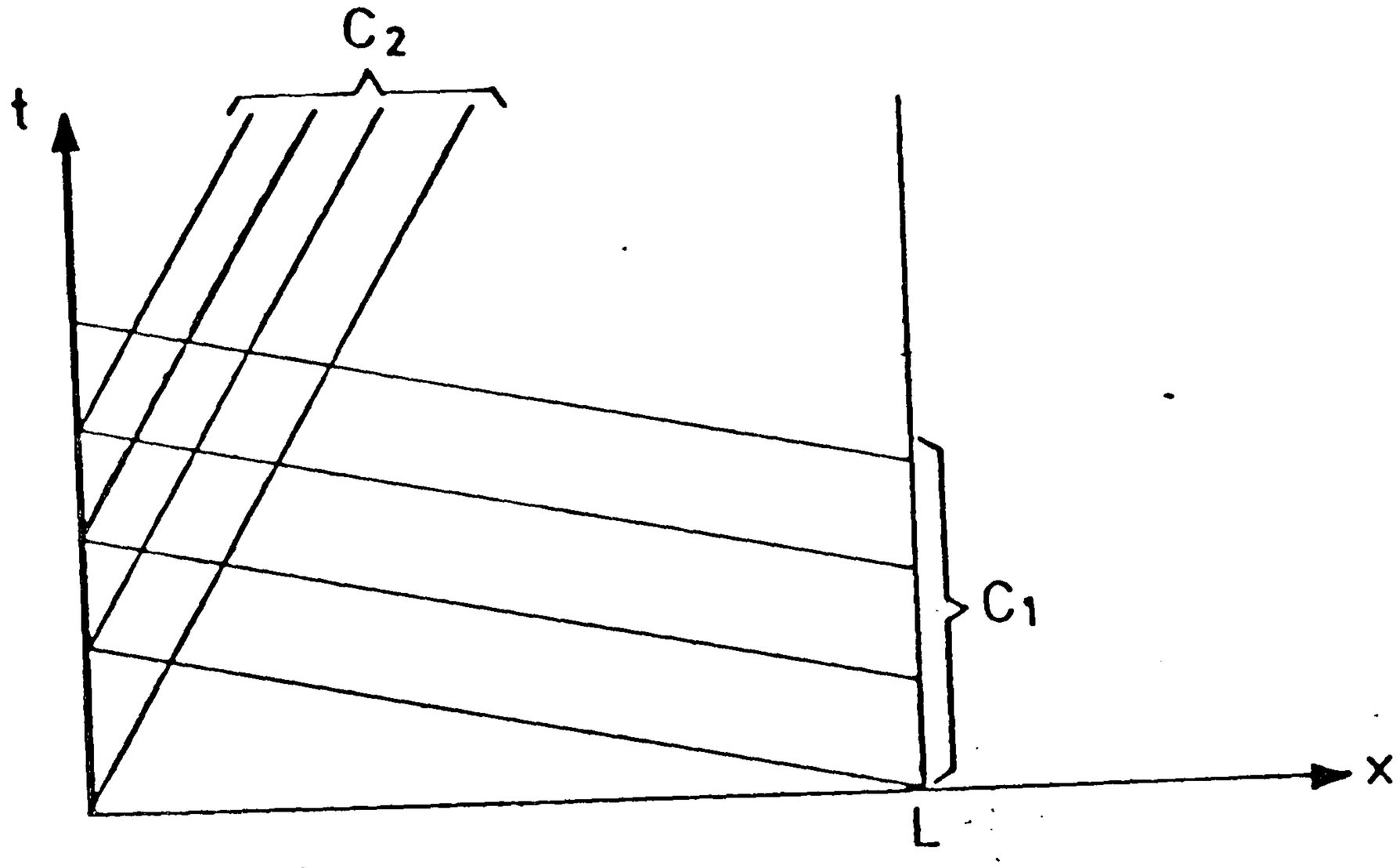

Figure 5. Families of characteristics for the counterflow equations.

From (1) and (2) it may be seen that there can be no jumps in the partial stresses t_1^1 and t_1^2. Thus it is again asserted that the partial stresses do not feature in the mathematical model, and that the jump conditions (1) to (4) reduce to

$$(U-V_a)[H] = 0, \quad (U-V_p)[M] = 0, \tag{5}$$

$$(U-V_a)\{c_a[T] + [H(e_v + c_v T)]\} = 0, \tag{6}$$

$$(U-V_p)\{c_p[\theta] + [M(e_w + c_w \theta)]\} = 0. \tag{7}$$

It is easily shown that jumps in H and T can only occur when $U = V_a$ and that jumps in M and θ can only occur when $U = V_p$. Thus there are two types of discontinuity. For a type 1 discontinuity H and T are discontinuous, while M and θ are continuous, and the path of the discontinuity in the (x,t) plane is along a C_1 characteristic. Similarly in a type 2 discontinuity M and θ are discontinuous while H and T are continuous, and the path of the discontinuity in the (x,t) plane is along a C_2 characteristic.

The significance of the jump conditions is now clear: any jump discontinuities which occur in the initial or boundary conditions will be propagated along the appropriate characteristic. In physical terms this is, perhaps, more easily appreciated by referring to Figure 4. Any discontinuity in the humidity (H) or temperature (T) of the incoming air is simply propagated through the bed with the speed of the air. Similarly, any discontinuity in the moisture content (M) or temperature (θ) of the incoming grain is carried through the bed with the speed of the grain. No further information is available from (5) to (7).

3.3 Constitutive Relations

A brief discussion of models for thin layer, or single kernel, drying was given in the Introduction. It was noted that such models are useful in providing estimates of the drying rate for use in deep bed models. These estimates are usually obtained with the aid of measurements of the average moisture content of a single (fixed) layer of grain at successive times during drying. In thin layer tests, the

drying air is normally at constant specific humidity and temperature. Henderson and Pabis (1962) observed from such tests that the speed of the drying air had no discernible effect on the rate of drying provided the airflow were turbulent. In this context turbulence amounts to saying that the air speed is greater than $10^{-1}ms^{-1}$. Clearly, in concurrent flow, for example, the magnitude of the relative speed $(V_a - V_p)$, rather than V_a, is the relevant variable. Usually V_p is much smaller than V_a and in most applications the airflow is turbulent. This leads one to the usual assumption that the drying rate is independent of V_a. This rate, and hence the function m, will therefore be assumed to depend on the four variables H, M, T and θ, and on various parameters of the particular type of grain being dried. These parameters may include representative dimensions defining the geometry of a typical grain kernel and values of the moisture and thermal diffusivities for such a kernel.

It was noted in the Introduction that, in view of their computational simplicity, empirical models such as those based on the Lewis type expression (1.2-1) are often preferred to the 'theoretical' diffusion equation models. Either type of model may be used to provide a constitutive relation for m. However, in the work of the following chapters, solely empirical models will be used for this purpose. In particular, for the work of the following chapters, it will be assumed that

$$\frac{dM}{dt} = -k(M - M_e). \qquad (1)$$

The e.m.c. M_e (the moisture content corresponding to vapour pressure equilibrium of the grain with the environment) is normally expressed as a non-linear function of the air temperature T and of the specific humidity H or the relative humidity $\phi = \phi(H,T)$. A number of different functional forms have been proposed to represent the e.m.c. data. Many early equations for M_e were based on theoretical or semi-theoretical considerations and a number of these were devised to account for the hysteresis effect observed between sorption and desorption data, see e.g. Young and Nelson (1967). More recently, empirical equations, which combine simplicity and flexibility, have been successfully used

for a number of crops. In particular Bakker-Arkema et al (1974) have given a spline fit to e.m.c. data for shelled corn. The drying rate coefficient k is determined either empirically or 'semi-theoretically'. In order, however, to appreciate the theoretical significance of k, it is necessary to elaborate on remarks made in the Introduction about diffusion equation models.

A general model for simultaneous heat and moisture transport in capillary-porous bodies was given by Luikov (1966). He considered the various fluxes, such as liquid and vapour transport due to capillary forces, both moisture and temperature concentration gradients, and total pressure differences within a four phase system consisting of air, vapour, liquid and solid. Using the basic laws of balance of mass and energy, he derived a system of equations of the form

$$\frac{\partial \underline{u}}{\partial t} = K\nabla^2 \underline{u} \quad , \tag{2}$$

where $\underline{u} = \underline{u}(x,t) = [\alpha, \Theta, P]^T$, and where α, Θ, and P represent the distributions of moisture content, temperature and total pressure within the body. In the 3×3 matrix $K = \{K_{ij}\}$, the elements of which depend on physical properties of the product such as diffusivity and thermal conductivity, the K_{ii}, $i = 1,2,3$ are phenomenological coefficients while the off-diagonal elements K_{ij}, $i \neq j$, represent coupling coefficients between the various transport mechanisms. Although equations of the form (2) have been shown to be widely applicable to biological products, they have not been used, in their most general form, to describe single kernel grain drying, since insufficient data is available for the estimation of all the coupling coefficients in the matrix K. However, under various simplifying assumptions, reduced versions of (2) have been adapted for the description of grain drying.

In the drying of cereal grains the temperatue attained by the grain is generally sufficiently low to regard the effects of a total pressure gradient as negligible (see Luikov (1966), p.243 for a discussion). Equations (2) then reduce to a two equation system involving only the grain moisture content and temperature distributions. The effects of temperature gradients on moisture diffusion only become

significant in conduction drying or where intensive heating methods, such as dielectric and microwave drying, are employed. This thermal diffusion is therefore usually assumed negligible in normal convective drying. If further, the effects of internal evaporation are assumed negligible, then (2) reduces to a system of the form

$$\frac{\partial \alpha}{\partial t} = D_m \nabla^2 \alpha \quad , \tag{3}$$

$$\frac{\partial \Theta}{\partial t} = D_t \nabla^2 \Theta \quad , \tag{4}$$

where D_m and D_t represent the mass and thermal diffusivities respectively. If D_m is assumed to depend on position in the grain, or on moisture content or temperature, then (3) may be replaced by

$$\frac{\partial \alpha}{\partial t} = \nabla.(D_m \nabla \alpha) \quad . \tag{5}$$

If the diffusivities are both assumed constant then (3) and (4) may be solved separately for α and Θ. The Lewis number, $Le = D_t/D_m$, representing the ratio of the relaxation rates of the mass to heat transfer potentials is of the order unity for air saturated with water vapour, whilst for air-dried solids Le is greater than unity. At high moisture contents Le is approximately constant whilst below the hygroscopic limit it increases with decreasing moisture content. For normally moist grain, however, Le is generally very much greater than unity and it is therefore usually assumed that the grain kernel attains a uniform temperature instantaneously. Such an assumption gives rise to a single diffusion equation model consisting of equation (3) or (5) together with appropriate initial and boundary (surface) conditions. Models of these forms have been used by several workers to obtain estimates of the moisture content profile and an 'average' moisture content throughout a single kernel for various types of cereal grain.

In order to obtain a solution to a diffusion equation model, an appropriate geometric shape is firstly assumed for the approximate representation of the individual grain kernel e.g. a sphere, cylinder or slab. The diffusion equation is then written in terms of the

appropriate coordinates e.g. spherical, cylindrical or rectangular. In some of these cases, series solutions such as those given by Crank (1975), may be used to provide estimates of the average moisture ratio, MR, where

$$MR(t) = \frac{(M - M_e)}{(M_o - M_e)} ,$$

and where $M = \bar{\alpha}(t)$ and the initial moisture content M_o, is assumed constant throughout the grain kernel. For example, if the kernel is assumed to be spherical, with D_m constant, then (3) may be written

$$\frac{\partial \alpha}{\partial t} = D_m\left(\frac{\partial^2 \alpha}{\partial r^2} + \frac{2}{r}\frac{\partial \alpha}{\partial r}\right) \qquad (6)$$

If further, constant initial and boundary conditions of the form

$$\left.\begin{aligned} &\alpha(r,o) = M_o, \quad |r| < a, \text{ where } a \text{ is the radius of the sphere} \\ &\alpha(a,t) = M_e, \quad t \geqq o, \end{aligned}\right\} \qquad (7)$$

are assumed, then, defining the average moisture content by

$$M(t) = \frac{1}{(\frac{4}{3}\pi a^3)} \int_o^a 4\pi r^2 \alpha(r,t)dt ,$$

the series solution

$$MR(t) = \sum_{n=1}^{\infty} \frac{6}{n^2\pi^2} \exp(-D_m n^2 \pi^2 t/a^2) \qquad (8)$$

may be easily obtained. For the more irregular geometries and in the nonlinear case (5). However, a numerical solution must generally be sought.

Now if k and M_e are assumed to be independent of time, then (1) may be integrated to give

$$MR = \exp(-kt). \qquad (9)$$

As a result of this expression, (1) is often referred to as the exponential (or logarithmic) drying law. In view of this single exponential solution, a number of workers have made use of series solutions, such as (8), to obtain estimates for the coefficient k in empirical drying rate expressions. Successive terms in such series converge rapidly for sufficiently large t. The first few terms dominate the series and subsequent terms may often be considered negligible, i.e. if $MR = \sum_{i=1}^{\infty} a_i \exp(-k_i t)$, then for t sufficiently large, a satisfactory approximation may be provided by taking $MR = \sum_{i=1}^{N} a_i \exp(-k_i t)$, for finite N. For example, Chen and Johnson (1969), assuming slab geometry in experiments on the drying of fish muscle, observed the maximum error in using only the first term in their series solution to be of the order of 10%. Nellist and O'Callaghan (1971) determined the coefficients of a two-term exponential fit of the form

$$M = M_e + A \exp(-k_1 t) + B \exp(-k_2 t)$$

to their experimental data on ryegrass seed. One term in this expression was taken to represent the effect of the first term in the series solution for sphere and the other to represent higher order terms in the series. In some of these truncated series expressions, the rate coefficients, k_i, and corresponding 'amplitudes', a_i, are determined by direct comparison with a series solution such as (8). In view, however, of the assumptions made concerning a typical kernel, it is generally necessary to use statistical techniques to determine some of the unknown coefficients in order to obtain a 'satisfactory fit'.

The above approach constitutes one means of estimating the drying rate coefficient k, which, however, requires the assumption of a particular goemetry for the grain kernel. Many workers make use of an Arrhenius relation of the form

$$k = a \exp(-b/T_{abs}) \quad , \qquad (10)$$

see e.g. Henderson and Pabis (1961), or a simple exponential relation of the form

$$k = c \exp(dT) \quad , \qquad (11)$$

see e.g. Simmonds et al (1953). Nellist (1976) investigated the dependence of k on himidity, H, and vapour pressure deficit, P_d, by fitting expressions of the form

$$k = a_1 \exp(b_1 T + c_1 H)$$

and

$$k = a_2 + b_2 P_d^{c_2}$$

to his data on ryegrass seed.

However, the drying rate is determined, since the moisture content, M, is measured on a bulk basis, i.e. per unit volume of mixture, the evaporation rate m, may be identified through

$$m = -\rho_p \frac{dM}{dt} \quad . \tag{12}$$

Hence from (1) one may obtain the constitutive relation

$$m = \rho_p k(M-M_e) \quad . \tag{13}$$

In view of the above discussion it is clear that m will, in general, depend on H, M and T. However, since diffusion theory provides the basis for (1), it is evident that k also depends on the grain temperature, θ. Further, in view of the way that most empirical drying rate expressions are presented, it will be assumed for simplicity that m is solely a function of the four primary variables, H, M, T and θ.

The question of the constitutive relation for ψ is now considered. In the foregoing discussion on diffusion equation models, it was pointed out that, in normal convective grain drying, the transport of heat within an individual kernel is very fast as compared with that of moisture. For this reason, it is assumed that instantaneous thermal equilibrium is attained throughout the kernel and that the difference in temperature, between the grain and the drying air at a point, is the potential for sensible heat transfer between the two constituents at that point in the mixture. In addition to this transfer, there will be heat exchanged in the water evaporated or vapour condensed, which in view of (13), is governed by the potential differences in moisture

contents of air and grain, $M - M_e$. Various constitutive relations have been implicitly assumed for the net energy transfer, ψ, in the literature. However, it would appear that a suitable assumption, embracing a number of these relations is to take

$$\psi = h(T - \theta) - m\, E_v(\theta_v) \quad , \tag{14}$$

where h is a volumetric heat transfer coefficient. The second term on the right hand side of (14) accounts for the internal energy of the liberated water vapour at some mean evaporation temperature θ_v with $\theta \leqq \theta_v \leqq T$. Most models implicitly assume that $\theta_v = T$, although in the model of Ingram (1976a) the assumption $\theta_v = \theta$ appears to have been made. In effect either choice amounts to making a constitutive assumption for θ_v. In practice, equilibration of temperatures is usually sufficiently fast for such a choice to make little difference to overall simulations. For a more detailed treatment of this question, however, see chapter 4.

From a more general point of view, there is no reason for θ_v not to be given a general constitutive relation but this possibility is not considered further here.

There is a substantial literature on the heat transfer coefficient h, see e.g. Gamson et al (1943). A number of expressions have been suggested for h in terms of appropriate dimensionless quantities such as the particle Reynolds number. However, as for the drying rate coefficient k, empirical expressions have also been given for a number of different cereal grains. In particular, Boyce (1966) obtained an expression of the form

$$h = a \left\{ \frac{\varepsilon \rho_a V_a (T + b)}{P_{atmos}} \right\}^c \quad , \tag{15}$$

where a, b and c are constants and P_{atmos} is the atmospheric pressure. This form for h has been used successfully in a number of simulations at both the NIAE and the SIAE and is therefore adopted for the present work.

Referring to the comment following equation (2.2-14), it is noted

that when (14) is substituted into the energy equations (2.2-13), it is noted that when (14) is substituted into the energy equations (2.2-13) and (2.2-14), it is easy to see that the resulting energy equations are independent of the base energies e_v and e_w (see (3.5-1) and (3.5-2)). The constitutive relations (13) and (14), together with the related assumptions, indicate that m and ψ are functions of H, M, T and θ. It may be recalled that the anlaytical work in section 3.1 was based on this premiss.

3.4 An Equilibrium Model

Partial differential equation models of the form (3.1-1) may be used to simulate the mass and heat transfer processes in low temperature, low airflow rate, fixed bed applications. However, in view of the near equilibrium conditions in such applications, some simplifications may be made to these models with a consequent reduction in complexity and hence in the computational effort required for their solution. Some of the earlier models, for example those of logarithmic type, mentioned in the Introduction, which were derived under simplifying assumptions, have been found suitable for these applications. However, one may deduce an 'equilibrium' model from the fixed bed equations (3.1-1) under the appropriate assumptions.

For instantaneous thermal and moisture equilibrium between the moist air and the moist grain at each point in the bed over the duration of drying, it must be assumed that there is no resistance to heat and mass transfer within the air-grain system. Such an assumption implies infinite heat and mass transfer rate coefficients, h and k respectively. Thus, if for example m and ψ are given by constitutive equations of the form (3.3-13) and (3.3-14) respectively, then the following relationships must hold

$$T(x,t) = \theta(x,t) \quad \text{and} \quad M(x,t) = M_e(x,t). \quad (1)$$

Now in view of the relation (3.3-12), together with the assumption that the e.m.c. is solely a function of the air humidity and temperature, i.e. $M_e = M_e(H,T)$, it follows that

$$m = - \rho_p \left(\frac{\partial M}{\partial H}^e \cdot \frac{\partial H}{\partial t} + \frac{\partial M}{\partial T}^e \cdot \frac{\partial T}{\partial t} \right) .$$

Then substituting this expression and (1) into the system (3.1-1) and re-arranging one may obtain a system of two partial differential equations of the form

$$A \frac{\partial \underline{u}}{\partial t} + B \frac{\partial \underline{u}}{\partial x} = \underline{0} \quad , \tag{2}$$

where $\underline{u} = [H,T]^T$ and the matrices A and B are given by

$$\left. \begin{aligned} A = & \begin{bmatrix} \varepsilon\rho_a + \rho_p \frac{\partial M}{\partial H}^e & \rho_p \frac{\partial M}{\partial T}^e \\ \rho_p \gamma \frac{\partial M}{\partial H}^e & \varepsilon\rho_a c_1 + \rho_p (c_2 + \gamma \frac{\partial M}{\partial T}^e) \end{bmatrix} \\ \text{and} \quad B = & \begin{bmatrix} \varepsilon\rho_a V_a & 0 \\ 0 & \varepsilon\rho_a V_a c_1 \end{bmatrix} , \end{aligned} \right\} \tag{3}$$

where

$$\left. \begin{aligned} \gamma &= c_w \theta - c_v T - h_{fg} , \\ c_1 &= c_a + c_v H \quad \text{and} \quad c_2 = c_p + c_w M . \end{aligned} \right\} \tag{4}$$

Now (2) is a reducible system of homogeneous, linear, first-order partial differential equations. It may be easily shown that characteristic directions for this system are given by

$$\left(\frac{dx}{dt} \right)^{-1} = V_a^{-1} + \frac{\omega}{2} \left\{ (\lambda + \sigma - \eta\psi) \pm \sqrt{[(\sigma - \lambda - \eta\psi)^2 - 4\eta\lambda\psi]} \right\} , \tag{5}$$

where

$$\left. \begin{aligned} \lambda &= \frac{\partial M}{\partial H}^e , \quad \psi = \frac{\partial M}{\partial T}^e , \quad \omega = \frac{\rho_p}{\varepsilon\rho_a V_a} , \\ \sigma &= \frac{c_2}{c_1} \quad \text{and} \quad \eta = \frac{-\gamma}{c_1} . \end{aligned} \right\} \tag{6}$$

Assuming average values for h_{fg}, c_w and c_v (see e.g. Parry (1983b), sections 2.3, 2.4), and that T and θ are measured in °C, it may be shown that $\gamma < 0$ provided that the condition $\theta < 0.45\,T + 597.5$ is approximately satisfied. This condition is always satisfied in practice. Further, from (6) and the definition of M_e, it may be seen that $\lambda > 0$ and $\psi < 0$. Therefore the product $\eta\lambda\psi$ is negative and hence the discriminant in (5) is positive. The characteristics defined by (5) are then two real and distinct families of curves in the x-t plane. It may be shown that the characteristic form of (2) along these directions may be written in the form

$$\frac{dH}{dT} = \frac{1}{2}\{(\sigma - \lambda - \eta\psi) \pm \sqrt{[(\sigma - \lambda - \eta\psi)^2 - 4\eta\lambda\psi]}\} \quad . \qquad (7)$$

It may also be shown that $\frac{dx}{dt} > 0$, always, and the theory of simple waves, as outlined in Courant and Friedrichs (1952), may be used to facilitate the sketching of the characteristics. Jump conditions, analogous to those given in section 3.2, may be used to define the relationship between the state variables, H and T, across the 'shock fronts' which occur in this case, and to determine the velocities of the fronts as they travel through the air-grain mixture. A number of authors have presented analyses of exchange processes under such equilibrium conditions. The basic theory is given by Amundson et al (1965). Nordon and Bainbridge (1972) examined such processes in wool beds, Sutherland et al (1971), used the theory to predict 'heating' and 'drying' front velocities in deep beds of grain, and, more recently, Ingram (1979) compared the results obtained using this theory with those from a detailed simulation for some grain cooling and drying problems.

3.5 Comparison with Other Models

Firstly, it is reiterated that the approach adopted in Chapters 2 and 3 constitutes a more general development of grain drying models than any in the available literature. Most published models of 'partial differential equation' type are formulated for fixed bed driers. For this reason the comments in this section refer to differences between such models and the general fixed bed model (3.1-1), unless

otherwise stated. Furthermore, the models referred to are those which may be written as a system of four partial differential equations in a one-to-one correspondence with those of(3.1-1), i.e. effectively two mass balance and two energy balance equations. This point is made since several of the models, see e.g. Bakker-Arkema et al (1974), consist of only three partial differential equations, one of which is a linear combination of the two mass balance equations, together with an appropriate drying rate equation, generally of the form (3.3-1) or similar, and two energy balance equations.

Most authors, with the exception of Van Arsdel (1955), neglect terms involving the time derivatives of the air properties, i.e. $\frac{\partial H}{\partial t}$ and $\frac{\partial T}{\partial t}$. In some cases these terms do not appear in the derivation of the model, see e.g. Klapp (1963). In others they may appear but are subsequently neglected. For example, Spencer (1969a) calculated that, for drying air at about 93°C, these terms are of the order of 2% of the corresponding space derivatives in magnitude. This observation does not, however, appear to be based on a non-dimensional analysis and its range of validity clearly depends on the length and time scales of the problem. The main reason for neglecting these terms appears to lie in the simplification of the model equations. The resulting system is then effectively treated as two coupled systems of ordinary differential equations in the directions of the two coordinate axes. As demonstrated in section 3.1, however, in view of the hyperbolic nature of the four equation system, such a simplification may be brought about without this neglect if the resulting equations are solved along the appropriate characteristic directions.

In practice, the model equations are usually written in terms of the mass flow rates, G_a and G_p, of the air and grain product respectively, through unit area of the drier, rather than in terms of their velocities. Now since, in the derivation of the general system (2.2-15), it was assumed that the grain density, ρ_p, is measured on a bulk basis, i.e. mass of grain per unit volume of the drier including any interstitial air, the relationship $G_p = \rho_p V_p$ is satisfied. The air density, ρ_a, is assumed to be measured in the usual sense and hence for the interstitial air the relationship $G_a = \varepsilon \rho_a V_a$ holds. However, the measured value for the air velocity, $\bigcup_a$, say, appearing

in some models, see e.g. Spencer (1969), is related to the mass flow rate through the relationship $G_a = \rho_a \mathcal{U}_a$, hence $\mathcal{U}_a = \varepsilon V_a$. Actually $\mathcal{U}_a$ represents the velocity assuming that the air occupies the whole of that part of the drier under consideration and is clearly smaller than V_a. In view, however, of the usual neglect of the time derivative terms, the difference between these two velocities is not always apparent since they need not appear explicitly in the equations.

The following discussion refers to the right hand side vector, $\underline{b}$, of the general system, given in section 2.2. The interaction force term, $\underline{\phi}.(\underline{v}^2 - \underline{v}^1)$, appearing in (2.2-11), is not present in any of the published models. In view, however, of the numerical evidence presented in Chapter 4, such an omission may be of limited significance in simulations.

The terms $-mE_v(T)$ and $mE_w(\theta)$, on the right hand sides of the energy balance equations for moist air and moist grain respectively, are due to the effects of differential changes in humidity and moisture content respectively on the internal energies of the moist air and moist grain. In view of their mode of derivation, none of the published models contain these terms explicitly. Further, in view of certain implicit assumptions, it is generally difficult to effect a direct comparison between models in respect of such terms. It is certainly apparent that most models do not take these terms fully into account. For example, Van Arsdel (1955) appears to have assumed that the 'humid heat capacities', c_1 and c_2 (defined in (3.4-4)), of moist air and moist grain respectively, are constant, for the purpose of deriving his equations. It would also appear that he made the implicit assumption that the mean evaporation temperature is given by $\theta_v = T$. In order, however, to facilitate a comparison of the various models, it is noted that (2.2-15) together with (3.3-14) yield, for the right hand sides of the energy balance equations for air and grain respectively

$$b_3 = [-h(T - \theta) + mc_v(\theta_v - T)]/[\varepsilon\rho_a(c_a + c_v H)] \qquad (1)$$

and

$$b_4 = [h(T - \theta) + m(c_w\theta - c_v\theta_v - h_{fg})]/[\rho_p(c_p + c_w M)] \qquad (2)$$

This form is consistent with most of the published models, the only remaining generality being the unspecified temperature θ_v.

If θ_v is taken to be the temperature, T, of the drying air, then the numerator of (1) reduces to $-h(T - \theta)$. The corresponding term in the models of Van Arsdel, Klapp, Spencer and Bakker-Arkema et al, is of this form. However, taking $\theta_v = T$ in (2) gives the numerator

$$h(T - \theta) + m(c_w\theta - c_vT - h_{fg}),$$

whereas in the first three models cited this term is effectively given as $h(T - \theta) - mh_{fg}$ and in the model of Bakker-Arkema et al as $h(T - \theta) + m(h_{fg} + c_v(T - \theta))$. Now under the constitutive assumptions (2.2-7) and (2.2-8), i.e. that the constituent energies depend linearly on temperature, it follows that the latent heat of vaporization, $h_{fg} = h_{fg}(0)$, may be written in the alternative forms

$$h_{fg} = h_{fg}(\theta) - (c_v - c_w)\theta = h_{fg}(T) - (c_v - c_w)T. \qquad (3)$$

Substituting the first expression in (3) into (2) with $\theta_v = T$ yields the term $h(T - \theta) - m(h_{fg}(\theta) + c_v(T - \theta))$. This would appear to suggest an incorrect sign in the model of Bakker-Arkema et al. This apparent error occurs in both the fixed bed and steady-state crossflow models of these authors, rendering their energy balance equations thermodynamically inconsistent. Their models for the steady state concurrent flow and steady state counterflow cases appear to be consistent, however, provided that the datum for h_{fg} is considered unimportant. In view of the second expression in (3), it may easily be seen that, for thermodynamic consistency, the other three models require the addition of a 'sensible heating' term of the form $-mc_w(T - \theta)$.

If, on the other hand, θ_v is taken to be the grain temperature, θ, then the numerators of (1) and (2) become

$$-(h + mc_v)(T - \theta)$$

and

$$h(T - \theta) - m(h_{fg} - (c_w - c_v)\theta)$$

respectively. These terms are of the same form as those in the corresponding equations given in a report by Ingram (1976a). His equations are therefore thermodynamically consistent. However, in a paper based on this report, Ingram (1976b) presented an energy balance equation for the the grain in which the numerator appears simply as $h(T - \theta)-mh_{fg}$, neglecting the 'sensible heating' term $m(c_w - c_v)\theta$ and rendering his new equations inconsistent.

Constitutive assumptions for m and h have been considered in section 3.3. The basic structure of the four equation system is not affected by any differences in these assumptions. Furthermore, as must be apparent from the discussion, several models exist to provide the constitutive equations, the choice of which must, to some extent, depend upon the individual crop to be dried.

Clearly, in the case of equilibrium exchange, there is no requirement to provide constitutive equations for the heat and mass transfer coefficients, h and k respectively. It is of course still necessary to prescribe some appropriate functional dependence on M_e on the air properties, H and T. The equilibrium model obtained by Ingran (1979) from his fixed bed model (Ingram (1976b)) is basically of the form (3.4-2). In view, however, of the various differences between his basic fixed bed model and that defined by (3.1-1) together with (2.2-17), there are corresponding differences between his equilibrium model and that presented in section 3.4. In particular, in view of his neglect of sensible heating terms, his expression for γ, corresponding to (3.4-4), is simply $\gamma = -h_{fg}$. Also, in view of his neglect of the terms in $\frac{\partial H}{\partial t}$ and $\frac{\partial T}{\partial t}$, his expression for the characteristic directions, corresponding to (3.4-5), does not contain the term V_a^{-1}. It must be added that in practice these omissions may only be of minor significance, particularly in view of the other assumptions made for such a model. Section 3.4 is included for completeness, as are the comments in this paragraph. Since, however, the present work is mainly concerned with the detailed simulation of more general drying processes, the equilibrium case will not be discussed any further in subsequent chapters.

CHAPTER FOUR: STEADY STATE CONCURRENT FLOW DRIER SIMULATION

Equations representing simultaneous heat and mass transfer in concurrent flow grain drying were presented in section 3.1(c). In particular, it was shown, subject to the given assumptions, that 'steady state' drying could be modelled by a system comprising the three ordinary differential equations (3.1-22) together with the single linear algebraic equation (3.1-23). In view of the nonlinear right-hand sides of these equations, it is not possible, in general, to obtain an analytical solution. In section 4.1, however, the results of a semi-analytical investigation of the steady state equations are summarised. Although it is concluded that such an approach does not lead directly to a practicable means of solving the equations, some useful information on the behaviour of the solution is thereby obtained.

In section 4.2 some of the problems of choosing a suitable technique for the 'purely' numerical solution of the steady state equations are discussed. An algorithm devised specifically for this purpose, and based on a numerical integration technique employing polynomial extrapolation of a 'modified' midpoint method, is then described. With the aid of a (FORTRAN) computer implementation of this algorithm, several test cases were 'run' to validate the model (together with the algorithm). Two such validation cases are presented and discussed in section 4.3. The results of these simulations indicate the need for further work on the constitutive equations used in the model.

In section 4.4 the first validation case is used as the basis for a study of various factors affecting the 'performance' of the algorithm. These include the 'user-prescribed' level of accuracy to which the solution is obtained and the sensitivity of the results to perturbations in the inlet conditions. Finally, in section 4.5, the relative contributions of the various energy transfer terms occurring on the right-hand sides of the steady state equations (3.1-22), and their effects on the solution, are considered.

4.1 A Linearised Model

4.1.1 The Linearised Equations

The algebraic relation (3.1-23) may be used, for example, to express the specific humidity, $H(x)$, in terms of the moisture content, $M(x)$, through

$$H(x) = H(0) - \frac{p}{G_a}\,(M(x) - M(0)) \qquad (1).$$

Now substituting (1) into the nonlinear right-hand sides b_2, b_3 and b_4, given by (2.2-17), the system of ordinary differential equations (3.1-22) may be written in the form

$$\left.\begin{aligned} &\frac{d\underline{u}}{dx} = \underline{f}(\underline{u}), \quad \text{for } x > 0, \\ &\text{subject to initial conditions of the form} \\ &\underline{u}(0) = \underline{u}_o \end{aligned}\right\} \qquad (2).$$

In (2), $\underline{u} = \{u_i\} = [M, T, \theta]^T$ only and the initial condition $H(0)$ may simply be regarded as a parameter of the problem.

If now $\underline{f}(\underline{u})$ is assumed to possess continuous first derivatives with respect to each of the variables u_i, $i=1,2,3$, then (2) may be expanded by Taylor series about $\underline{u} = \underline{u}_o$ to yield

$$\frac{d\underline{u}(x)}{dx} = \underline{f}(\underline{u}_o) + J(\underline{u}_o)(\underline{u}(x) - \underline{u}_o) + \underline{R}(\underline{u}(x), \underline{u}_o) \qquad (3).$$

In (3) $J(\underline{u}_o)$ is the Jacobian matrix of $\underline{f}(\underline{u})$ evaluated at $\underline{u} = \underline{u}_o$ i.e. the 3×3 matrix with elements

$$J_{ij} = \left(\frac{\partial f_i}{\partial u_j}\right)\Bigg|_{\underline{u} = \underline{u}_o}.$$

The remainder term $\underline{R}$ is such that

$$\left\|\underline{R}(\underline{u}(x), \underline{u}_o)\right\|_\infty = 0\left\|\underline{u}(x) - \underline{u}_o\right\|_\infty \text{ as } \left\|\underline{u} - \underline{u}_o\right\|_\infty \to 0^*.$$

*Here the order symbol 0 is taken to have the following meaning: $\|\phi\|_\infty = 0\|\mu\|_\infty$ as $\|\mu\|_\infty \to 0$ means a scalar function $\phi(\mu)$ such that $\lim_{\mu\to 0}(\phi(\mu)/\mu) = 0$.

If then the variation of $\underline{u}(x)$ over the interval $(x_o, x]$ is 'sufficiently small', (3) may be approximately represented over this range by the 'quasi-linearised' form

$$\frac{d\underline{u}(x)}{dx} = \underline{f}(\underline{u}_o) + J(\underline{u}_o)(\underline{u}(x) - \underline{u}_o) \qquad (4).$$

Now (4) is a system of three linear ordinary differential equations with constant coefficients. The theory for such equations is well established (see e.g. Leighton (1976)), and, provided that the elements of $J(\underline{u}_o)$ are known, it is possible, at least in theory, to obtain an analytical solution to this sytem. This solution may be written in the 'spectral' form

$$\underline{u}(x) = \underline{u}_o + \sum_{i=1}^{3} \alpha_i \underline{v}_i \exp\{\lambda_i(x - x_o)\} - [J(\underline{u}_o)]^{-1} \underline{f}(\underline{u}_o) \qquad (5),$$

where $(\lambda_i, \underline{v}_i)$, i=1,2,3 are the eigenpairs of the matrix $J(\underline{u}_o)$. Equations (5) together with the initial conditions given in (2) then yield the 3 × 3 system of linear equations

$$\sum_{i=1}^{3} \alpha_i \underline{v}_i = [J(\underline{u}_o)]^{-1} \underline{f}(\underline{u}_o) \qquad (6),$$

which may be solved for the constant coefficients α_i, i=1,2,3, provided of course, that the coefficient matrix $[\underline{v}_1, \underline{v}_2, \underline{v}_3]$ is non-singular.

4.1.2 Some Observations

Clearly (5) only provides a valid approximation to the solution of (2) within a sufficiently small neighbourhood of the point $x = x_o$. Equations (5) and (6) may, however, be applied over successive intervals, say $(x_i, x_{i+1}]$, i=0,1,..., the initial condition for each application being taken as $\underline{U}(x_i)$, i=0,1,..., where $\underline{U}(x)$ represents the approximation to $\underline{u}(x)$. The size of each interval (x_i, x_{i+1}) in such a scheme could, for example, be determined by some measure of the variation in the propagated solution.

The attainable accuracy in using the scheme described above obviously depends upon the behaviour of $J(\underline{U}(x_i))$ and its eigenpairs,

since these are assumed constant over each interval. Therefore, a preliminary investigation of this behaviour was conducted before attempting to compute a solution to the linearised system (4).

Assuming constitutive equations of the form given in appendix A, the elements of the Jacobian matrix J may be shown to be of the form given in appendix B. These (partial derivative) elements may be shown to be well-defined for the range of dependent variables i.e. temperatures and moisture contents, encountered in most problems of interest. In view, however, of the constitutive equations used for the equilibrium moisture content, M_e, the relative humidity, $\emptyset$ must be assumed to satisfy the condition $\emptyset < 1.0$ i.e. the air must never reach 100% saturation.

In order to obtain some idea of the behaviour of J and its eigenpairs, the NAG library routine D02QBF (NAGFLIB:1640/0:MK7:Dec.78) was firstly used to obtain a numerical solution to the system comprising (1) and (2) at a discrete number of intervals over the depth of the grain bed, for a variety of cases i.e. different inlet conditions and bed depths. This NAG routine, based on an algorithm due to Gear (1971a,b), contains a facility for the automatic choice of step-size and order of method as well as an option for stiff systems. The routine was incorporated into a FORTRAN program which was run for a number of prescribed levels of accuracy and with various criteria i.e. absolute, relative and mixed error tests. The results were found to be consistent and not too sensitive to small changes in inlet conditions.

The numerical values $\underline{U}(x_i)$, $i=1,2,\ldots,N$, say, where $x_i = iL/N$ and L is the bed depth, obtained as described above, were then used for the following:

(a) To obtain approximate values for $\underline{f}(\underline{U}(x))$, the elements of $J(\underline{U}(x))$, and the eigenpairs $(\lambda_i(x), \underline{v}_i(x))$, at the points $x = x_i$, $i=0,1,\ldots,N$.

(b) To produce plots of the state variables H, M, T and θ, together with various functions of interest, against bed depth x.

The elements of J were obtained using expressions of the form given in Appendix B and the corresponding eigenpairs were obtained using the NAG library routine F02AGA/F.

The results of the computations described above are not presented in detail in this work. However, the results of one such investigation, the initial conditions for which are given near the end of this section, are summarised in Tables 1a,b. Figures 6a-e illustrate the behaviour of the solution for this case. With regard to the results obtained overall, the following general observations were made:

(i) The grain moisture content, M, and air temperature, T, are strictly decreasing functions of the distance, x, from the air inlet point, x=0. Both functions drop very steeply at first over a short initial period and then 'flatten out' very rapidly. The air humidity, H, exhibits the opposite behaviour. The grain temperature, θ, however, increases steeply at first, flattening out rapidly and subsequently diminishes, converging towards the air temperature from below. The grain, therefore, attains a maximum temperature, θ_{max}, say, soon after the start of drying. An examination of the elements of $\underline{f}(\underline{U})$ (see e.g. Table 1b) indicates the nearly equal gradients of air and grain temperatures as drying progresses.

(ii) Over the initial period of rapid change in both temperatures and moisture contents of air and grain, the elements of the Jacobian matrix, J change rapidly with x.

(iii) An examination of the eigenpairs of $J(\underline{U})$ led to the observation that the range $0 \leqq x \leqq L$ could be divided, albeit artificially, into three distinct intervals, according to the nature of the eigenvalue spectrum in each interval. (see Figure 6a).

In the first interval, I_1, defined by $0 \leqq x < x_1$, say, the eigenvalue spectrum comprises a complex conjugate pair of roots with large negative real parts, together with a single positive real root of much smaller magnitude.

In the second interval, I_2, defined by $x_1 \leqq x < x_2$, say, the complex pair separate into two distinct real negative roots, one of increasing magnitude and the other of decreasing magnitude, as x increases, whilst the positive real root remains positive but also decreases in magnitude with increasing x. In order of decreasing magnitude, these

distinct real roots will be denoted by λ_1, λ_2, and λ_3

In the third interval, I_3, defined by $x_2 \leqq x \leqq L$, the root λ_1 continues to increase negatively and λ_2 to decrease negatively, whilst λ_3 also becomes negative and real, decreasing negatively with increasing x (although in some cases this root was observed to oscillate in sign within a very small neighbourhood of zero).

Now the solution (5) to the linearised form (4) may be re-written in the form

$$\underline{u}(x) = \tilde{\underline{u}}(x) + \sum_{i=1}^{3} c_i \, \underline{v}_i \, \exp(\lambda_i \, x) \qquad (7).$$

The term $\tilde{\underline{u}}(x)$ in (7) represents the contribution of the 'steady-state'* part of the solution and the eigensolutions, $\exp(\lambda_i \, x)$ characterise the local response of the system to small perturbations about $\tilde{\underline{u}}(x)$. Now if the real parts of all the eigenvalues are negative i.e. $Re(\lambda_i) < 0$, for $i=1,2,3$, then as x increases this 'transient' part of the solution decays and the system is said to be locally stable. Now the assumptions made concerning the remainder term R in (3) imply 'near-linearity' of the non-linear system (2) over suitably small intervals. It may be shown (see e.g. Jordan and Smith (1979)) that such a system is stable if the corresponding linearised system is stable. From the observations noted in (iii) above, it may therefore be seen that the steady state equations for concurrent flow grain drying, (2), are, at best, locally stable only over the interval I_3 defined in (iii). It must of course be stressed that the above comments are made on the basis of a limited range of test cases.

An initial value problem of the form (2) is said to be stiff in some interval $a \leqq x \leqq b$ if, over this interval,

(a) $Re(\lambda_i) < 0$, for $i=1,2,3$

and

(b) $S(x) = \max Re(-\lambda_i)/\min Re(-\lambda_i) >> 0.$

* Not to be confused with the generally adopted meaning of the term throughout this work i.e. time-invariance.

The stiffness ratio S(x) may be equivalently defined in terms of the 'time constants', tc_i, of the system, given by $tc_i = 1/Re(-\lambda_i)$, as

$$S(x) = \max tc_i / \min tc_i \qquad (8).$$

The above definition of stiffness is that used by Lambert (1973) and it is noted that other definitions appear in the literature. In view of (8), the stiffness ratio may be seen to be the ratio of the numerically largest to the numerically smallest time constants and so represents a measure of the spread of decay rates of the exponential 'components' in the solution.

Lambert refers to problems with a stiffness ratio $0(10)$ as marginally stiff whilst he notes that it is not uncommon, in fields such as chemical kinetics, process control and electrical circuit theory, to find systems with stiffness ratios $0(10^6)$. Over the range of drying problems investigated, stiffness ratios $0(10^5)$ were found, using the above definition, indicating a high degree of stiffness in the steady state concurrent flow drying equations.

4.1.3 Solution of the Model

A computer program was written to facilitate propagation of the solution (5) of the linearised approximation (4) to the concurrent flow equations (1) and (2). The program incorporated the NAG library routine FO2AGA/F for computation of the eigenpairs of J. The constants α_i, i=1,2,3, were computed by simple elimination. All computations were carried out in double precision arithmetic. Whilst the results of the computations carried out for a variety of test cases, are not presented in detail here, some results corresponding to the case presented in Table 1 are given in Table 2. For this case, the initial (inlet) conditions were as follows

for the grain: $M(0) = 25.00$ % d.b. , $\theta(0) = 15°C$

$G_p = 6.7$ kg./m²/min.

for the air : $H(0) = 0.006$, $T(0) = 150°C$

$G_a = 18.0$ kg./m²/min.

the residence time of the grain was approximately 38.6 minutes.

Firstly, the NAG routine D02QBF was used to obtain values of the solution, to approximately five significant figure (local) accuracy, at equal intervals throughout the bed (see e.g. Table 1a). Then, taking the initial conditions to be the approximate computed values at the first output point (e.g. $x = 0.01$ for the results given in Table 2), the linear approximation (5) was obtained at successive equidistant points in the bed. In Table 2, the figures in parentheses give a measure of the % error relative to the absolute change in the solution over the previous step

i.e.
$$\text{ERROR}(u(x_i)) = \left| \frac{u_i^{NAG} - u_i^{linear}}{u_i^{NAG} - u_{i-1}^{NAG}} \right| \times 100, \quad i=1,\ldots,$$

with the obvious notation.

The results presented in Table 2 are characteristic of those obtained overall. Implementation of the technique described above was hampered by a number of problems. Most of these appeared to be conditioning problems connected with the various matrix operations involved. In particular, it is felt that the near linear dependence of air and grain temperatures in the region I_3 (see Figure 6a) was, in part, responsible for ill-conditioning of the coefficient matrix in (6). Attempts made at 'equilibrating' the matrices were only partially successful.

It may be seen from Table 2 that the errors, as defined above, are unacceptably large and increasing with x. In view of the conditioning problems mentioned above, computations could not be carried out for $x > 0.04$, approximately.

	GRAIN		AIR	
X	M.C.%	TEMP.	TEMP.	SP.HUM.
0.000	25.00	15.000	150.000	0.0060
0.020	21.72	58.197	84.347	0.0182
0.040	20.94	65.425	72.184	0.0210
0.060	20.41	64.818	68.170	0.0230
0.080	19.96	63.182	65.703	0.0247
0.100	19.58	61.569	63.720	0.0261
0.120	19.24	60.109	62.004	0.0273
0.140	18.94	58.800	60.491	0.0284
0.160	18.67	57.621	59.141	0.0294
0.180	18.43	56.555	57.930	0.0303
0.200	18.22	55.587	56.836	0.0311
0.220	18.02	54.705	55.844	0.0319
0.240	17.84	53.898	54.940	0.0325
0.260	17.68	53.159	54.115	0.0331
0.280	17.53	52.479	53.358	0.0337
0.300	17.39	51.854	52.664	0.0342
0.320	17.26	51.278	52.025	0.0347
0.340	17.15	50.746	51.436	0.0351
0.360	17.04	50.254	50.893	0.0355
0.380	16.94	49.799	50.391	0.0359
0.400	16.85	49.379	49.926	0.0362

Table 1a. Results of a concurrent flow simulation using NAG library subroutine D02QBF. (Temperatures given in °C)

x	f	J			Re(λ)	Im(λ)	Re($\underline{v}^T$)	Im($\underline{v}^T$)
0.0	-5	-23	-.153	0	6.8	-	(-.0040, .746, .666)	-
	-7340	-7203	-78	54	-81	75	(0.0007, .027, .840	(-.0005, -.542, 0)
	2187	-28429	-90	-54	-81	-75	(0.0007, .027, .840)	(0.0005, 0.542, 0)
0.1	-.2	-1.9	-.010	0	-.019	-	(-.0034, .708, .706)	-
	-92	-63	-43	43	-6.4	-	(0.0015, .759, .651)	-
	-77	-1954	47	-57	-95.3	-	(-.0001, -.63, .776)	-
0.2	-.1	-1.6	-.006	0	-.011	-	(-.0030, .708, .707)	-
	-52	-35	-42	42	-4.8	-	(0.0015, .747, .664)	-
	-46	-1708	51	-58	-96.5	-	(.0000, -.606, .796)	-
0.3	-.07	-1.4	-.005	0	-.006	-	(-.0027, .707, .707)	-
	-33	-22	-41	41	-4.1	-	(0.0015, .743, .670)	-
	-30	-1626	52	-59	-97.0	-	(.0000, -.59, -.805)	-
0.4	-.04	-1.4	-.005	0	-.004	-	(-.0025, .707, .707)	-
	-22	-15	-41	41	-3.9	-	(0.0015, .741, .672)	-
	-20	-1615	53	-59	-97.2		(.0000, -.585, .811)	-

Table 1b. Computed values of the Jacobian matrix and its eigenpairs for a concurrent flow simulation.
(The eigenvectors $\underline{v}$ are normalised to give $\|\underline{v}\|_2 = 1.0$)

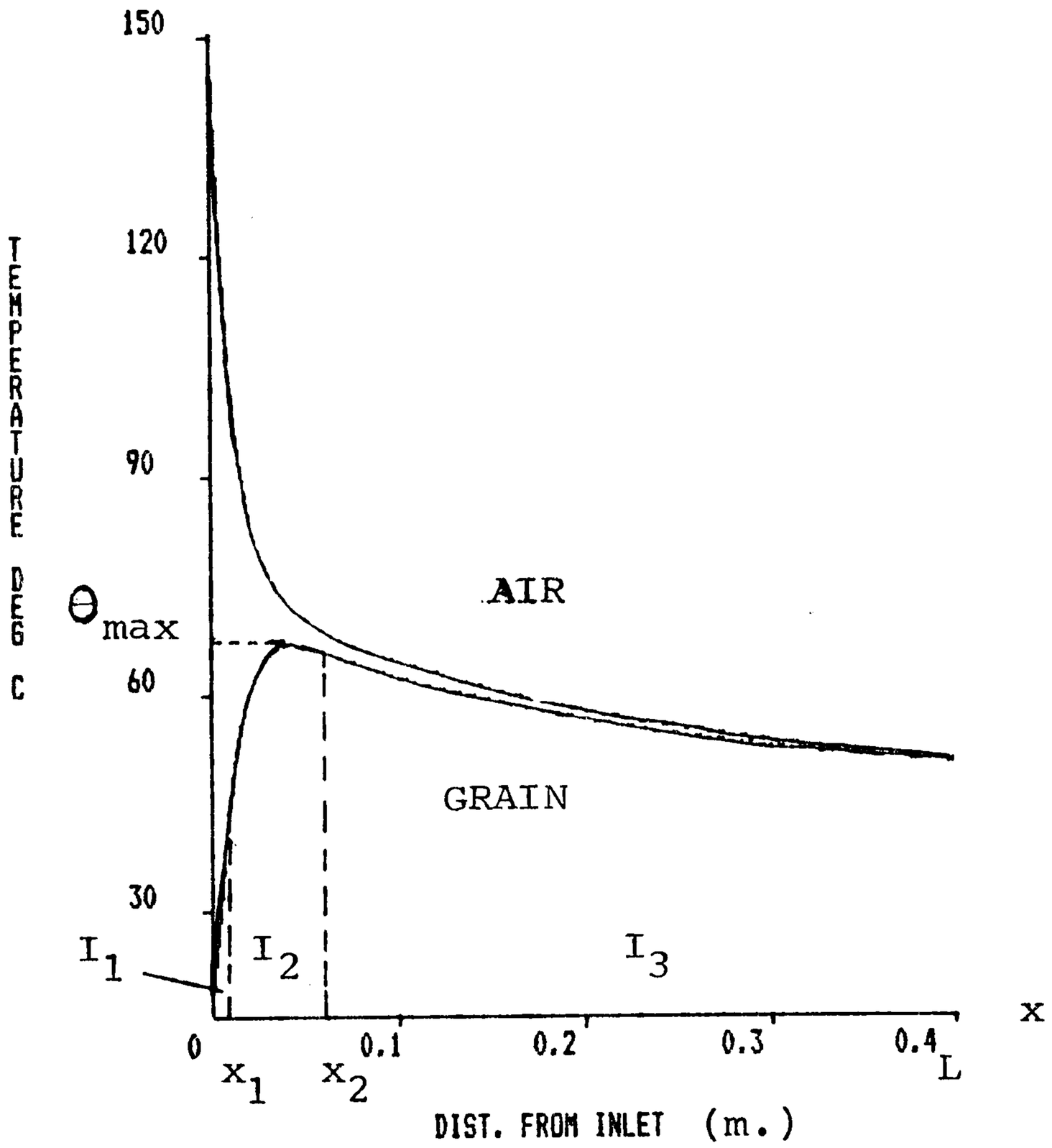

Figure 6a. Plot of predicted air and grain temperatures against depth for a concurrent flow simulation.

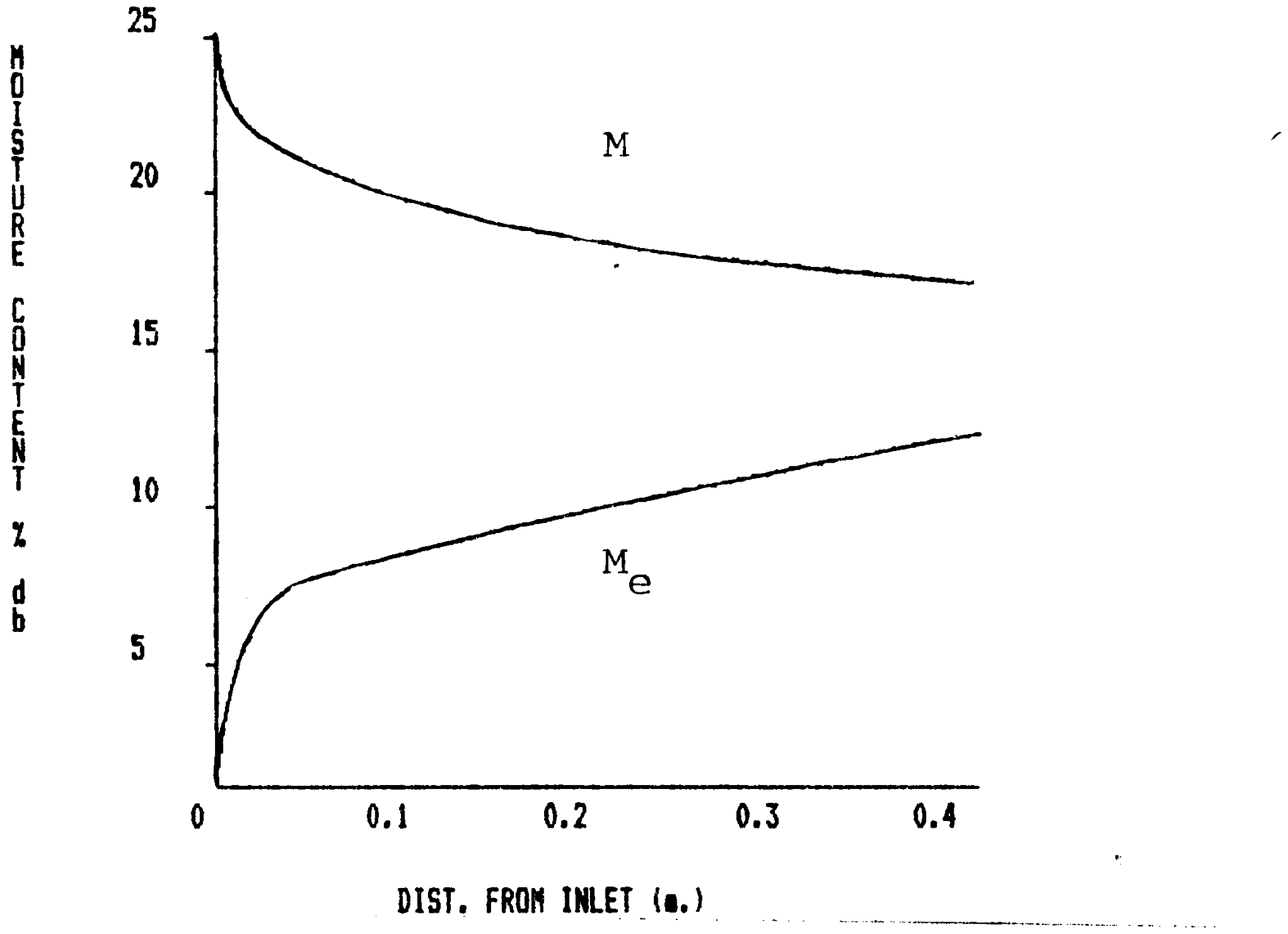

Figure 6b. Plot of predicted moisture content and e.m.c. against depth for a concurrent flow simulation.

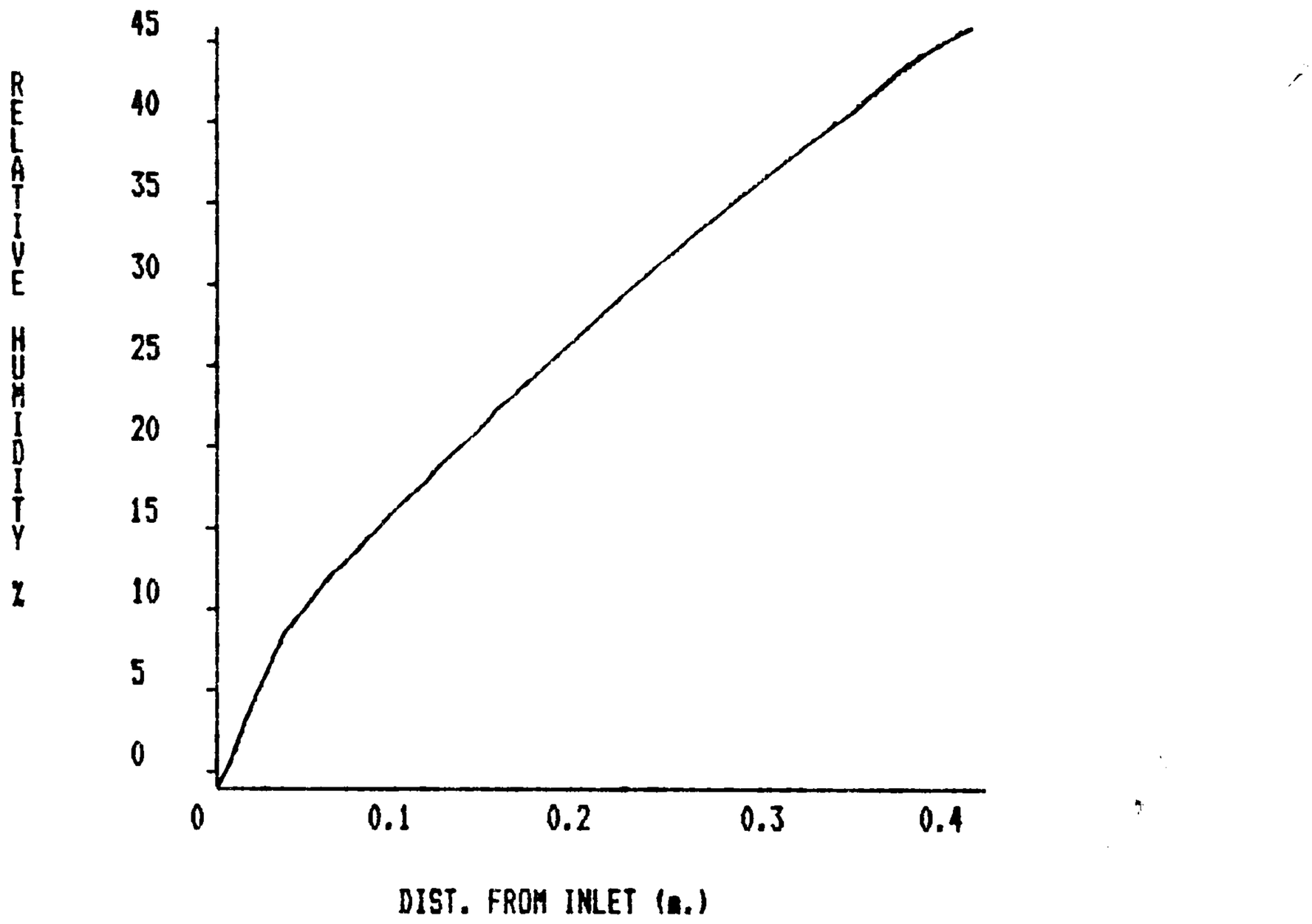

Figure 6c. Plot of predicted relative humidity of drying air against depth for a concurrent flow simulation.

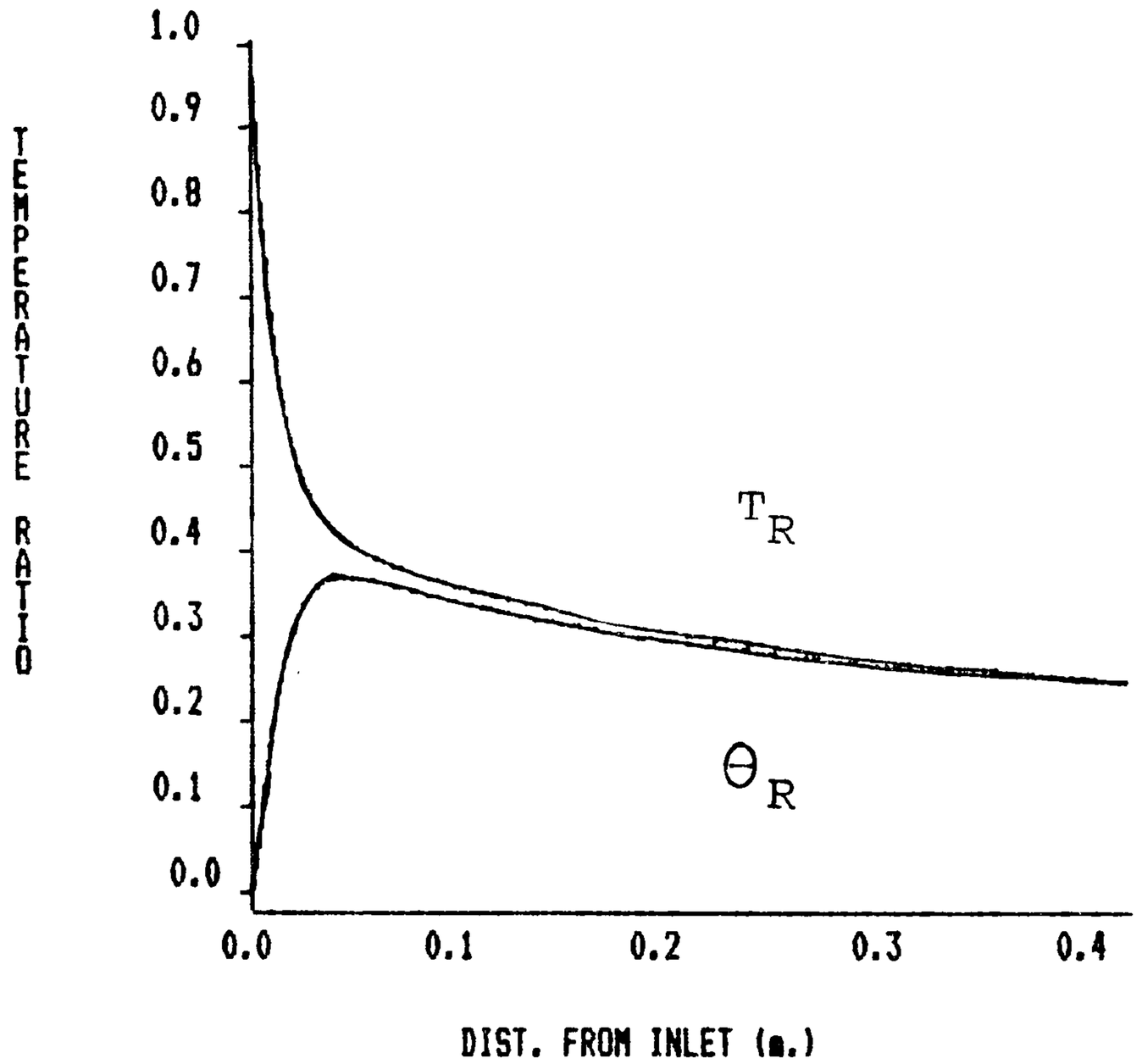

Figure 6d. Plot of temperature ratios, T_R and Θ_R against depth for a concurrent flow simulation.
(see 5.1-14 for a definition of T_R and Θ_R)

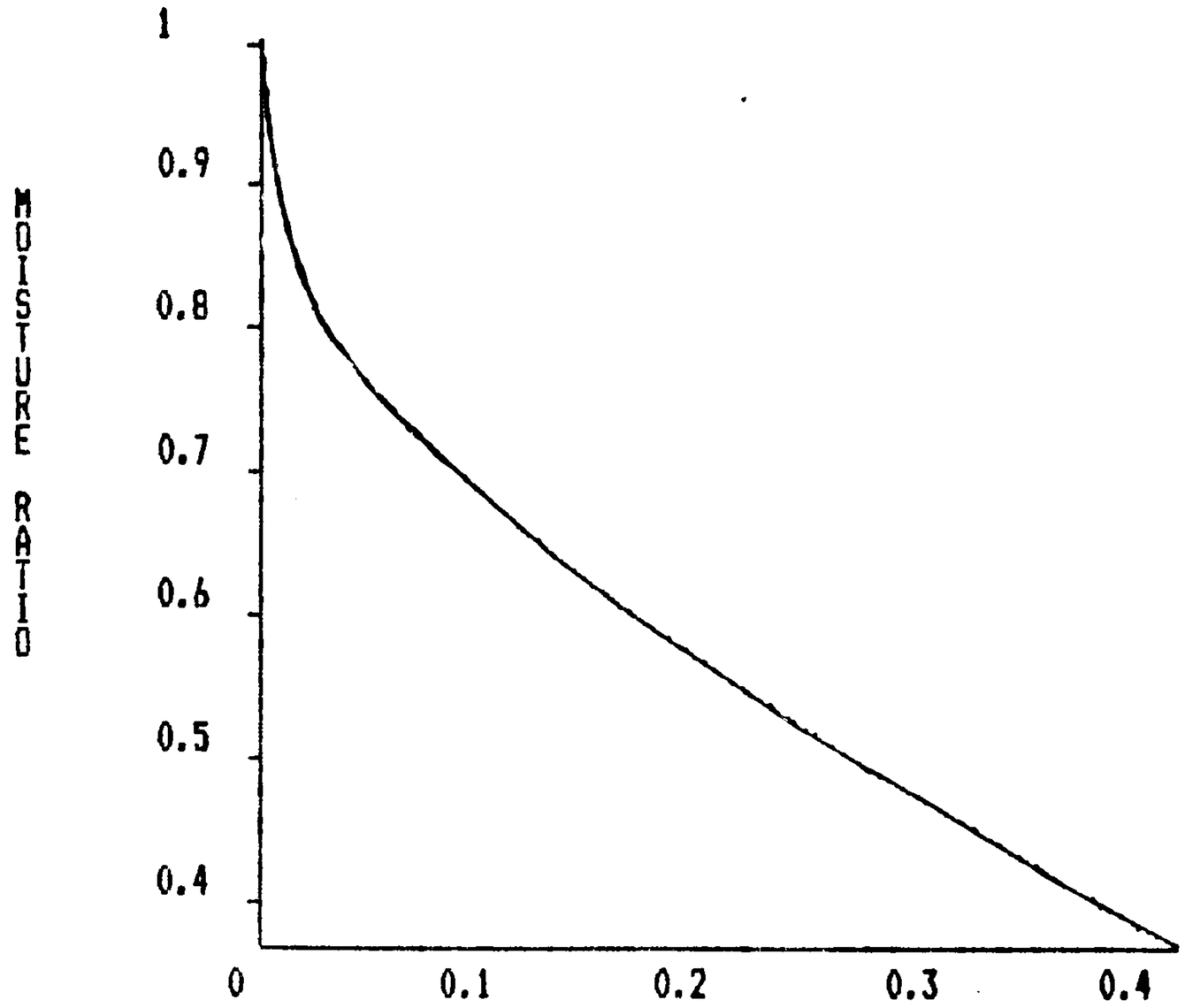

Figure 6e. Plot of moisture ratio, MR, against depth for a concurrent flow simulation.

	X		
	0.02	0.03	0.04
M	21.80 (10)	21.36 (18)	21.02 (23)
θ	58.869 (4)	64.393 (10)	65.425 (30)
T	84.702 (2)	76.679 (6)	72.668 (12)
H	0.0178 (14)	0.0194 (25)	0.0207 (25)

Table 2. Results of a concurrent flow simulation using a linearised approximation. (Compare columns 1 and 3 with 2nd, 3rd rows in Table 1a).

4.2 An Algorithm for the Numerical Solution of the Steady State Model

4.2.1 General Considerations

The work described in section 4.1 gives some insight into the nature of the solution to steady state concurrent flow problems. However, in trying to construct a means for the propagation of this solution semi-analytically, a number of serious problems were encountered. Furthermore, since the NAG routine D02QBF was found to give consistent and accurate results over the range of cases tried, the search for a suitable numerical technique was instituted.

In choosing a numerical technique, a number of factors need to be taken into account. Firstly, the solution to any drying problem of practical interest must be propagated in a stable and 'sufficiently accurate' manner throughout the grain bed. Secondly, the implementation of the chosen technique must be reasonably economical in terms of computer processing time. This consideration is important in view of the possible use of the technique in an 'iterative' manner e.g. in drier control applications (not considered further in this work). Finally, the technique should possess the attribute of 'portability' i.e. it should be relatively simple to program and independent of the support of software 'packages' such as the NAG library. This latter consideration is especially important in view of the possible future implementation of the technique on a micro-computer system which does not possess the requisite 'software support' for a sophisticated routine.

It was stated in the previous section that a high degree of stiffness was observed in the concurrent flow equations. Now in the numerical solution of stiff systems of differential equations, instability problems may occur if the step-size used in numerical integrations is inappropriately chosen. Referring to (4.1-7), it may be seen that if our purpose is to find the 'steady-state' part of the solution i.e. $\underline{u}(x)$, then the system must be solved until the slowest decaying exponential term i.e. that corresponding to the eigenvalue λ_3, is negligible. Thus the magnitude of λ_3 determines the range of integration for this purpose. However, the applicability of any numerical integration technique is dependent on the stability properties of that technique, as distinct from those of the system to be solved.

Consider for example, a numerical method of the general form

$$\sum_{i=0}^{k} \alpha_i \, u_{n+i} = h \sum_{i=0}^{k} \beta_i \, f(x_{n+i}, u_{n+i}) \qquad (1),$$

for solving the scalar equation

$$\frac{du}{dx} = f(x,u(x)), \quad \text{given} \quad u_o = u(x_o) \ ,$$

where α_i and β_i are constants and $u_{n+i} = u(x_{n+i})$. Such a technique is referred to as a linear multistep (k-step) method. If $\beta_k = 0$ then (1) constitutes an explicit method, otherwise it is implicit. In either case, the method is said to be absolutely stable, for a given value of the product $h\lambda$ (where h is the step-size and λ an eigenvalue of J), if all the roots t_i, $i=1,\ldots,k$, of the 'stability polynomial' π, given by

$$\pi(t, h\lambda) = \sum_{i=0}^{k} (\alpha_i - h\lambda\beta_i) \, t^i \qquad (2),$$

lie within the unit circle. Further, a region $\mathcal{R}_A$ of the complex plane is said to be a region of absolute stability if the method is absolutely stable for all $h\lambda \varepsilon \mathcal{R}_A$. For real λ this region is referred to as an interval of absolute stability. If $\mathcal{R}_A$ contains the whole of the half plane $Re(h\lambda) < 0$, then the method is said to be A-stable. Therefore the region of stability is dependent on the magnitude of λ_1.

It may be seen from the above discussion that to preserve numerical stability, the choice of method and integrating step, h, which may be used at any point, should, ideally, be determined with reference to the eigenvalue spectrum of the Jacobian matrix, J. There are a number of definitions of numerical stability in addition to those given above (see e.g. Lambert (1973)). However, on the basis of the above discussion, the following observations provide some general guidelines for choosing a suitable technique:

(i) Explicit methods have finite intervals of absolute stability,

(ii) Implicit methods usually have larger intervals of absolute stability than explicit methods of corresponding accuracy.

(iii) Usually for predictor-corrector type methods (but not for Runge-Kutta type) the higher the order of accuracy, the smaller the interval of absolute stability.

(iv) The order of an A-stable linear multistep method cannot exceed two - the trapezoidal rule is the most accurate such method.

4.2.2 Preliminary Numerical Investigations

In order to construct a suitable algorithm, a number of different numerical integration techniques were implemented to solve the system of three ordinary differential equations (2). These included the following:

a) The NAG library routine D02QBF used in the work described in section 4.1 .

b) The (implicit) trapezoidal rule with polynomial extrapolation of the solution to accelerate convergence (see e.g. Van Der Houwen (1977)).

c) Rational and polynomial extrapolation of Gragg's modified midpoint rule (see e.g. Bulirsch and Stoer (1966)).

The NAG routine comprises a highly sophisticated 'package' of options for solving systems of ordinary differential equations, particularly stiff systems. The routine incorporates a variable order Adams-Bashforth-Moulton method (see e.g. Lambert (1973), p.112). The order of this method and the integration step-size are automatically adjusted at each step so as to minimise the computational effort required to maintain a specified level of local accuracy in the computed solution. The routine also contains an (automatic) option to replace the Adams-Bashforth-Moulton method by special predictor-corrector formulae appropriate for the solution of stiff systems. In order to 'adapt' according to the nature of the system being solved, the routine allows for specification of the elements of the Jacobian matrix, J, in a user-written subroutine. Alternatively, these elements are computed numerically by the routine if required.

In view of its level of sophistication, D02QBF is obviously capable of propagating the solution to equations such as system (4.1-2) in a stable and accurate manner. However, the routine calls upon other NAG routines and is far too complex to be considered as 'portable' for the

purposes of this work. Its use, therefore, was restricted to that of providing a basis for the 'validation' and comparison of other, more suitable, techniques. The results of solving (4.1-1,2), using DO2QBF, for the case presented in section 4.1, are given in Table 1a.

The trapezoidal rule is given by

$$\underline{u}_{n+1} = \underline{u}_n + \frac{h_n}{2} (f(\underline{u}_n) + f(\underline{u}_{n+1})) \qquad (3),$$

where $h_n = x_{n+1} - x_n$. Since the unknown $\underline{u}_{n+1}$ appears on both sides of (3), the rule is implicit and an estimate must be provided for $\underline{u}_{n+1}$ to initiate the iterative solution of the equation. This was accomplished as follows:

(i) A first estimate of $\underline{u}_{n+1}$ was obtained by setting $\underline{f}_{n+1} = f_n$, i.e. using the basic Euler method

$$\underline{u}_{n+1} = \underline{u}_n + h_n \underline{f}(\underline{u}_n), \quad \text{for } n=0,1,2,... \qquad (4).$$

(ii) Equation (3) was then solved iteratively at each step using Newton iteration i.e.

$$\underline{u}_{n+1}^{(k+1)} = \underline{u}_{n+1}^{(k)} - J_F^{-1}(\underline{u}_{n+1}^{(k)}) \; \underline{F}(\underline{u}_{n+1}^{(k)}) \qquad (5),$$

for $k=1,2,...;\ n=0,1,...$.

In (5) the vector function $\underline{F}(\underline{u})$ is defined by

$$\underline{F}(\underline{u}) = \underline{u}_n + \frac{h_n}{2} (\underline{f}(\underline{u}_n) + \underline{f}(\underline{u})) - \underline{u}$$

and the matrix $J_F(\underline{u})$ is given by

$$J_F(\underline{u}) = \frac{h_n}{2} J(\underline{u}) - I \ ,$$

where J is the Jacobian matrix of $\underline{f}(\underline{u})$.

Convergence to the solution $\underline{u}(x)$ was accelerated using polynomial extrapolation (see the discussion of this in section 4.2.3).

The results of the test case referred to in section 4.1, obtained using this scheme for one integration step, are given in Table 3. However, in trying to use the trapezoidal rule over the entire depth of the grain bed, conditioning problems, similar to those described in section 4.1, were encountered. Furthermore, a great deal of computer time was required to solve the resulting system of nonlinear equations at each step a sufficient number of times in order to compute $\underline{u}_{n+1}$ to the requisite degree of local accuracy. In addition, convergence of the solution through polynomial extrapolation was found to require an inordinate level of local accuracy in the computed values of $\underline{u}_{n+1}$ i.e. those obtained through the application of (5). This convergence was also found to be hampered by the growth of rounding errors, although, unlike the use of D02QBF, computations were only carried out in single precision arithmetic.

	step-size				extrapd values	NAG values
	0.010	0.005	0.0025	0.00125		
M	21.07	21.56	21.68	21.71	21.72	21.72
θ	55.610	57.575	58.044	58.159	58.198	58.197
T	79.740	83.190	84.058	84.275	84.347	84.347
H	0.0205	0.0187	0.0183	0.0182	0.0182	0.0182
total its	(15)	(19)	(31)	(45)		

Table 3. Concurrent flow simulation results using trapezoidal rule.

(Results given for $x = 0.02$ only. The final column of values taken from Table 1a.)

In view of the above comments, it was decided that the implementational problems and attendant computational cost outweighed the otherwise beneficial stability properties of the technique.

4.2.3 The Numerical Integration Technique

In view of the experience gained with implicit techniques, such as that just described, it became evident that a more 'robust' and economical scheme should be sought from amongst the variety of explicit numerical integration techniques.

The scalar form of the basic midpoint rule is given by

$$u_{n+2} = u_n + 2h\, f_{n+1} \quad , \; n = 0,1,... \qquad (6),$$

given $u_o = u(x_o)$, and with u_1 calculated using a suitable starting procedure. This is an explicit 2-step method.

Now from the stability polynomial (2), it may easily be seen that the (one-step implicit) trapezoidal rule (3) has the root

$$t = (1 + h\lambda/2)/(1 - h\lambda) \; .$$

Clearly for real $\lambda < 0$, we have $|t| < 1$, so that the method is A-stable. In the case of (6), however, the two roots are given by

$$t = h\lambda \pm \sqrt{(1 + h^2\lambda^2)} \; ,$$

from which it may be seen that $|t| > 1$. The midpoint rule thus has no region of absolute stability. It is, however, 'zero-stable' (i.e. as $h \to 0$) and consistent (i.e. its truncation error tends to zero as $h \to 0$) and hence convergent. Such a method is referred to (by some authors) as <u>weakly stable</u>.

Clearly the basic midpoint rule is not suitable for our application. However, Gragg (in a private communication to H.J.Stetter) proposed a modified form of this rule, which, in scalar form, may be written

$$u_1 = u_o + h_s\, f(x_o,u_o)$$

then

$$u_{m+2} = u_m + 2h_s\, f(x_{m+1},u_{m+1}), \quad \text{for} \quad m=0,1,\ldots N_{s-1} \qquad (7),$$

together with the 'smoothed' approximation to $u(x_o+ H)$

$$u(x_o+ H;h_s) = (u_{N_{s+1}} + 2u_{N_s} + u_{N_{s-1}})/4$$

where $h_s = H/N_s$ for integral N_s. With $N_s = 2$, for example, it may easily be shown that (7) is equivalent to a second order, 3-stage, explicit Runge-Kutta method (see e.g. Lambert (1973)) with steplength $2h_s$. Such a method has a finite interval of absolute stability. In fact, it is absolutely stable in the approximate interval

$$-3.1 < H\lambda < 0.0 \quad , \quad \text{for real} \quad \lambda \quad .$$

From the results of section 4.1, in which it was observed that values of the order 10^2 were common for λ_1 in the cases simulated, this condition means that, in order to maintain absolute stability of the method, the integration step-size must satisfy the constraint

$$H < 0.03$$

approximately.

Gragg (1963) showed that the approximation obtained through (7) may be improved upon using polynomial extrapolation. Furthermore, it has been proven that the interval of absolute stability of the resulting scheme is extended.

Extrapolation methods are based on the assumed existence of an asymptotic expansion for the solution of the form

$$u(x_o+ H;h_s) = u(x_o+ H) + \sum_{i=1}^{N} A_i h^i + R_N(h) \qquad (8),$$

where $R_N(h) = O(h^{N+1})$ as $h \to 0$. Then evaluating $u(x_o+ H;h_s)$ for

a sequence of distinct step-sizes h_s, $s = 0,1,\ldots S$,
where

$$h_o > h_1 > \ldots > h_S > 0 \qquad (9),$$

it is possible, in general, to find a linear combination of these values, $P_S(h)$, say, such that, as $h \to 0$,

$$P_S(h) = \sum_{s=0}^{S} c_{s,S}\, u(x_o + H; h_s) = u(x_o + H) + O(h_o^{S+1}) \qquad (10).$$

This approach is equivalent to fitting a polynomial, $P_S(h)$, of degree S in h, through the data points $(h_s, u(x_o + H; h_s))$, $s=0,1,\ldots S$. Then, letting $h \to 0$ in this interpolating polynomial yields an 'extrapolated' approximation to $u(x_o + H)$ with error $O(h_o^{S+1})$. In practice the extrapolation is performed 'iteratively' using Neville's algorithm which produces successive approximations with error $O(h_o^i)$, $i=2,3,\ldots$, and the coefficients $c_{s,S}$ in (10) are not explicitly evaluated.

Successive approximations may be written in the form of a tableau, to illustrate convergence, as follows

$$\begin{array}{lllll} h_o & a_o^o & & & \\ h_1 & a_1^o & a_o^1 & & \\ h_2 & a_2^o & a_1^1 & a_o^2 & \\ h_3 & a_3^o & a_2^1 & a_1^2 & a_o^3 \\ \cdot & \cdot & \cdot & \cdot & \cdot \\ \cdot & \cdot & \cdot & \cdot & \cdot \\ \cdot & \cdot & \cdot & \cdot & \cdot \end{array} \qquad (11),$$

where

$$\left.\begin{aligned} a_s^o &= u(x_o + H; h_s), \quad s = 0,1,\ldots \\ a_s^m &= a_{s+1}^{m-1} + \frac{(a_{s+1}^{m-1} - a_s^{m-1})}{(h_s/h_{m+s}) - 1}, \quad s = 0,1,\ldots; \quad m = 1,2,\ldots \end{aligned}\right\} \qquad (12).$$

Now Gragg showed that, if the coefficients $A_i(h)$ in (8) are continuous

at $h = 0$, as $h \to 0_+$, then a necessary and sufficient condition for $a_o^m \to u(x_o + H)$, as $m \to \infty$ is that $\sup_{m>0} (h_{m+1}/h_m) < 1$. Effectively, this condition simply means that, provided the stepsizes h_s are chosen to satisfy condition (9), then the diagonal entries in the tableau (11) will converge to the true solution at the point $x = x_o + H$. Gragg further showed that, in the case of (7), the expansion (8) could be written

$$u(x_o + H;h_s) = u(x_o + H) + \sum_{i=1}^{M} A_{2i} H^{2i} + R_{2M}(h) \qquad (13),$$

assuming $N = 2M$, even, and where

$$R_{2M}(h) = O(h^{2m+2}), \quad \text{as} \quad h \to 0.$$

In this case (12) is replaced by

$$\left.\begin{aligned} a_s^o &= u(x_o + H;h_s) \ , \ s = 0,1,\ldots \\ a_s^m &= a_{s+1}^{m-1} + \frac{a_{s+1}^{m-1} - a_s^{m-1}}{(h_s/h_{m+s})^2 - 1} \ , \ s = 0,1,\ldots ; \\ &\qquad\qquad m = 1,2,\ldots \end{aligned}\right\} \qquad (14).$$

Whilst it is impossible to say anything quantitatively about regions or intervals of absolute stability for an arbitrary sequence N_s, s=0,1,.., Stetter has produced tables of absolute stability intervals for Gragg's method with polynomial extrapolation, for the two sequences

$$\left.\begin{aligned} F_1 &= (2,4,6,8,12,16,24,\ldots) \\ F_2 &= (2,4,8,16,32,64,\ldots) \end{aligned}\right\} \qquad (15),$$

(see e.g. Lambert (1973)). In either case, extrapolation using the first six or seven terms of the sequence was shown to produce an approximate doubling of the interval of absolute stability (slightly more for F_2).

Burlirsch and Stoer (1966) presented a scheme employing rational extraploation of Gragg's method (the GBS, i.e. Gragg-Bulirsch-Stoer, method). In tableau (11), the column of entries a_s^m, $s = 0,1,\ldots,$ represent values of the solution extrapolated using m^{th} degree polynomial extrapolation of approximations to $u(x_o + H)$, obtained taking step h_i, for $i = 0,\ldots,s+1$. In the GBS scheme, these entries correspond to extrapolation by the quotient of polynomials $P_i(h)/Q_j(h)$, say, where the degree of numerator and denominator are alternately increased by one as follows:

$$\left.\begin{aligned} &\text{for} \quad m = 0, \; i = j = 0 \\ &\text{for} \quad m = 1, \; i = 0, \; j = 1, \\ \text{then} \quad &\text{for} \quad m > 1, \; i = i + (1 + (-1)^m)/2 \\ &\qquad\quad \text{and} \quad j = j + (1 - (-1)^m)/2. \end{aligned}\right\}$$

Then, assuming an asymptotic expansion of the form (13), the scheme (14) is replaced by

$$\left.\begin{aligned} &a_s^{-1} = 0, \; a_s^o = u(x_o + H; h_s) \;, \quad s = 0,1,\ldots \\ &a_s^m = a_{s+1}^{m-1} + \frac{a_{s+1}^{m-1} - a_s^{m-1}}{(h_s/h_{m+s})^2 \left[1 - (a_{s+1}^{m-1} - a_s^{m-1})/(a_{s+1}^{m-1} - a_{s+1}^{m-2})\right] - 1}, \end{aligned}\right\} \quad (16)$$

$$s = 0,1,\ldots \; ;$$

$$m = 1,2,\ldots \; .$$

Both of the schemes described above were implemented in a program to solve equations (4.1-1,2). The results obtained using the GBS scheme were not found to differ significantly (i.e. in terms of the required number of derivative evaluations for a solution to a specified accuracy) from those obtained using polynomial extrapolation of Gragg's rule. In view, therefore, of the better established theoretical background to the latter scheme, and of its slightly greater computational simplicity, it was decided to employ polynomial rather than rational extrapolation. Thus, the numerical integration scheme chosen for solving the system of three ODEs in (4.1-2) consists of the first approximations $u(x_o+H:h_s)$, $s = 0,1,\ldots,$ given by (7), improved upon

using the extrapolation scheme (14).

Both sequences in (15) were used to generate the first column of approximations a_s^o in (11). However, it was observed for a number of test cases, over a range of prescribed accuracies, that the use of the sequence F_2 generally required a significantly greater number of derivative evaluations than did the use of F_1 to produce results of the specified accuracy. Therefore the sequence F_1 was assumed for use in the work subsequently described.

In practice, suitable convergence criteria must be applied, following the evaluation of each approximation to $u(x_i+H)$ at the current point, to determine when the required accuracy has been attained. For the implementation used in this work, these criteria are applied as follows:

Assume a prescribed relative accuracy of magnitude ε, and that the solution is to be advanced from the point x_{i-1} to $x_i = x_{i-1} + H_i$. Then, 'convergence' to the required accuracy is assumed if the following condition is satisfied

$$\left.\begin{aligned} &\left|a_o^m - a_o^{m-1}\right| < \varepsilon u_{max} , \\ &\text{for some value of } m \text{ in the range} \\ &3 \leqq m \leqq 6 \end{aligned}\right\} \quad (17),$$

where

$$u_{max} = \max \left\{ |u_o|, |u_1|, \ldots, |u_{i-1}|, |a_o^m| \right\} .$$

If this condition is satisfied, then a_o^m is taken as the required approximation to $u(x_i)$. In this case, the next integration step is then performed. If, however, (17) is not satisfied, then the basic step-size, H_i, is halved and the step re-calculated i.e. a value is computed for $u(x_{i-1} + H_i/2)$, and the test re-applied.

If (17) is satisfied then the size of the next step, H_{i+1}, is

determined by

$$H_{i+1} = \begin{cases} H_i , & \text{if } m = 6, \\ 1.5\, H_i , & \text{if } m < 6 \end{cases} .$$

The step adjustment stratagem depends, of course, on the remaining interval over which the integration is to be performed. Appropriate adjustments are therefore made to the step-size near the end of this interval (corresponding to the outlet end of the drying chamber). This stratagem represents a 'rule of thumb' compromise to ensure that excessive halving and re-doubling does not occur. It also has some theoretical justification, being based on an expression for the error in the extrapolated values (see e.g. Bulirsch and Stoer (1966)).

For simplicity, the numerical integration scheme described above was presented in scalar form, for the solution of the single ODE

$$\frac{du}{dx} = f(x,u), \quad \text{given} \quad u(x_o) = u_o .$$

The scheme is readily extended, however, for the solution of system (4.1-2), by the simultaneous application of (7) and (14), at each integration step, to obtain approximate values for the state variables M, T and θ. The linear algebraic relation (4.1-1) is then used to obtain a corresponding value for H. The 'convergence' test (17) is applied to each of the four dependent variables and must be satisfied simultaneously in all four in order for the integration to proceed.

The purpose of condition (17), together with the step-control mechanism described, is to maintain a specified level in the local relative accuracy. Other tests are possible, for example (17) may be replaced by the 'mixed' condition

$$\left| a_o^m - a_o^{m-1} \right| < \varepsilon(1.0 + u_{max}),$$

for m in the same range. This condition is equivalent to a relative error test if $u_{max} >> 1$ and an absolute error test if $u_{max} << 1$*.

* This test was found to be unsuitable since humidity values were predicted with too little accuracy.

The results obtained using the above scheme appear to be propagated in a stable and accurate manner over a range of accuracies suited to present requirements (see section 4.4 for a fuller discussion). The main advantages of the technique over others considered are:

(i) The explicit nature of the basic integration rule and hence no requirement to solve a system of non-linear algebraic equations at each step.

(ii) The 'economy' with which higher order approximations to the solution may be found, facilitated by the use of an appropriate extrapolation procedure.

It is acknowledged that the scheme does not possess very good stability properties and that the use of such schemes for the solution of very stiff systems of ODEs is not generally advised. However, subject to certain constraints (see section 4.4), the scheme, as implemented, appears to be sufficiently 'robust' and, in view of its adaptive nature, well able to cope with the rapidly changing gradients in some concurrent flow drying applications.

4.2.4 Interpolation of the State Variables

Interpolation of the state variables M, T and θ, at arbitrary bed depths is achieved using cubic Hermite interpolation (see e.g. Davis (1963)). Relation (4.1) is then used to obtain corresponding values for H. Over each depth interval $(x_{i-1},x_i]$ i.e. each basic integration step, H_i, the interpolated value, $\tilde{u}(x)$, of a state variable u at some specified depth x, for $x_{i-1} < x \leq x_i$, is computed from

$$\tilde{u}(x) = \frac{(x_i-x)^2(x-x_{i-1})}{H_i^2} m_{i-1} - \frac{(x-x_{i-1})^2(x_i-x)}{H_i^2} m_i$$

(18).

$$+ \frac{(x_i-x)^2[2(x-x_{i-1})+H_i]}{H_i^3} u_{i-1} + \frac{(x-x_{i-1})^2[2(x_i-x)+H_i]}{H_i^3} u_i$$

In (18), $H_i = x_i - x_{i-1}$, u_j represents the approximate value for $u(x_j)$ and m_j the approximate computed value of the derivative

$$\left.\frac{du}{dx}\right|_{x=x_j} \quad , \quad \text{for} \quad j = i-1, i,$$

both obtained in the course of the numerical integration.

One advantage of (18) is that, in view of its low degree and piece-wise nature, it constitutes a flexible fit to the data i.e. the state variables and their gradients with respect to depth. The fit is also continuously differentiable i.e. $\tilde{u}(x) \in C^1(0,L)$, and so possesses a certain degree of smoothness across the 'knots' x_i, $i=1,\ldots,N-1$, where N is the number of intervals.

In order to obtain further smoothness in the interpolated values of the solution, using (18), a system of linear algebraic equations must be solved for the m_j's. These equations express the condition of second derivative continuity at each of the interior knots (see e.g. Ahlberg et al (1967)), and, with appropriately prescribed end conditions, (18) then represents cubic spline interpolation (see Chapter 5 for more detail). In order to effect a comparison with the spline, a number of test cases, such as those described in the next section, were run using both (18) and a cubic spline fit. The differences in interpolated values in all cases were found to be negligible and the calculated m_j values were found to be of the same order as those obtained from the numerical integration. Clearly less stringent continuity conditions are required by (18), which might therefore be more suited than the spline for the representation of the high gradients which occur, particularly near the inlet, in high temperature concurrent flow drying.* Furthermore, the m_j's, having been previously computed in the numerical integration stage, are already available.

Now the error, $E\{u(x)\}$, say, in using (18) to interpolate over the range $(x_{i-1}, x_i]$, and assuming that $m_j = (du/dx)\Big|_{x=x_j}$, may be shown to be bounded by

$$\left| E\{u(x)\} \right| \leq H_i^4 \max_{x_{i-1} < x \leq x_i} \left| \frac{d^4u(x)}{dx^4} \right| /384 \qquad (19)$$

* It is well known that the 'conditioning' of the continuity equations is adversely affected by large differences in the size of adjacent intervals.

Clearly, the higher derivatives of the dependent variable u(x) may be very large during the initial stages of drying. However, in view of the adaptive nature of the integration scheme, the knots will tend to be distributed according to the degree of variation of u(x) over the bed. For example, they will be closest near the inlet point, where large gradients in both temperature and moisture content occur, and will spread out as drying progresses (see Table 4b). It might therefore be expected that the effect of large fourth derivatives in (19) is, to some extent, counteracted by correspondingly small step-sizes H_j. It is possible, in theory, to obtain analytical expressions for these derivatives. However, a glimpse at the elements of the Jacobian matrix, J, given in Appendix B, will serve to indicate the difficulty of such an approach. Numerical differentiation provides a more generally applicable alternative (if used with caution). However, neither of these approaches were pursued to obtain such a bound on the error of interpolation, which would, in any event, tend to be an over-estimate of the actual error. It is simply noted here that actual computations indicate that the error of interpolation is generally small as compared to that incurred by numerical integration.

4.2.5 Computer Implementation of the Algorithm

The algorithm described in sections (4.2-3,4) was implemented as the FORTRAN program CONFLO on the ICL 470/472 computer system at the ARC Computing Centre at Harpenden. A separate program CFPLOT was written to produce graphical output of the results on a BENSON plotter, making prior use of the GHOST graphical system on a TEKTRONIX terminal. This work is fully documented in Parry (1983b). A cursory description only is presented here.

The program CONFLO comprises a MAIN segment together with six subroutines and six inter-related function subprograms. The relation-ship between these segments is schematically indicated in Figure 7. The MAIN segment firstly calls SUBROUTINE IPDATA to read data from a user-supplied file. Solution of the heat and mass transfer equations is then accomplished in SUBROUTINE SOLVEX, using the extrapolated, modified midpoint rule described herein. SUBROUTINE OPHEAD writes a heading together with some of the input data to an appropriately

defined output file. Finally, SUBROUTINE OPFILE creates two output files of results interpolated at the required bed depths. The first of these files may be printed for presentation of the solution (see e.g. Table 4a). The second file contains information used by the plotting program CFPLOT (this program is not described here but see Figure 8 for a sample of its output).

In addition to the four main subroutines described above, the right hand side of system (4.1-2) is evaluated in SUBROUTINE DERIV, which may be user written, and is called by SUBROUTINE SOLVEX. At each integration step, the derivatives are calculated at the values of the dependent variables H, M, T and θ, supplied by SOLVEX. Estimates for the heat and mass transfer rates required for this calculation, defined empirically in terms of the state variables (see Appendices A, C) are evaluated in function subprograms HTRANS and DRYRAT respectively. The drying rate coefficient, k, and equilibrium moisture content (emc), M_e, are evaluated in FUNCTION's DRYK and EMC respectively. The emc, in turn, requires values for the relative humidity and saturation vapour pressure of the air, obtained from RELHUM and SATPRE respectively. Finally, the values output by OPFILE are interpolated in SUBROUTINE SPLINT, at the user-specified depths, by means of (18).

The input data file, created by the user, must contain values for the specific heats c_a, c_v, c_w and c_p of dry air, water vapour, liquid water and product (dry grain) respectively, together with the latent heat and vaporisation, h_{fg}, of free water, and the atmospheric pressure. Typical values for these quantities, in the appropriate units, are given in Parry (1983b), pp.22-24. The mass flow rate of drying air, G_a, and throughput of moist grain, G_p must be specified, as well as initial values for the temperatures and moisture contents of drying air and moist grain. Finally, the (effective) bed depth, L, percentage (local) relative accuracy, ε, and, in the current implementation, the number of (equal) intervals at which output of the results is required.

In order to validate the numerical technique, comparisons (not presented here) were made between results obtained using both CONFLO and the NAG routine D02QBF, for a number of cases. Whilst a direct

comparison is difficult, in view of slightly different error tests employed, the results of both programs were found to be very close overall. For example, with a prescribed local accuracy corresponding to approximately five significant figure accuracy, these results were found to agree to three or four significant figures, or better.

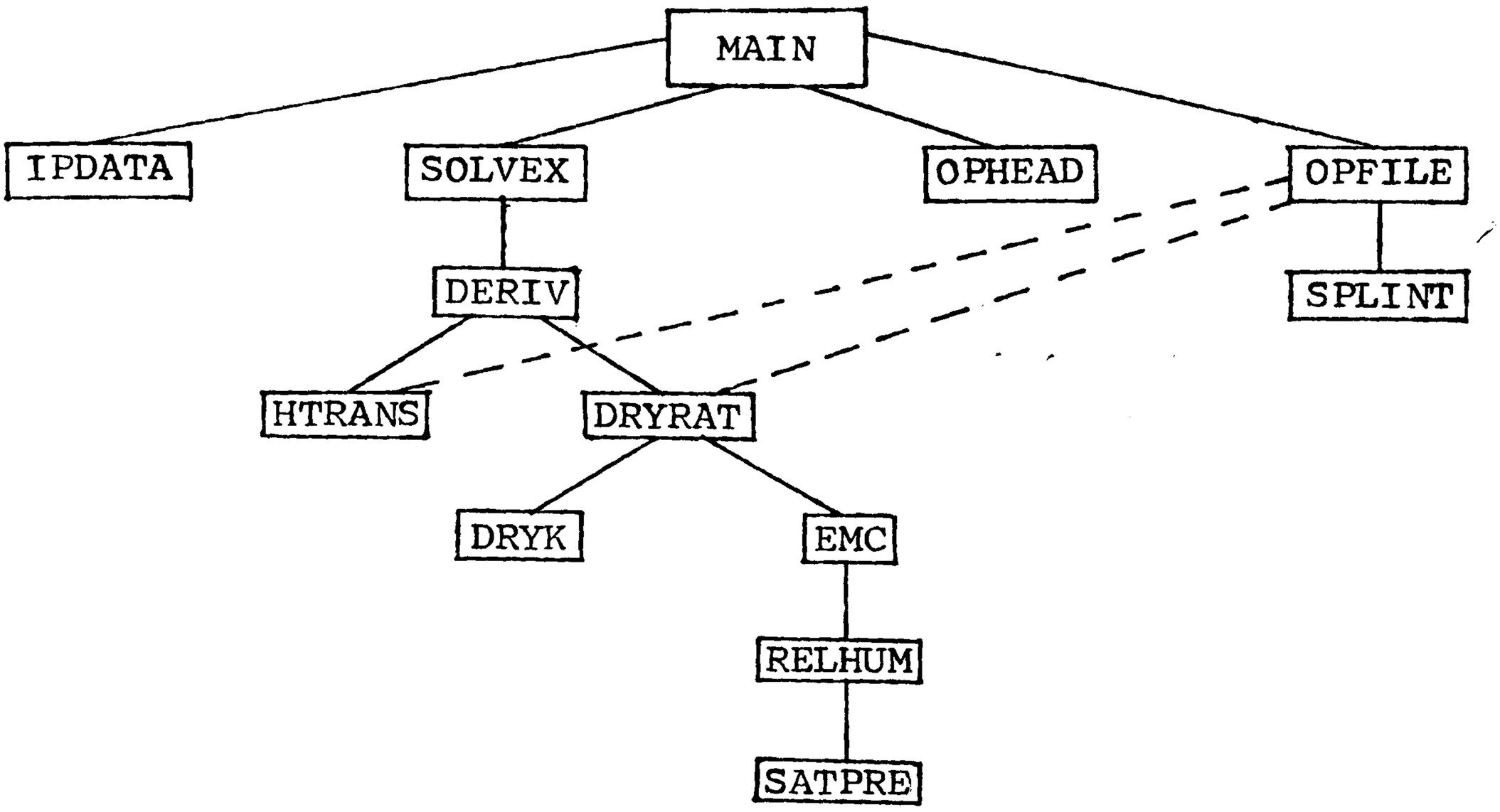

Figure 7. Flow diagram for the program CONFLO

4.3 Validation of the Model

CASE 1

Firstly, results obtained using the program CONFLO were compared with those given by another program SIMUL*. The latter was developed at NIAE, see Nellist (1974), and subsequently modified to facilitate the simulation of a range of drying applications, see Bruce (1983).

It was found that, although the models differ in their formulation and method of solution, they give, what are for practical purposes, the same results when using the same constitutive relations for the grain and air properties (see Appendix A). For example, Table 4a and Figure 8 present results for a drying bed of depth 0.4m. deep with grain entering at 25% m.c.d.b. and being ventilated with air temperature and flow of 200°C and 17.1 kg/min/m^2 respectively.

These results were obtained when, in the present model, the water was assumed to have been evaporated at the air temperature, i.e. $\theta_v = T$. When θ_v was set to θ, the maximum grain temperature, occurring in the region 0.07-0.08m. from the inlet, was found to be approximately 3 °C higher than that predicted by the NIAE program. Overall, however, this difference would still appear to be relatively small.

Table 4b gives the distribution of knots in the piecewise smooth cubic fit (4.2-18) to the state variables. In this case eleven knots are required to represent the solution to a relative accuracy of approximately 0.1% over the given bed depth. The values DX represent the basic integration step-sizes between knots (see section 4.4 for further comment).

Total Mass and Energy Balance

As a further check on the numerical simulation, assuming negligible loss of heat and moisture through the walls of the drying chamber, the following overall balance equations should be approximately satisfied:

* The NIAE program will be referred to by this name throughout the remainder of this work.

1. The increase in the moisture content of the drying air

   = The decrease in moisture content of the moist grain

   i.e.

$$G_a(H_{out} - H_{in}) = -G_p(M_{out} - M_{in}) \qquad (1).$$

2. The increase in internal energy of the moist grain

   = The decrease in internal energy of the drying air

   i.e.

$$G_p\,[(E_p + ME_w)]\,\Big|_{\theta_{in}}^{\theta_{out}} = -G_a\,[(E_a + HE_v)]\,\Big|_{T_{in}}^{T_{out}},$$

   which may be written in the form

$$G_p[(c_p + c_w M_{out})\,\theta_{out} - (c_p + c_w M_{in})\,\theta_{in} - h_{fg}\,(M_{out} - M_{in})]$$

$$= G_a[(c_a + c_v H_{in})T_{in} - (c_a + c_v H_{out})T_{out}] \qquad (2).$$

Now from Table 4a we have for a moisture balance:

1.h.s. of (1) $\cong$ 17.1(.0511 - .008) $\cong$ 0.737(kg./min./sq.m.),

r.h.s. of (1) $\cong$ -12.2(.1896 - .2500) $\cong$ 0.737(kg./min./sq.m.).

Similarly, for an energy balance:

1.h.s. of (2) $\cong$ 2.60×10^6 (J./sq.m./min.),

r.h.s. of (2) $\cong$ 2.55×10^6 (" ").

From the above, it may be seen that a moisture balance was obtained to 3 d.p., in the given units, but that a difference of approximately 2% was found between the two sides of the overall energy balance equation.

CASE 2

The importance of using appropriate constitutive relationships was highlighted when some experimental results obtained by Bakker-Arkema et al (1977) were simulated using CONFLO. These results comprise drying data for a one-stage concurrent flow wheat drier of 0.61. i.e. 2ft depth, drying soft wheat. The following inlet conditions were given

for the grain: $M(0) = 28.2\%$ d.b., $\theta(0) = 29.44°C$ (85°F)

$G_p = 15.56$ kg/m^2/min.

for the air : $H(0) = 0.0061$, $T(0)$ - various (see Table 5),

$G_a = 19.81$ kg/m²/min.

At first, the simulated results were disappointing because, over a range of drying air temperatures from 120 to 204 °C, the predicted maximum grain temperature rose by only 6°C and indeed at 204°C was still below 60°C. Now it was known from the extent of reduction in grain viability* in these and other experiments that in reality grain temperatures well in excess of 60°C are attained in such concurrent flow beds. Furthermore, Bakker-Arkema et al themselves present, what appear to be experimental, but which are now known to be simulated, maximum grain temperatures which do rise in the expected manner. It was then realised that the latter results had been obtained using constitutive relationships not for wheat but for maize. Comparison of the data for the two grains then showed that extrapolation of that for wheat into the temperature range 120-200°C gave unrealistically high values of the drying rate (and hence m) when compared with experimental drying rates for maize in that temperature range, i.e. the extrapolated values were several times greater than would have been expected from the difference in grain size between the two cereals.

In view of the above observations, the simulations were re-run using the same constitutive relationships for maize as used by Bakker-Arkema et al (see Appendix C). The new results, presented in Table 5 and Figure 9, are in very close agreement with the reported experimental values of outlet grain temperature and moisture content and predicted maximum grain temperature.

It may be concluded that these validation cases have demonstrated that three differently formulated and programmed models give similar results when the same constitutive equations are used for the grain and air properties. It has further emphasised the importance of using data valid for the physical conditions being simulated. As regards agreement with experimental data, the second case in particular, demonstrates that model predictions are of the same order as experimental results. Clearly, however, it will be necessary to carry out a thorough comparison with more and better experimental data when this becomes available.

* Private communication - M.E.Nellist.

CONCURRENT FLOW SIMULATION
****

INLET CONDITIONS

GRAIN

M.C.(%D.B.)=25.00
TEMP.DEG.C.=15.00
THROUGHPUT = 12.200
KG.(D.M.)/MIN./SQ.M.
BED DEPTH=0.4000 M.

AIR

SPEC.HUMIDITY=0.008
TEMP.DEG.C.=200.00
MASS FLOW RATE = 17.100
KG./MIN./SQ.M.

STEADY-STATE CONDITIONS AT DIST. X FROM INLET
(VALUES COMPUTED TO APPROX. 0.10000 % LOCAL REL.ACC.)
RESIDENCE TIME OF GRAIN= 21.08 MINS

	GRAIN			AIR			
X	M.C.%	EMC%	TEMP.	TEMP.	SP.HUM	R.H.%	DRYING RATE
0.000	25.000	2.955	15.000	200.000	0.0080	0.08	0.27E-02
0.020	20.883	4.848	37.389	90.818	0.0374	7.90	0.12E-03
0.040	20.477	6.943	50.718	65.097	0.0403	24.41	0.39E-04
0.060	20.278	8.315	53.516	57.986	0.0417	34.92	0.26E-04
0.080	20.128	9.056	53.597	55.515	0.0428	40.19	0.22E-04
0.100	19.998	9.537	53.005	54.305	0.0437	43.46	0.20E-04
0.120	19.879	9.973	52.349	53.369	0.0445	46.29	0.18E-04
0.140	19.770	10.377	51.679	52.610	0.0453	48.81	0.16E-04
0.160	19.671	10.782	51.059	51.918	0.0460	51.22	0.15E-04
0.180	19.579	11.197	50.498	51.266	0.0467	53.59	0.14E-04
0.200	19.495	11.596	49.960	50.701	0.0473	55.76	0.13E-04
0.220	19.418	11.990	49.463	50.186	0.0478	57.82	0.12E-04
0.240	19.347	12.398	49.024	49.687	0.0483	59.85	0.11E-04
0.260	19.282	12.822	48.642	49.200	0.0488	61.86	0.98E-05
0.280	19.223	13.218	48.271	48.788	0.0492	63.65	0.90E-05
0.300	19.169	13.597	47.925	48.425	0.0496	65.29	0.82E-05
0.320	19.120	13.981	47.622	48.075	0.0500	66.88	0.74E-05
0.340	19.075	14.372	47.359	47.739	0.0503	68.43	0.67E-05
0.360	19.034	14.734	47.110	47.451	0.0506	69.80	0.61E-05
0.380	18.998	15.075	46.881	47.197	0.0508	71.03	0.55E-05
0.400	18.965	15.406	46.679	46.963	0.0511	72.19	0.49E-05

Table 4a. Simulation of a concurrent flow section of a mixed flow drier

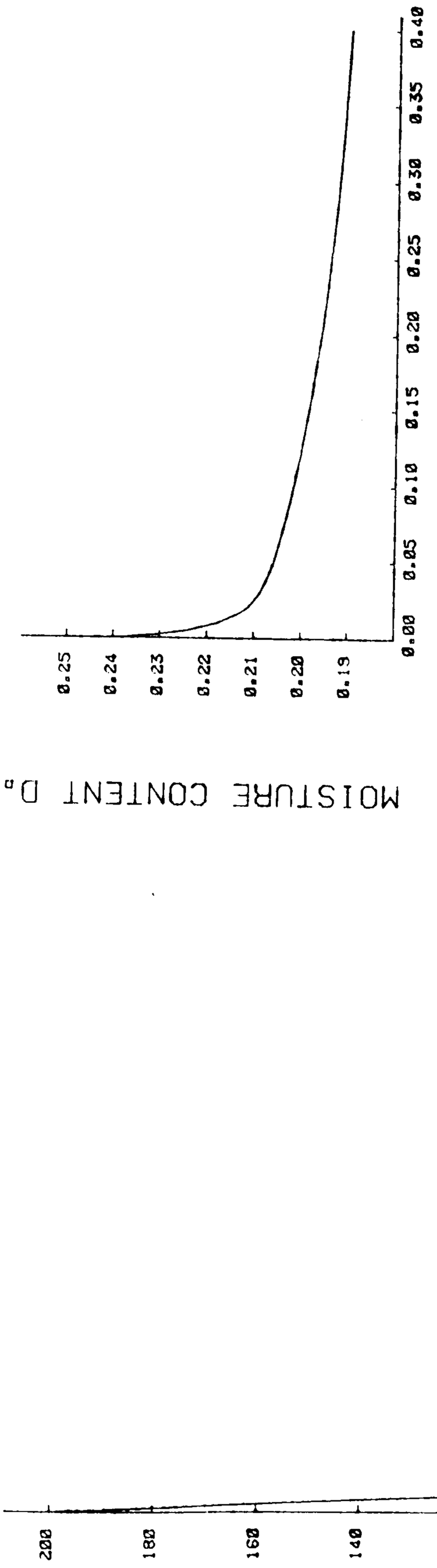

Figure 8. Plot of results of simulation of mixed flow drier of concurrent flow section

knot no.	knot	DX
1	0.0000	0.00500
2	0.0050	0.00750
3	0.0125	0.01125
4	0.0237	0.01687
5	0.0406	0.02531
6	0.0659	0.03797
7	0.1039	0.05695
8	0.1609	0.08543
9	0.2463	0.07686
10	0.3231	0.07686
11	0.4000	

Table 4b. Distribution of knots for concurrent flow simulation.

INLET AIR TEMP.DEG C	OUTLET GRAIN TEMP.DEG C		MAX.GRAIN TEMP.DEG C		OUTLET M.C.%db	
	EXP.	PRED.	EXP.	PRED.	EXP.	PRED.
121.1	37.20	37.51	47.80	50.80	24.40	24.56
148.9	40.60	40.93	55.60	56.37	23.50	23.60
176.7	44.40	44.82	62.80	64.08	22.50	22.69
204.4	47.78	48.63	70.60	71.95	21.70	21.77
232.2	52.22	51.99	78.30	79.94	20.90	20.79
260.0	57.22	55.50	86.70	87.98	20.20	19.80

Table 5. Comparison of simulated with experimental results for a one-stage concurrent flow wheat drier.

(In the above table all maximum grain temperatures were simulated).

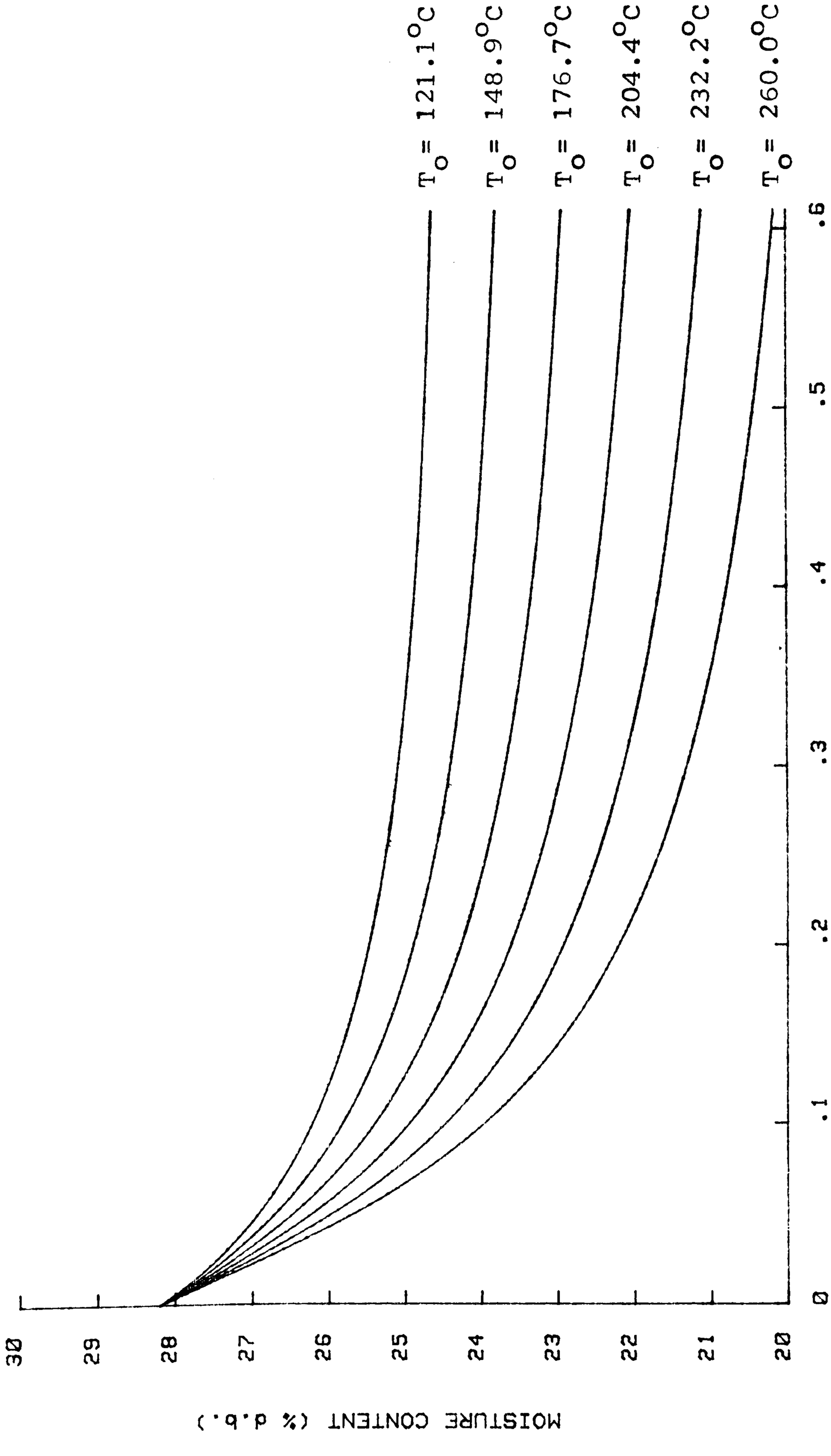

Figure 9a. Plot of predicted moisture content against depth, for various temperatures, for a one-stage concurrent flow wheat drier.

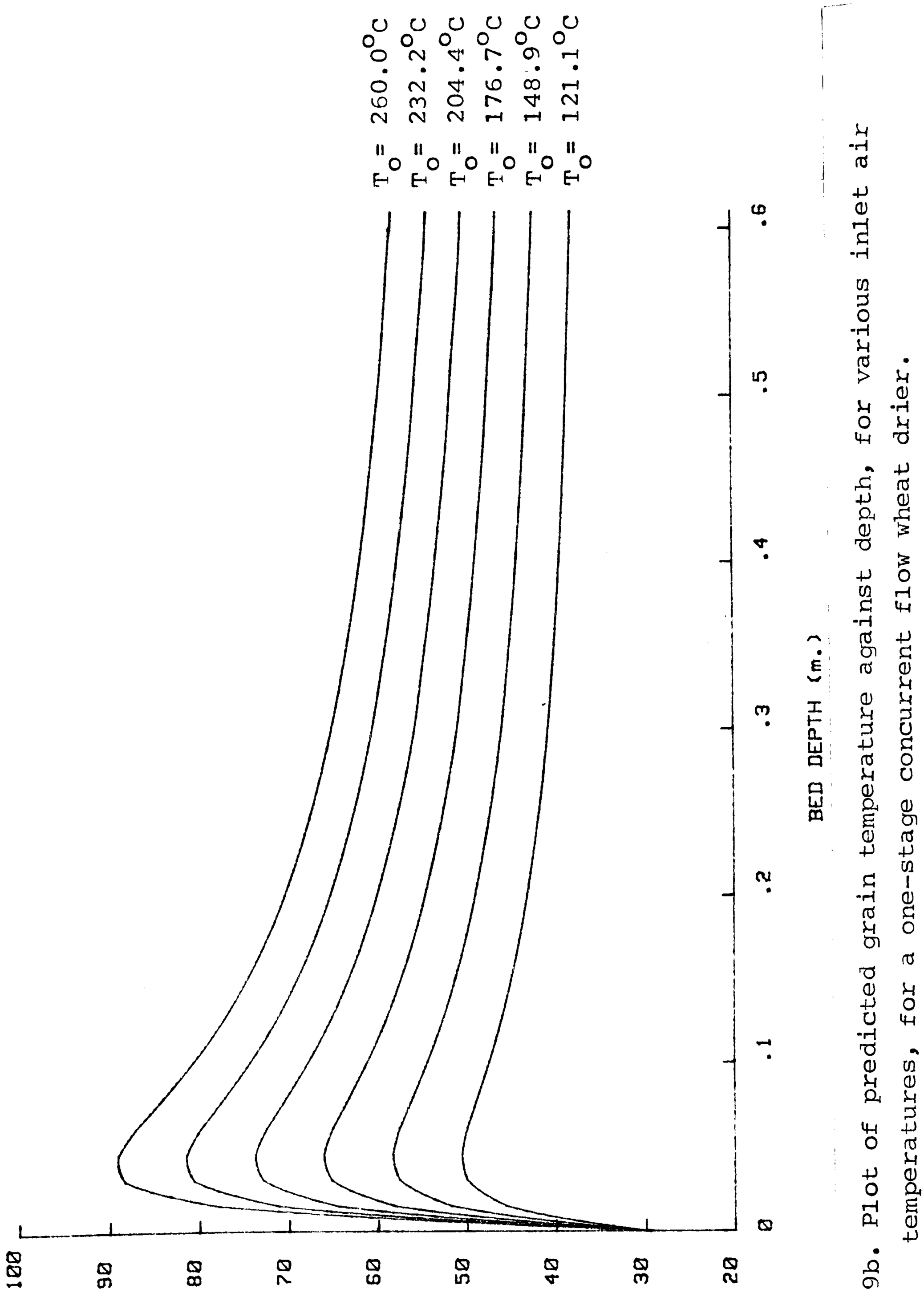

Figure 9b. Plot of predicted grain temperature against depth, for various inlet air temperatures, for a one-stage concurrent flow wheat drier.

4.4 Factors Affecting the Performance of the Algorithm

The numerical integration technique, described in section 4.2, is 'adaptive' in the sense that it incorporates a step adjustment strategy to ensure that the required stepwise accuracy is maintained during the integration stage. The cubic Hermite interpolation formula (4.2-18) then collocates with the predicted values of the state variables, H, M, T and θ, and their gradients with respect to depth, at each of the 'knots' i.e. end points of each basic interval of integration, in order to preserve the overall accuracy of the required order in any interpolated values.

Table 4a gives the results of a simulation of a drier of 0.4 m. 'effective' depth, obtained to a local relative accuracy of 0.1%. It may be seen from Table 4b that successive integration intervals for this case, the lengths of which are given by DX, tend to increase in size with distance from the inlet (there will of course be some adjustment of this step at the outlet end of the drier). The distribution of knots, therefore, illustrates the way in which the algorithm adapts to varying gradients in the solution.

The total number of 'derivative evaluations' required during the course of a numerical integration gives, in general, some indication of the computational effort required and of the efficiency of the technique used. In the present context, one derivative evaluation represents an evaluation of the right-hand sides b_2, b_3 and b_4 of (3.1-22). For the simulation presented in Table 4a, the required number of such evaluations was found to be 163.

The run-time for a single concurrent flow simulation is fairly small and the number of derivative evaluations in such a case is of limited significance. Such a simulation might, however, be performed iteratively, for example in controlling the output of a drier. In this case it would clearly be sensible to attempt to 'optimise' the number of derivative evaluations and hence the overall simulation time. Obviously this time will vary depending on how the algorithm is implemented on a particular computer. Assuming sufficient arithmetic accuracy on all computers, however, the number of derivative evaluations will be independent of the implementation and may therefore

be taken as an invariant measure of the performance of the algorithm.

In addition to considerations of time-wise economy, the total number of knots required for the representation (4.2-18) determines the total internal memory utilised by the program. Whilst for the cases presented here the number of knots is very small, it is possible that in some cases this number could significantly affect the internal memory utilisation. Clearly then, the permissible number of knots must be limited in some way, and an arbitrary limit of 50 has been built into the present implementation of the program CONFLO (an error message indicates if this limit has been attained).

A number of factors affect both the number of derivative evaluations and the number of knots. These include the length of the drier to be simulated, the required accuracy, and moisture and temperature gradients throughout the bed, but particularly near the inlet. A further factor is the stepsize, H_o say, taken for the first integration step.

Table 6 is a summary of results obtained from a number of simulations with the same inlet conditions as those given in Table 4a. Each entry in the table gives the number of derivative evaluations, followed by the number of knots, N_{knots}, say, in parentheses (the number of basic integration steps taken by the algorithm is then simply N_{knots}-1). These entries are given for three drier depths, L, five values of local relative accuracy, eps, and three initial stepsizes, H_o.

In view of the fairly arbitrary choice of values for the parameters L, eps and H_o, it is only possible to make a few general observations concerning the performance of the algorithm over this limited range of these parameters. Obviously, in general, the deeper the bed and the greater the required accuracy, the greater is the number of derivative evaluations needed. However, it is evident that for eps = 10^{-4}, a greatly increased number is required, together with a much larger number of basic integration steps/knots. The value of N_{knots}, however, remains approximately constant for eps in the range

$$1.0 \leqq \text{eps} \leqq 10^{-3} \ .$$

Thus increased storage is not required for greater accuracy within this range (this is due to the required accuracy being attained within the specified number of levels (six) of extrapolation). However, in view of likely inaccuracies in the initial data and of the various simplifying assumptions made in deriving the basic model, a request for a very high accuracy in the computed results would seem unwarranted.

The problem of finding an optimal value for H_o is complex. In view of the number of different factors affecting such a choice, no attempt was made to even formualte such a problem (note, for example, the behaviour of the algorithm for $L = 1.6$). For higher accuracies it is obviously better to start with a commensurately small integration step to avoid excessive interval reduction initially. Any estimate of a suitable value for H_o, in a given case, would, however, involve extra computation, for example in the approximate calculation of derivatives near the inlet, and might not result in much saving in the total computational effort. A compromise must therefore be made and the value of $H_o = 0.01$ was deemed suitable for the present implementation of CONFLO, although in general this value should be determined relative to other factors. The point is not pursued further here.

In order to gain some notion of the 'convergence' of the solution obtained, an analysis was performed, of the differences in the values of the state variables obtained to a variety of different accuracies. The following approach was adopted:

the sequence $\underline{u}^k(x) = \underline{u}(x;\varepsilon_k)$, $k = 0,1,\ldots,4$, it taken to denote the solution $\underline{u}(x) = [M,T,\theta,H]^T$, at some point x, obtained using prescribed accuracies of $\varepsilon_k = 10^{-k}$. Then, writing the difference between two successive terms in the sequence as

$$\underline{d}_k(x) = \underline{u}^k(x) - \underline{u}^{k-1}(x), \quad k = 1,\ldots,4,$$

a measure of the convergence of the sequence may be obtained by examining terms in the sequence of relative differences

$$\underline{rd}_k = [rd_{k1},\ldots,rd_{k4}]^T, \quad \text{for } k = 1,\ldots,4,$$

where

$$rd_{ki} = \max_x \left| \frac{d_{ki}(x)}{u_i^k(x)} \right| .$$

Values of $\underline{u}^k(x)$ were obtained for $x = x_j = jL/10$, $j = 1,\ldots,10$, and Table 7 gives the corresponding values of $\max_j |d_i^k(x_j)|$ and rd_{ki} for each of the state variables.

From Table 7 it may be seen that the differences diminish, if somewhat slowly, as the prescribed accuracy is increased, indicating some measure of convergence. The relative changes in moisture content and humidity are, however, smaller for any given accuracy, than those in the air and grain temperatures. Thus convergence seems to depend on the latter variables to a greater extent. Corresponding to $k = 4$, there appears to be anomalous behaviour, in both absolute and relative differences. These differences increase in the vicinity of the maximum grain temperature, diminishing thereafter (a maximum for this region is given in parentheses).

The results of this analysis would seem to indicate that the algorithm is fairly 'well-behaved' over the range

$$10^{-1} \leqq \text{eps} \leqq 10^{-4} .$$

In view of this and the previous comments a relative accuracy of eps = 0.1% would seem perfectly adequate for most applications. This would ensure, for example, that air temperatures of up to 1000°C, predicted by the model, would be computed to a (local) accuracy of ± 1°C.

A somewhat cursory 'sensitivity analysis' was carried out in order to investigate the effects on the solution of perturbations in the inlet (initial) conditions of both air and grain. From the results of this analysis (see Table 8), the following effects were observed:

(i) perturbations in the initial humidity had a very small effect on the computed predictions of the other variables,

(ii) perturbations of ± 10% in initial air temperatures affected the predicted humidity by up to 21% and grain temperature and moisture content by up to 5%,

(iii) perturbations in the grain inlet temperature appeared to have less effect on the other variables than corresponding perturbations in the air temperature,

(iv) perturbations in the grain moisture content at the inlet were propagated throughout the bed i.e. with little change. This might be expected in view of the greater 'bulk' of the grain.

Overall, the results of the sensitivity analysis (not presented in detail in Table 8) would seem to indicate that values of the state variables are not significantly affected by small perturbations (e.g. small errors, perhaps due to physical measurements) in the inlet conditions.

Bed depth L (m.)	relative accuracy eps (%)	Initial step-size, H_o		
		0.020	0.010	0.005
0.4	1.0	113 (9)	113 (9)	131 (11)
	10^{-1}	177 (9)	177 (9)	155 (11)
	10^{-2}	257 (9)	257 (9)	239 (11)
	10^{-3}	433 (9)	365 (9)	335 (11)
	10^{-4}	1583 (31)	1583 (31)	1511 (31)
0.8	1.0	204 (14)	204 (14)	364 (16)
	10^{-1}	409 (14)	401 (14)	476 (16)
	10^{-2}	549 (14)	501 (14)	512 (16)
	10^{-3}	764 (16)	706 (14)	724 (16)
	10^{-4}	2143 (39)	2143 (39)	2071 (39)
1.6	1.0	451 (25)	493 (25)	630 (28)
	10^{-1}	866 (24)	*	970 (24)
	10^{-2}	1069 (24)	*	1001 (25)
	10^{-3}	1422 (26)	*	1127 (26)
	10^{-4}	*	*	*

Table 6. Number of derivative evaluations and knots for a variety of concurrent flow simulations.

(N.B. The asterisk (*) indicates that the required number of basic integration steps exceeded 50).

k	$\max_{x_j} \lvert d_{ki}(x_j) \rvert$				rd_{ki}			
	M	T	θ	H	M	T	θ	H
1	$.2\times10^{-4}$	.400	.230	$.1\times10^{-4}$	$.1\times10^{-3}$	$.8\times10^{-2}$	$.5\times10^{-2}$	$.3\times10^{-3}$
2	$.9\times10^{-5}$	.120	.078	$.6\times10^{-5}$	$.5\times10^{-4}$	$.3\times10^{-2}$	$.2\times10^{-2}$	$.1\times10^{-3}$
3	$.3\times10^{-5}$	.030	.019	$.2\times10^{-5}$	$.2\times10^{-4}$	$.6\times10^{-3}$	$.4\times10^{-3}$	$.5\times10^{-4}$
4	$.1\times10^{-5}$	.015	.010	$.9\times10^{-6}$	$.6\times10^{-5}$	$.3\times10^{-3}$	$.2\times10^{-3}$	$.2\times10^{-4}$
	$(.3\times10^{-4}$	.140	.060	$.2\times10^{-4}$	$.1\times10^{-3}$	$.2\times10^{-2}$	$.1\times10^{-2}$	$.5\times10^{-3}$

Table 7. Differences in the computed solution for various accuracies.

pert.	M		T		θ		H	
i.c.	+10%	-10%	+10%	-10%	+10%	-10%	+10%	-10%
M_o	12 (")	-12(")	-6(-4)	7 (6)	-7(-4)	8 (5)	7 (3)	-7(-4)
T_o	-6(-5)	5 (5)	4 (")	-4 (")	4(")	-5(")	21(13)	-19(-12)
θ_o	*	*	1 (")	-1 (")	1(")	-1(")	1 (")	-1 (")
H_o	*	*	*	*	*	*	2 (")	-2 (")

Table 8. Effects on the solution of perturbing individual initial conditions by ± 10%.

(Entries represent percentage relative changes of maximum magnitude followed by corresponding changes in outlet conditions (in parentheses). Quote marks (") indicate max. values at outlet point and asterisk (*) indicates values below 1%).

4.5 An Examination of the Contributions of the Various Energy Terms in the Model

A number of simulations, similar to that given in Table 4a, were carried out in order to determine the following:

(i) the relative magnitudes of various transfer terms on the right-hand sides of the system (4.1-2),

(ii) the effects, on the solution of system (4.1-2), of making various assumptions concerning the 'mean' evaporation temperature θ_v (see section 3.3).

Inclusion of the kinetic energy transfer terms due to moisture evaporation, i.e. $\frac{1}{2}mV_a^2$ and $\frac{1}{2}mV_p^2$ in equations (2.2-11,12), was found to produce a maximum difference of approximately 0.005% in any output value of the state variables. The effects due to the interaction force, $\underline{\phi}$, (see section 2.2), cannot, however, be so readily evaluated. Nonetheless, in view of the relatively low airflow rates involved, these effects were neglected in the current work. In any event, insufficient information was available to determine the form of ϕ.

Table 9 gives the approximate relative orders of magnitude of the various terms appearing in the energy balance equations. The given values represent the approximate maximum magnitudes as well as the maximum relative magnitudes, both of which occur near the inlet point and diminish with depth.

Table 10 illustrates the differences obtained in changing the value of θ_v from θ to T. The figures represent absolute differences followed by the percentage change in parentheses. Clearly, whilst the outlet conditions are little affected by these two extremes of choice for θ_v, the predicted maximum grain temperature may differ significantly (by as much as a few degrees for the given results c.f. the comment in section 4.3.

A number of models, particularly the earlier ones, do not fully take account of the 'sensible' heating terms $mc_v(\theta_v - T)$ and $-m(c_v\theta_v - c_w\theta)$. Taking $\theta_v = \theta$, the differences obtained by solving the model with and without these terms are summarised in Table 11. From this table it may be seen that the effects of neglecting these terms are of a comparable order to those given in Table 10.

θ_v	$h(T - \theta)$	$mc_v(\theta_v - T)$	mh_{fg}	$m(c_w\theta - c_v\theta_v)$
θ	10^7	10^4	10^6	10^6
T	10^7	0.0	10^6	10^6

Table 9. Relative magnitudes of transfer terms (units of J $m^{-3}s^{-1}$)

difference	M (% d.b.)	T (°C)	θ (°C)	H
maximum	-.22 (-1%)	1.05 (1.1%)	-3.25 (-8.7%)	4.5%
at outlet	-.05 (-.2%)	-.42 (0.9%)	-0.21 (-0.4%)	0.8%

Table 10. Effects of different assumptions for θ_v

difference	M (% d.b.)	T (°C)	θ(°C)	H
maximum	0.3 (1.5%)	2.6 (2.9%)	-0.66 (1.6%)	5.5%
at outlet	0.25(1.3%)	0.4 (0.9%)	0.42 (0.9%)	3.5%

Table 11. Effects of neglecting sensible heating terms.

CHAPTER FIVE: FIXED BED DRIER SIMULATION

Equations representing the general processes of heat and mass transfer in fixed bed grain drying are presented in section 3.1(a). In section 5.1.2 an analytical solution to a linearised form of the corresponding 'pure heat transfer' problem is obtained in terms of Bessel functions. This is shown to be a generalisation of a solution obtained previously by Klapp (1963). This solution is then utilised in section 5.1.3 in demonstrating a 'perturbation' type approach for obtaining a semi-analytical solution to the simultaneous heat and mass transfer problem, under further simplifying assumptions. In view of the restrictive nature of these assumptions and of the inordinate complexity of the solution, this approach is not, however, pursued further. Instead, a numerical solution is again sought.

The numerical algorithm devised for the solution of the fixed bed problem, and which makes use of a combination of existing techniques, is described in section 5.2.2. Its computer implementation is briefly described in section 5.2.3.

In section 5.3, the results of three validation simulations are presented in tabular/graphical form. These cases serve to both illustrate the nature of the solution to the fixed bed equations and to provide a comparison with both experimental and previously simulated results. Finally, in section 5.4, factors affecting the performance of the algorithm are discussed with reference to a set of sample simulations. In particular, some guidance is given on the effective use of the program FIXBED.

5.1 A Linearised Model

5.1.1 The Fixed Bed Equations

The 'characteristic form' (3.1-4,5), of the fixed bed equations (3.1-1), may be written, in terms of the transformed independent variables

$$\zeta = x \qquad \text{and} \qquad \eta = t - x/V_a,$$

in the form

$$G_a \frac{\partial H}{\partial \zeta} = m \tag{1}$$

$$\rho_p \frac{\partial M}{\partial \eta} = -m \tag{2}$$

$$G_a(c_a + c_v H) \frac{\partial T}{\partial \zeta} = -h(T - \theta) - mc_v(T - \theta_v) \tag{3}$$

$$\rho_p(c_p + c_w M) \frac{\partial \theta}{\partial \eta} = h(T - \theta) - m(h_{fg} + c_v\theta_v - c_w\theta) \tag{4}.$$

The lines η = constant and ζ = constant represent respectively the families C_1 and C_2 of straight line characteristics shown in Figure 2.

5.1.2 Solution of the Pure Heat Transfer Problem

Assuming that no mass transfer takes place, we have that

$$m = 0 \tag{5}.$$

Then, from (1) and (2), it follows that

$$H = H(\eta) \text{ only}, \quad \text{and} \quad M = M(\zeta) \text{ only}.$$

It will be assumed in what follows that

$$H = 0 \quad \text{and} \quad M = 0 \tag{6},$$

and the fixed bed problem reduces to consideration of the system of two partial differential equations

$$G_a c_a \frac{\partial T}{\partial \zeta} = -h(T - \theta) \tag{7}$$

and

$$\rho_p c_p \frac{\partial \theta}{\partial \eta} = h(T - \theta) \tag{8}.$$

Now in general it may be assumed that $h = h(T,\theta)$ and further that $h \in C^{1,1}$ i.e. that this function is continuously differentiable with respect to T and θ. In this case we may write

$$h(T - \theta) = f(T,\theta) = a + b(T - T_o) + c(\theta - \theta_o)$$

$$+ \quad O\left((T - T_o)^2, \ (\theta - \theta_o)^2\right) \qquad (9),*$$

where

$$a = f(T_o,\theta_o) = h(T_o,\theta_o)(T_o - \theta_o),$$

$$b = \frac{\partial f}{\partial T}\Big|_{(T_o,\theta_o)} \quad \text{and} \quad c = \frac{\partial f}{\partial \theta}\Big|_{(T_o,\theta_o)} .$$

It may then be assumed that, in a 'sufficiently small' neighbourhood of (T_o,θ_o), we may replace (9) by the 'bi-linear' approximation

$$f = a + b(T - T_o) + c(\theta - \theta_o). \qquad (10).$$

The system (7,8) may then be written

$$G_a c_a \frac{\partial T}{\partial \zeta} = - [a + b(T - T_o) + c(\theta - \theta_o)] \qquad (11)$$

and

$$\rho_p c_p \frac{\partial \theta}{\partial \eta} = \quad a + b(T - T_o) + c(\theta - \theta_o) \qquad (12).$$

Now, introducing dimensionless independent variables X and τ through

$$X = \frac{h_o \zeta}{c_a G_a} \quad , \qquad \tau = \frac{h_o \eta}{\rho_p c_p} \qquad (13),$$

where $h_o = h(T_o,\theta_o)$, and dimensionless temperature ratios, T_R and θ_R through

* The order symbol has the meaning given in section 4.1.1.

$$T_R = \frac{T - \theta_o}{T_o - \theta_o} \quad , \qquad \theta_R = \frac{\theta - \theta_o}{T_o - \theta_o} \qquad (14),$$

equations (11,12) may be written in the form

$$\frac{\partial T_R}{\partial X} + BT_R + C\theta_R = -(1 - B) \qquad (15)$$

and

$$\frac{\partial \theta_R}{\partial \tau} - BT_R - C\theta_R = 1 - B \qquad (16),$$

where $B = b/h_o$ and $C = c/h_o$. The boundary/initial conditions corresponding to this dimensionless formulation are then

$$T_R(0,\tau) = 1 \quad \text{and} \quad \theta_R(X,0) = 0 \qquad (17)$$

respectively.

Now taking Laplace transforms of (15,16) with respect to X, and making use of (17), gives

$$(p + B)\bar{T}_R + C\bar{\theta}_R = 1 - p^{-1}(1 - B) \qquad (18)$$

and

$$\frac{\partial \bar{\theta}_R}{\partial \tau} - B\bar{T}_R - C\,\bar{\theta}_R = p^{-1}(1 - B) \qquad (19),$$

where $\bar{\theta}_R(p,\tau) = \int_o^\infty \theta_R(t,\tau)\exp(-pt)\,dt.$

Then (18,19) yield

$$\frac{\partial \bar{\theta}_R}{\partial \tau} - \frac{Cp}{p + B}\,\bar{\theta}_R = (p + B)^{-1} \quad ,$$

which has the solution

$$\bar{\theta}_R(p,\tau) = \int_o^\tau (p + B)^{-1}\exp\left[\frac{Cp}{p + B}\,(\tau - t)\right] dt \qquad (20).$$

Now making use of relationships for the inverse Laplace transform, as given for example in Erdélyi et al (1954), it may be shown from (20) that

$$\theta_R(X,\tau) = \begin{cases} (-BC)^{-1} \int_o^{(-BC)\tau} \exp(-\frac{t}{B} - BX)\, I_o(2\sqrt{Xt})\, dt, & \text{for } BC < 0 \\ (BC)^{-1} \int_o^{(BC)\tau} \exp(\frac{t}{B} - BX)\, J_o(2\sqrt{Xt})\, dt, & \text{for } BC > 0 \end{cases} \qquad (21).$$

Substituting these results into (18), it may then be shown that

$$T_R(X,\tau) = -\frac{(1-B)}{B} + \frac{e^{-BX}}{B} - \begin{cases} B^{-1} \int_o^{(-BC)\tau} e^{-\frac{t}{B} - BX}\, I_1(2\sqrt{Xt})\sqrt{\frac{X}{t}}\, dt, & \text{for } BC < 0 \\ B^{-1} \int_o^{(BC)\tau} e^{\frac{t}{B} - BX}\, J_1(2\sqrt{Xt})\sqrt{\frac{X}{t}}\, dt, & \text{for } BC > 0 \end{cases} \qquad (22).$$

In (21,22) the functions $J_\nu(z)$, and $I_\nu(z)$, representing respectively the Bessel function and modified Bessel function of the first kind, of order ν, are defined by

$$J_\nu(z) = (\tfrac{1}{2}z) \sum_{m=0}^{\infty} \frac{(-1)^m (\tfrac{1}{2}z)^{2m}}{m!\ (\Gamma+m+1)}, \quad I_\nu(z) = \sum_{m=0}^{\infty} \frac{(\tfrac{1}{2}z)^{\nu+2m}}{m!\Gamma(\nu+m+1)},$$

and where

$$\Gamma(m+1) = m!, \quad \text{for integral } m > 0.$$

For the applications considered in this work, an expression of the form (A-5) is usually assumed for the volumetric heat transfer coefficient, h. Furthermore, for the fixed bed applications considered, it is assumed that

$$T(x,t) > \theta(x,t),$$

although this is not always necessarily the case. It readily follows from these assumptions that

$$b > 0 \quad \text{and} \quad c < 0,$$

and hence that the appropriate expressions for θ_R and T_R are given by the first of these in both (21) and (22).

In particular, if we take

$$B = 1 \quad \text{and} \quad C = -1,$$

corresponding to

$$f = h_o(T - \theta),$$

where $h = h_o$, assumed constant, these expressions reduce to

$$\theta_R(X,\tau) = \int_o^\tau e^{-t-X} I_o(2\sqrt{Xt})\, dt \qquad (23)$$

and

$$T_R(X,\tau) = e^{-X} - \int_o^\tau e^{-t-X} I_1(2\sqrt{Xt}) \sqrt{\frac{X}{t}}\, dt \qquad (24)$$

This special case was considered by Klapp (1963), who obtained expressions of the form (23,24) under the assumption of constant h.

For pure heat transfer problems in which it may be assumed that an appropriate volumetric heat transfer coefficient is given by $h(T,\theta)$ as defined above, (21,22) represent a 'local' approximation to the analtyical solution of (7,8). This approximation, however, is only valid within an 'appropriately small' neighbourhood of the 'point' (T_o,θ_o) (c.f. comment in section 4.1).

5.1.3 A Solution of the Simultaneous Heat and Mass Transfer Problem

Inclusion of the mass transfer terms in equations (1-4) further complicates the problem of finding a solution to this system. Instead, therefore, of proceeding in the same manner as for the pure heat transfer problem, some simplifying assumptions will firstly be made.

The following local approximations will be assumed to hold in

some neighbourhood of the point (x_o, t_o) (initially the origin):

(i) The 'composite' specific heats of moist air and moist grain are given by

$$c_a + c_v H = \bar{c}_a \qquad \text{and} \qquad c_p + c_w M = \bar{c}_p \qquad (25),$$

where $\bar{c}_a$, $\bar{c}_p$ are constant.

(ii) Terms due to 'sensible' heating of air and grain are 'small' in magnitude as compared to those representing latent heat of vaporisation/condensation and 'convective' heat transfer. (A typical comparison of the relative orders of magnitude of such terms is presented for a concurrent flow drier simulation in Table 9, section 4.5).

Furthermore, in view of differences in magnitude of terms of the same order of magnitude (not readily apparent from the table), it will be assumed that cancellation does not affect the overall order of magnitude of the right hand sides of (3) and (4). These assumptions may be briefly stated as

$$\left.\begin{aligned} |mc_v(T - \theta_v)| \;\; &<< \;\; |h(T - \theta)| \quad \text{in (3)} \\ \text{and} \qquad\qquad & \\ |m(c_v\theta_v - c_w\theta)| \;\; &<< \;\; \min\{\, |mh_{fg}| \,,\, |h(T - \theta)|\,\} \\ & \qquad\qquad \text{in (4)} \end{aligned}\right\} \qquad (26).$$

(iii) The heat and mass transfer coefficients are piecewise constant,

$$\text{i.e.} \qquad k = k_o \quad \text{and} \quad h = h_o, \quad \text{say} \qquad (27).$$

Under assumptions (i) - (iii), the fixed bed equations, (1)-(4), become

$$\left.\begin{aligned} G_a \frac{\partial H}{\partial \zeta} &= \rho_p k_o (M - M_e) \\ \rho_p \frac{\partial M}{\partial \eta} &= -\rho_p k_o (M - M_e) \\ G_a \bar{c}_a \frac{\partial T}{\partial \zeta} &= -h_o (T - \theta) \\ \rho_p \bar{c}_p \frac{\partial \theta}{\partial \eta} &= h_o (T - \theta) - \rho_p k_o (M - M_e) h_{fg} \end{aligned}\right\} \qquad (28).$$

Now, in addition to (13,14), introducing dimensionless dependent variables

$$M_R = \frac{h_{fg} M}{\bar{c}_p (T_o - \theta_o)} \quad , \qquad H_R = \frac{h_{fg} H}{\bar{c}_a (T_o - \theta_o)} \qquad (29)$$

and dimensionless function

$$M_{eR} = \frac{h_{fg} M_e}{\bar{c}_p (T_o - \theta_o)} \qquad (30),$$

equations (28) may be written in the form

$$\frac{\partial H_R}{\partial X} = \gamma (M_R - M_{eR}) \qquad (31)$$

$$\frac{\partial M_R}{\partial \tau} = -\gamma (M_R - M_{eR}) \qquad (32)$$

$$\frac{\partial T_R}{\partial X} + T_R - \theta_R = 0 \qquad (33)$$

$$\frac{\partial \theta_R}{\partial \tau} - T_R + \theta_R = -\gamma (M_R - M_{eR}) \qquad (34),$$

where

$$\gamma = \frac{\rho_p \bar{c}_p k_o}{h_o} \qquad (35).$$

Assuming constant inlet air conditions and uniform initial grain conditions, the boundary/initial conditions for the dimensionless formulation (31-34) are

$$\left.\begin{aligned} T_R(0,\tau) &= 1, \quad H_R(0,\tau) = H_{Ro}, \text{ constant} \\ \text{and} \\ \theta_R(X,0) &= 0, \quad M_R(X,0) = M_{Ro}, \text{ constant} \end{aligned}\right\} \qquad (36).$$

A 'perturbation' approach is now adopted to find a solution to this problem. Firstly, it is assumed, for small values of the parameter γ, that each of the dependent variables may be represented by a

* Not to be confused with the previously defined moisture ratio, MR.

series expansion i.e.

$$\left.\begin{aligned} H_R(X,\tau) &= \sum_{m=0}^{\infty} \gamma^m H_{R,m}(X,\tau) \\ M_R(X,\tau) &= \sum_{m=0}^{\infty} \gamma^m M_{R,m}(X,\tau) \\ T_R(X,\tau) &= \sum_{m=0}^{\infty} \gamma^m T_{R,m}(X,\tau) \\ \theta_R(X,\tau) &= \sum_{m=0}^{\infty} \gamma^m \theta_{R,m}(X,\tau) \end{aligned}\right\} \quad (37).$$

In addition, in view of (A-3,4), it is assumed that

$$M_{eR}(X,\tau) = \sum_{m=0}^{\infty} \gamma^m M_{eR,m}(X,\tau) \quad (38).$$

In (37,38), $H_{R,m}$ etc. are sequences of linearly independent functions.

Substituting these expansions into equations (31-34) yields

$$\left.\begin{aligned} \sum_{m=0}^{\infty} \gamma^m \frac{\partial H_{R,m}}{\partial X} &= \sum_{m=0}^{\infty} \gamma^{m+1}(M_{R,m} - M_{eR,m}) \\ \sum_{m=0}^{\infty} \gamma^m \frac{\partial M_{R,m}}{\partial \tau} &= -\sum_{m=0}^{\infty} \gamma^{m+1}(M_{R,m} - M_{eR,m}) \\ \sum_{m=0}^{\infty} \gamma^m \left\{\frac{\partial T_{R,m}}{\partial X} + T_{R,m} - \theta_{R,m}\right\} &= 0 \\ \sum_{m=0}^{\infty} \gamma^m \left\{\frac{\partial \theta_{R,m}}{\partial \tau} - T_{R,m}\ \theta_{R,m}\right\} &= -\sum_{m=0}^{\infty} \gamma^{m+1}(M_{R,m} - M_{eR,m}) \end{aligned}\right\} \quad (39).$$

The sum of the first n terms in each of the series expansions (37) is then taken as the nth approximation to the solution of (31-34), subject to (36), i.e.

$$H_R^{(n)}(X,\tau) = \sum_{m=0}^{n} \gamma^n H_{R,m}(X,\tau) \quad \text{etc.}$$

Successive approximations may be found by solving the systems of

differential equations obtained from a comparison of the coefficients of ascending powers of γ on both sides of equations (39). Thus for a 'zeroth' approximate solution:

comparing coefficients of γ^o gives

$$\left.\begin{aligned} \frac{\partial H_{R,O}}{\partial X} &= 0 \\ \frac{\partial M_{R,O}}{\partial \tau} &= 0 \\ \frac{\partial T_{R,O}}{\partial X} + T_{R,O} - \theta_{R,O} &= 0 \\ \frac{\partial \theta_{R,O}}{\partial \tau} - T_{R,O} + \theta_{R,O} &= 0 \end{aligned}\right\} \qquad (40)$$

The boundary/initial conditions corresponding to system (40) are

$$\left.\begin{aligned} T_{R,O}(0,\tau) = 1, \quad H_R(0,\tau) = H_{R,O} \\ \theta_{R,O}(X,0) = 0, \quad M_{R,O}(X,0) = M_{R,O} \end{aligned}\right\} \qquad (41).$$

and

The system (40,41) represents the pure heat transfer problem (15-17), with $B = 1$ and $C = -1$, and with solution $\theta_{R,O}(X,\tau)$ and $T_{R,O}(X,\tau)$ given by (23) and (24) respectively.

For a 'first' approximate solution:

comparing coefficients of γ^1 gives

$$\left.\begin{aligned} \frac{\partial H_{R,1}}{\partial X} &= M_{R,O} - M_{eR,O} \\ \frac{\partial M_{R,1}}{\partial \tau} &= -(M_{R,O} - M_{eR,O}) \\ \frac{\partial T_{R,1}}{\partial X} + T_{R,1} - \theta_{R,1} &= 0 \\ \frac{\partial \theta_{R,1}}{\partial \tau} - T_{R,1} + \theta_{R,1} &= -(M_{R,O} - M_{eR,O}) \end{aligned}\right\} \qquad (42).$$

The boundary/initial conditions corresponding to this system are

$$\left.\begin{aligned} T_{R,1}(0,\tau) &= 0, \qquad H_{R,1}(0,\tau) = 0 \\ \theta_{R,1}(X,0) &= 0, \qquad M_{R,1}(X,0) = 0 \end{aligned}\right\} \qquad (43).$$

Now since the right-hand sides of system (42) are functions of the (known) zeroth solution, this system may be solved in similar fashion to system (40). The 'first' approximate solution, i.e. first partial sum

$$H_R^{(1)}(X,\tau) = H_{R,0} + H_{R,1} \quad \text{etc.} ,$$

is then obtained with the aid of (23,24), and may be written

$$\left.\begin{aligned} H_R^{(1)}(X,\tau) &= H_{Ro} + \gamma \int_0^X f(x,\tau)\, dx \\ M_R^{(1)}(X,\tau) &= M_{Ro} - \gamma \int_0^\tau f(X,t)\, dt \\ T_R^{(1)}(X,\tau) &= e^{-X} + \int_0^\tau e^{-t-X} \sqrt{\frac{X}{t}}\, I_1(2\sqrt{Xt})\, dt \\ &\quad + \gamma \int_0^\tau \int_0^X e^{-t-X+u}\, f(u,\tau-t)\, I_o(2\sqrt{(X-u)t})\, du\, dt \\ \theta_R^{1}(X,\tau) &= \int_0^\tau e^{-t-X}\, I_o(2\sqrt{Xt})\, dt + \gamma \int_0^\tau \int_0^X e^{-t} f(u,\tau-t)\, du\, dt \\ &\quad + \int_0^\tau \int_0^X e^{-t-X+u} f(u,\tau-t)\, I_1(2\sqrt{t(X-u)}) \sqrt{\frac{t}{X-u}}\, du\, dt \end{aligned}\right\} \qquad (44)$$

where

$$f(X,\tau) = M_{R,0} - M_{eR,0} \quad .$$

Clearly, solutions such as (44) require the use of suitable numerical integration techniques for their evaluation. In view, however, of the various simplifying assumptions made in setting up the system (28), such approximate solutions must be of limited value. Therefore, the approach described in this section was not pursued further.

5.2 An Algorithm for the Numerical Solution of the Fixed Bed Model

5.2.1 Preliminary Considerations

Before devising a scheme for the numerical solution of the fixed bed equations, the available literature on the numerical solution of hyperbolic equations was briefly surveyed. The results of this survey are not presented here. The schemes considered, however, include the well-known implicit Lax-Wendroff method. This technique (see e.g. Smith (1978)) is of second-order accuracy and is unconditionally stable. The scheme may be re-written in explicit form in view of the known boundary/initial conditions. The work of Hackbusch (1977a,b), who devised extrapolation techniques for some discretisations was also given consideration. None of the schemes considered, however, appear to combine accuracy and stability with a ready facility for incorporating a suitably simple step-control mechanism.

A number of problems concerning the 'feasibility' of predicted air and grain states arise in attempting to simulate fixed bed grain drying. A detailed treatment of these is beyond the scope of the present work. However, it is noted that some such problems are caused, at least in part, by possible inconsistencies in the forms of constitutive equations (see e.g. the discussion in section 4.3). Clearly, any assumptions made in the derivation of the model, together with inaccuracies propagated in finding an approximate solution, also contribute to the prediction of 'infeasible state points'.

Inaccurate prediction of both temperatures and moisture contents of air and grain can lead to thermodynamic inconsistencies. For example, in drying moist grain with air at a higher temperature, it is possible, particularly in regions of high temperature gradients, for the predicted grain temperature to 'overshoot' that of the air. This problem is much more likely to arise, however, in concurrent flow drier simulation and was catered for in the program CONFLO, described in section 4.2.5.

A second problem is that of predicting relative humidities outside of the range $0.0 \leqq \phi \leqq 1.0$. This event has been catered for in a number of different ways by different workers. For example, Thompson et al (1968) incorporated a 'condensation' procedure in their model.

On the other hand, Nellist (1974) used an iterative scheme to adjust the predicted values of his state variables so that a prescribed maximum relative humidity resulted. In CONFLO this problem was solved by nominally setting $\phi = 1-\varepsilon$, where ε is some small preset tolerance. In both of the above problems, the current integration step is then repeated with a smaller step-size. Such an approach was found to give feasible predictions in all cases.

In view of the above discussion and the satisfactory results obtained for the concurrent flow case, it was decided to incorporate a modified version of the scheme described in section 4.2 in an algorithm for the numerical solution of the fixed bed model.

5.2.2 The Numerical Algorithm

The general scheme for adaptive numerical integration of the fixed bed equations is described with reference to Figure 10.

It is firstly assumed that the solution is known along the characteristic $C_{1,j}$, in terms of cubic spline parameters determined at the previous integration step (see description below). The current integration step is then as follows:

1. Grain boundary conditions, i.e. values for $M(0,t)$ and $\theta(0,t)$ are obtained by integration of equations (3.1-5) along the characteristic $C_{2,o}$ i.e. Ot. Values for all 4 state variables are then known at $(0,t_{j+1})$ - see description of integration along the C_2 characteristics below.

2. Equations (3.1-4) are integrated along the C_1 characteristic $C_{1,j+1}$ through the point $(0,t_{j+1})$, defined by

$$x = V_a(t - t_{t+1}), \qquad (1)$$

for the air state variables $H(x,t)$ and $T(x,t)$, throughput the grain bed.

The technique employed for integration along the C_1 characteristics is the modified midpoint rule with polynomial extrapolation, described in sec.4.2.3. In this case, however, only two ordinary differential equations are integrated.

In order to evaluate the right-hand side functions, b_1 and b_3, of system (3.1-4) at any point along $C_{1,j+1}$, it is necessary, in view of the constitutive assumptions discussed in section 3.3, to know values of all the dependent variables, H, M, T and θ at that point. The integration scheme, which is explicit in nature, demands the evaluation of these functions at an (initially) indeterminate number of points over each basic integration interval. The actual number of such function evaluations is determined by the 'convergence' criteria discussed in section 4.2 and, in particular, by the extrapolation sequence F_1 given in (4.2-15).

Values for H and T are naturally obtained in the course of the integration. Values for M and θ must, however, be obtained by integrating system (3.1-5) along the appropriate C_2 characteristics i.e. for all values of x corresponding to the intermediate integration points, x_s, say, where $s = 1,2,\ldots$.

The scheme employed for integration along a typical C_2 characteristic, say $C_{2,s}$ is as follows. Firstly, values of all four dependent variables are obtained at (x_s,t_j) using the cubic spline fit along $C_{1,j}$. These are required for the evaluation of the right-hand side functions b_2 and b_4 of system (3.1-5). The basic Euler method, given by

$$\underline{v}_{j+1}^{(0)} = \underline{v}_j + k\underline{f}\,(\underline{u}_j) \quad , \qquad (2)$$

where $\underline{v}_j = (M,\theta)^T$, $\underline{u}_j = (H,M,T,\theta)^T$ and $\underline{f} = (b_2,b_4)^T$,

all evaluated at (x_s,t_j), and where $k = t_{j+1} - t_j$,

is used as a 'predictor' to obtain a first approximation to the grain state variables at the point (x_s,t_{j+1}). An improved value for $\underline{u}_{j+1}$ is then obtained using the improved Euler (trapezoidal) scheme

$$\underline{v}_{j+1}^{(n+1)} = \underline{v}_j^{(n)} + k/2\,(\underline{f}^{(n)}(\underline{u}_j) + \underline{f}^{(n)}(\underline{u}_{j+1})) \qquad (3),$$

$$n = 0,1,2,\ldots .$$

Equation (3) is then used iteratively to obtain a sequence of improved approximations to M and θ.

Then, if the 'adaptive option' is chosen (see section 5.2.3), the following additional steps are executed:

3. Step 2 is repeated taking two half time steps. Firstly an approximate solution along the characteristic $C_{1,j+1/2}$ is obtained as described above but taking $k=k/2$. The solution along $C_{1,j+1}$ is then obtained by integrating in the same manner from $C_{1,j+1/2}$.

4. The two approximate solutions, $\underline{u}_{j+1}(x;k)$ and $\underline{u}_{j+1}(x;k/2)$, say, along $C_{1,j+1}$, are then compared to determine whether any step adjustment is necessary for the time-wise integrations. This comparison may be affected in a number of ways. In testing out this algorithm, however, relative error tests were implemented as follows.

Interpolated values of both approximate solutions are firstly obtained at a number of equidistant points $x=x_i = iL/N$, $i=1,2,..N$, along $C_{1,j+1}$, where N is some prescribed integer. The resulting 'vectors' of values for the dependent variables, obtained with time-step k, will be written

$$\underline{u}^{\ell}_{j+1}(k) = [u^{\ell}_{j+1,1}(k), u^{\ell}_{j+1,2}(k), \ldots, u^{\ell}_{j+1,N}(k)]^T, \quad 1=1,..4,$$

with a similar notation for the 'half-step' values.

The following inequality is then used as the basis for controlling the time-step, k.

$$\left\| \underline{u}^{\ell}_{j+1}(k) - \underline{u}^{\ell}_{j+1}(k/2) \right\| \leq \varepsilon \left\| \underline{u}^{\ell}_{j+1}(k/2) \right\| \qquad (4)$$

$$\text{for } \ell = 1, \ldots, 4,$$

where ε is a prescribed 'tolerance factor'. In (4) both 2 (Euclidean) and ∞ (maximum) 'discrete' norms $\| \cdot \|$ were used.

If (4) is not satisfied, with $\varepsilon = \varepsilon'$, say then the step is halved i.e. $k=k/2$ and the integration re-started from $C_{1,j}$. If the inequality is satisfied with $\varepsilon = 10^{-\tau}\varepsilon'$, then, provided

that the prescribed termination conditions for the simulation are not satisfied (see section 5.2.3), the time-step is increased i.e. k=1.5*k and j=j+1. If, however, the interval inequality

$$10^{-\tau}\varepsilon' \leqq \left\| \underline{u}^{\ell}_{j+1}(k) - \underline{u}^{\ell}_{j+1}(k/2) \right\| \Big/ \left\| \underline{u}^{\ell}_{j+1}(k/2) \right\| \leqq \varepsilon'$$

is satisfied, then the current time-step k is retained and $j=j+1$. In the latter two cases, $\underline{u}_{j+1}(x;k/2)$ is taken as the solution along $C_{1,j+1}$. In all three cases steps 1 to 4 are then repeated.

In testing the 'timewise' adaptive option described in steps 3 and 4, a variety of values were taken for both the exponent τ and tolerance ε'. Only limited success was, however, obtained with this option (see further comment in section 5.4).

Interpolation of the solution is achieved through the parametric representation of each of the state variables along a given characteristic, in terms of its cubic spline parameters. The basic form of this cubic is given by the Hermite interpolation formula (4.2-18). The values u_i in this formula represent the solution at the knots or ends of each basic integration range. In the concurrent flow case, the required derivative values, m_i, are obtained during the course of each integration. In the fixed bed case, however, values for the derivatives of M and θ are only obtained along the C_2 characteristics. Approximations to the derivatives of the grain state variables along C_1 characteristics must therefore be obtained by other means.

The theory of splines as used here is adequately described in Ahlberg et al (1967). Using the notation of section 4.2.4, however, it is noted that, for (4.2-18) to be defined over the N intervals along a C_1 characteristic it is necessary to provide values for the $N+1$ parameters m_i, $i=0,1,...N$. Applying the constraint of second derivative continuity at each of the interior knots x_i, $i=1,2,...N-1$, gives $N-1$ equations in these parameters. The remaining two conditions required to uniquely determine the m_i are usually obtained from some 'difference approximation' at either end of the range. In the present implementation of the algorithm, the following simple 'weighted average' derivative approximations are used

$$2m_0 + m_1 = 3/h_1(u_1 - u_0)$$

$$m_{N-1} + 2m_N = 3/h_N(u_N - u_{N-1}) \qquad (5).$$

(see e.g. Ahlberg et al). These end conditions may of course be replaced by other, more accurate formulae. The choice (5), however, facilitates writing the system of linear equations for the m_i's in the tri-diagonal form

$$A\underline{m} = \underline{d} \qquad (6),$$

where the matrix A is given by

$$A = \begin{bmatrix} b_0 & c_0 & & & & \\ a_1 & 2 & c_1 & & & \\ & a_2 & 2 & c_2 & & \\ & & \cdot & \cdot & \cdot & \\ & & & \cdot & \cdot & \\ & & & a_{N-1} & 2 & c_{N-1} \\ & & & & a_N & b_N \end{bmatrix}$$

The elements of A are given by

$$b_0 = 2 = b_N, \quad a_N = 1 = c_0,$$

$$a_j = h_{j+1}/(h_j + h_{j+1}), \quad c_j = h_j/(h_j + h_{j+1}), \quad j = 1,2,\ldots N-1.$$

The right-hand side vector $\underline{d} = [d_0, d_1, \ldots, d_N]^T$, has elements

$$d_0 = 3(u_1 - u_0)/h_1 ,$$

$$d_j = 3a_j(u_j - u_{j-1})/h_j + 3c_j(u_{j+1} - u_j)/h_{j+1}, \quad j=1,\ldots N,$$

$$d_N = 3(u_N - u_{N-1})/h_N ,$$

and the vector of spline parameters to be determined is $\underline{m} = [m_0, m_1, \ldots, M_N]^T$.

Now the matrix A is diagonally dominant and irreducible (see e.g. Forsythe and Moler (1967)) and hence for a system such as (6) there exists a particularly simple elimination algorithm without pivoting. This may be written as follows (see e.g. Ahlberg et al).

To perform the elimination:

set $q_{-1} = 0 = r_{-1}$,

then, for $k = 0,1,\ldots,N$, evaluate

$$p_k = a_k q_{k-1} + b_k,$$

$$q_k = -c_k/p_k,$$

$$r_k = (d_k - a_k r_{k-1})/p_k.$$

The m_i's are then evaluated successively from

$$m_N = r_N$$

$$m_i = m_{i+1} q_i + r_i, \quad \text{for} \quad i = N-1,N-2,\ldots 0 .$$

The above procedure is carried out to obtain the spline parameters of each of the four dependent variables. In view of the comments in section 4.2.4 comparable accuracy might be obtained using the approximate derivatives of H and T evaluated in the course of the integration. Since, however, the time required to compute $\underline{m}$ is negligible as compared to that required to perform an integration step, this economy was considered not to be worthwhile.

The path of the first 'front' of air through the grain bed is represented by the characteristic $C_{1,1}$. That region of the x-t plane bounded by this line, the line x=L, and Ox, is a 'constant state' region for the grain (see comment in section 3.1(a)). The air state along $C_{1,1}$ is therefore determined by the initial grain conditions. Thus initial conditions for the problem are obtained by solving system (3.1-4), subject to (3.1-6).

In view of its mixed nature, the overall integration scheme

described above is not amenable to any of the standard analyses. Some aspects of stability and convergence for the modified midpoint scheme were briefly discussed in section 4.2.3. With regard to the 'predictor-corrector' type scheme employed for 'timewise' integrations, stability will generally depend upon the (improved Euler) corrector. Convergence of the scheme only depends on the derivatives of M and θ satisfying an appropriate Lipschitz condition, which these functions may clearly be assumed to do. In addition, both formulae (2,3) may easily be shown to be relatively stable in the usual sense.

The above comments apply to the two integration techniques used separately. To maintain stability of the computed solution in the overall scheme, it is necessary to compute the solution to a relatively high degree of accuracy along the C_1 characteristics. Any growth in the absolute error due to the midpoint scheme will then be sufficiently small to facilitate 'convergence' of the timewise integrations. Clearly, the level of required accuracy will depend, in part, on the duration of drying. More will be said in quantitative terms about the choice of accuracy levels in section 5.4.

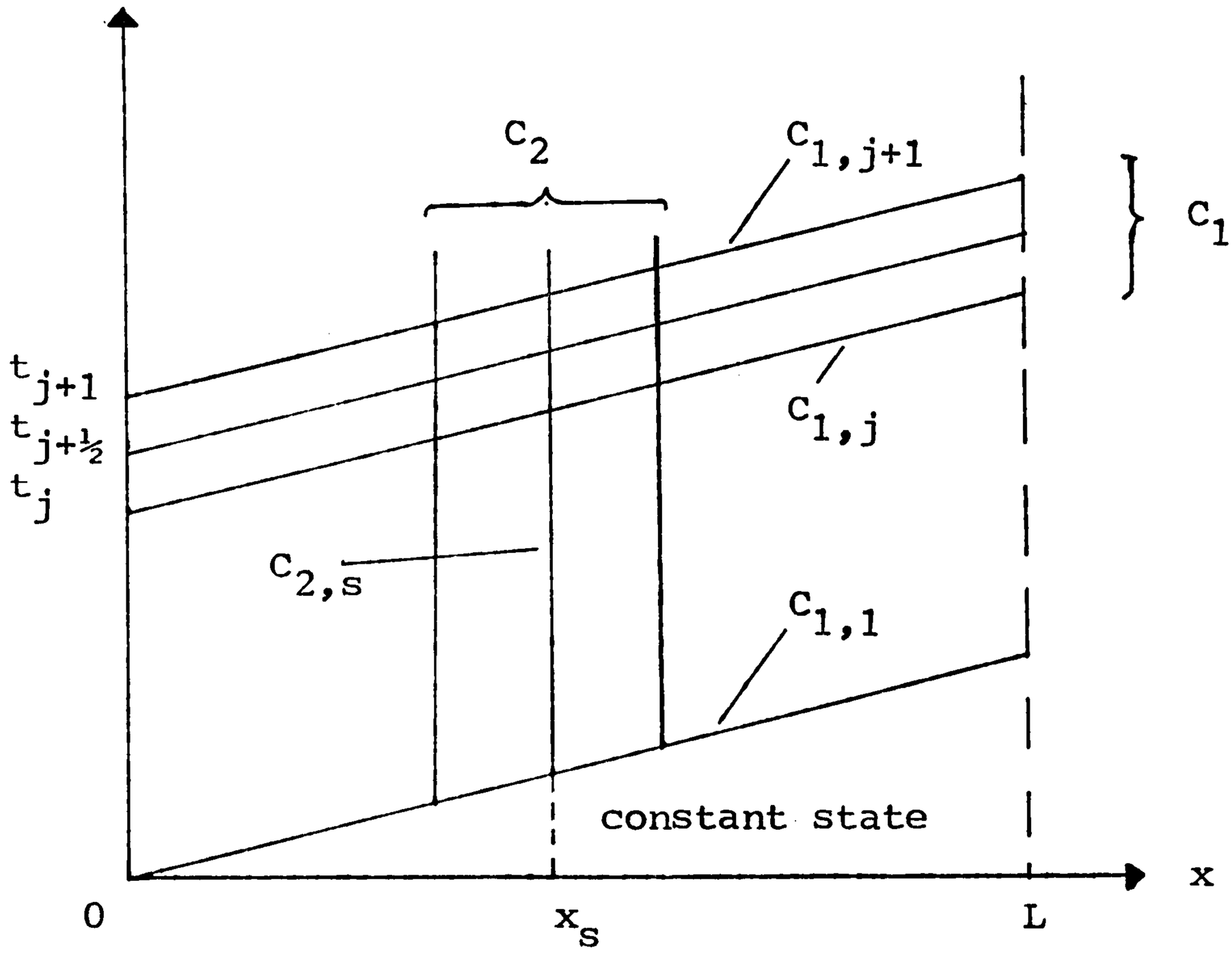

Figure 10. Characteristic grid for integration of the fixed bed equations.

5.2.3 Computer Implementation of the Algorithm

The algorithm described in section 5.2.2 has been implemented as the FORTRAN program FIXBED. As in the case of CONFLO, a separate program, FBPLOT, has been written to produce graphical output of a simulation c.f. comment in 4.2.5. The two programs have been fully documented in Parry (1983c) and a cursory description only is presented here.

The program FIXBED comprises a MAIN segment together with four main subroutines. These subroutines pass control to a further thirteen subroutines and seven function subprograms. The relationship between these segments is schematically indicated in Figure 11. Much of the structure of the program CONFLO, as illustrated in Figure 7, has been preserved in FIXBED. However, various additional features have, of necessity, been added.

The MAIN setment firstly calls SUBROUTINE IPDATA to read data from a user-written file. Input data is appropriately modified and any additional data required is set up for later use. For example, the required air density ρ_a is computed using the inlet air temperature and atmospheric pressure. The main computational part of the program is then effected through a call to SUBROUTINE SOLVDE. Final results are output via subroutines OPHEAD and OPSOLN, which perform the same functions as subroutines OPHEAD and OPFILE respectively in CONFLO.

Boundary conditions and initial conditions are set up in subroutines BCDNS and ICDNS respectively. In the present implementation, inlet air conditions are assumed constant and initial grain conditions uniform throughout the bed. Varying inlet conditions may be easily catered for by appropriate changes to BCDNS. If, however, varying initial conditions are to be admitted, some minor changes are required in both subroutines ICDNS and SOLVEX, in which the solution is propagated along C_1 characteristics.

The basic integration intervals along the C_1 characteristics are determined by the modified midpoint scheme implemented in SOLVEX. The latter therefore calls SUBROUTINE SOLVET to obtain the requisite values

of M and θ as described in step 2, section 5.2.2. The right-hand sides of systems (3.1-4) and (3.1-5) are evaluated in subroutines DERIVX and DERIVT respectively. At the end of each complete integration along a C_1 characteristic, the spline parameters m_i, i=0,1,...N, are evaluated in SUBROUTINE SPLINE, by solving system (6). These are stored in a real array for later use.

The individual functions of the 'suite' of six function subprograms (see Figure 11) representing transfer rates and psychrometric relationships are the same as for CONFLO (see section 4.2.5).

In SUBROUTINE COMPAR, the approximate solution obtained taking a time-step k, say, is compared with that obtained taking a step of k/2, as described in step 4. Values of H, M, T and θ are interpolated at the required bed depths in SUBROUTINE SPLINT using the cubic spline parameters evaluated in SPLINE. The arrays required for storing these parameters are updated after each time-step in SUBROUTINE UPDATE.

After each time-step, diagnostic and plotting information is written to the appropriate output files by subroutines OPINFO and OPPLOT respectively. The diagnostic information includes a measure of the average moisture content of the grain at the current time, evaluated in FUNCTION AVERMC.

Finally, on completion of a simulation, interpolated values of the dependent variables are obtained, at the required depths, in SUBROUTINE INTERP.

The user-created input data file must contain the specific and latent heats and atmospheric pressure, as for CONFLO. Either the mass flow rate or the corresponding speed must be specified along with the void ratio . The bulk grain density must be given, although that of the air is computed in IPDATA. In the present implementation, the (constant) air inlet and initial grain conditions must be specified in the input data file. Finally, the bed depth and percentage relative local accuracy, and, in the current implementation, the number of (equal) intervals at which output is required of the results at the completion of drying, must be specified.

In addition to the fixed set of data input values described above, a number of parameters may be input to determine which of the various options are effected. The program may be run according to the scheme outlined in steps 1-4 i.e. as a fully adaptive scheme. Alternatively, it may be run with equal-interval time-steps, specified by the user. This option is intended largely to allow for a less accurate, though often speedier solution to the equations which might be required in the initial stages of an investigation.

Options exist to simulate a drying run of fixed duration or one which terminates when a specified average moisture content has been attained throughout the bed. If the second option is chosen, a 'target' moisture content must be supplied. In either case, a maximum run time for the simulation must be specified. A further option allows for the addition of a 'conditioning' period in which, for example, cooling of the grain with ambient air may be simulated. In this case, the new inlet air conditions must be specified.

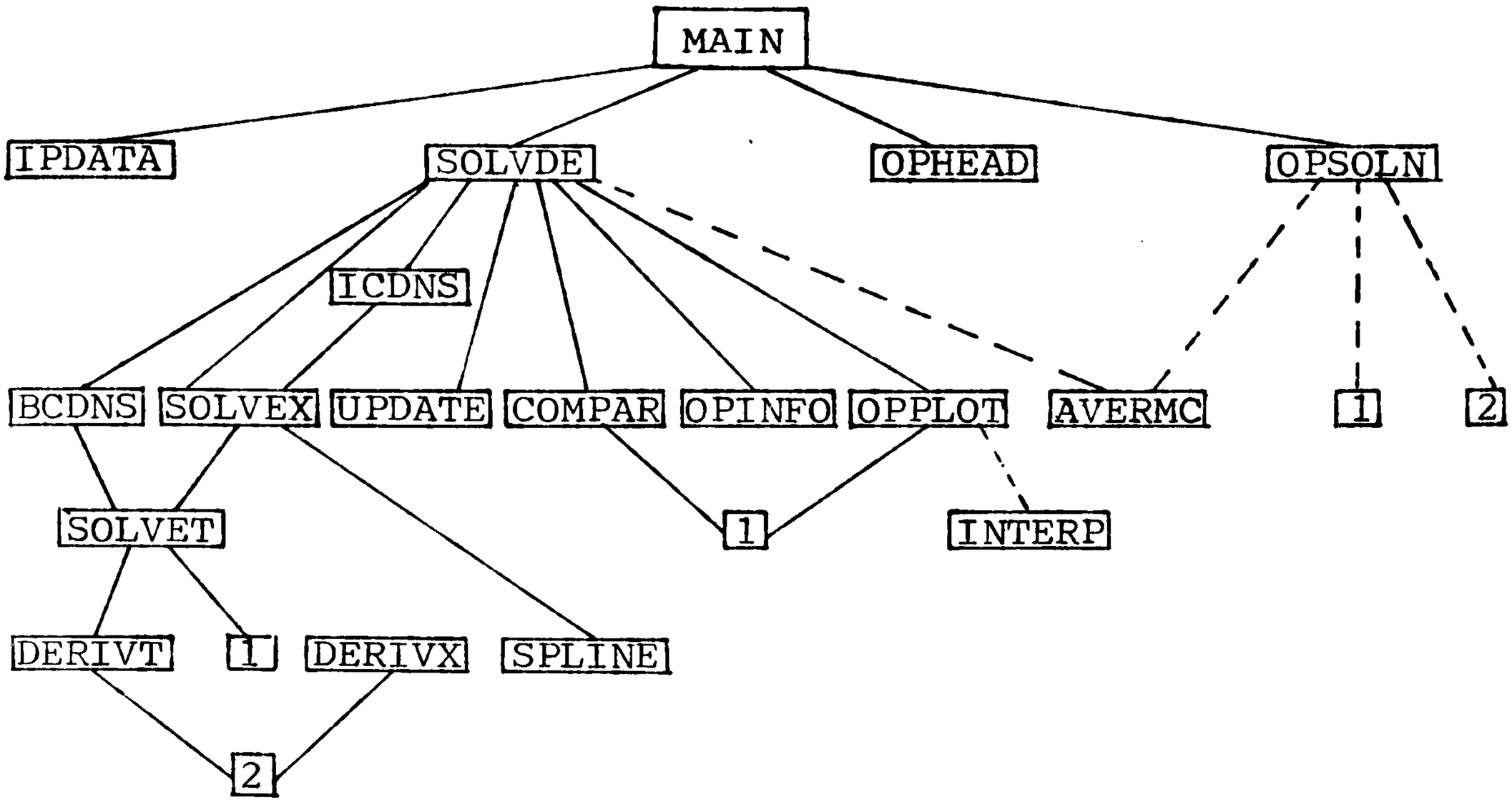

In the above diagram, the following abbreviations are used :

1 for SUBROUTINE SPLINT

2 for the suite of FUNCTION subprograms:

HTRANS, DRYRAT, DRYK, EMC, RELHUM and SATPRE.

The relationship between the latter five of these functions is as indicated in the following diagram:

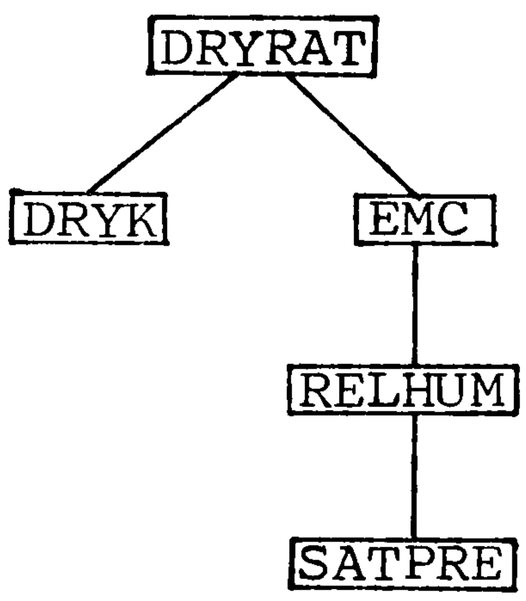

Figure 11. Flow diagram for the program FIXBED.

5.3 Validation of the Model

Case 1

The first case is taken from a series of experiments conducted by O'Callaghan et al (1971) to verify predictions obtained using their empirical drying rate equation. In the particular experiment to be simulated, a 0.3048 m. depth of barley, initially at 34% m.c.d.b. and 21°C was ventilated with air temperature and flow of 68.3°C and 10.644 kg/min/m² respectively. The results from a simulation of the first five minutes of drying are presented in tabular form in Ingram (1976a)* (not reproduced here) and those obtained using FIXBED are given in Table 12.

As far as can be determined, the same constitutive relationships were used in FIXBED as in GERALD for this case. These are the heat transfer expression (A-5), due to Boyce, together with an empirical drying rate expression of the form (A-1) with drying coefficient k given by (A-2) and e.m.c. by (A-3). There are, however, some differences in the two mathematical models (see section 3.5). In addition, Ingram's numerical solution technique is simpler and does not incorporate such strict 'convergence' criteria as those in FIXBED. Having regard for these differences, the following observations were made on the two sets of predicted results.

The grain conditions at the top of the bed, as predicted by both programs, were relatively unchanged from their initial values. Clearly, this is consistent with the short duration of drying. The drying air became 'saturated', i.e. with relative humidity approaching unity, a short distance from the inlet, at $x = x_{sat}$, say. At this point, about 5 cm. for GERALD and about 9 cm. for FIXBED, the drying rate became negative (since $M_e > M$), and remained negative† for $x > x_{sat}$, both programs consequently modelling sorption or 'condensation' from this point. The differences in predicted grain boundary temperatures after 5 minutes was less than 1°C (corresponding to an increase of approxim-

* Ingram's simulation program will subsequently be referred to as GERALD.

† N.B. 'drying rate' values in Ingram (1976a) have the opposite sign convention to those in Table 12.

ately 25°C in predicted values). The predicted boundary moisture contents differed by less than ½% m.c.d.b. (corresponding to a decrease of the order 5-6% m.c.d.b.). Some appreciable differences were, however, observed in propagated values of the solution, particularly over the region of greatest variation, i.e. $0 < x < x_{sat}$. Overall, the qualitative behaviour of both sets of predictions appear similar and consistent with that expected in practice.

Case 2

The next case is taken from Greig & Boyce (1967). In the experiment to be simulated, a bed of barley of nominal depth 0.3300 m. at an assumed uniform temperature of 21°C was ventilated with drying air, initially at 82.20°C and with flow rate of 8.4 kg/min/m². After 200 minutes of drying, the heating was switched off and a final period of cooling took place with air at 15°C and at the same flow rate. The simulation thus consists of a 200 minute drying period followed by a 110 minute cooling period.

It was noted that significant shrinkage, perhaps as much as 10%, may have occurred in such an experiment, and that the model used herein does not, in its present form, allow for bed shrinkage*. In addition, the airflow rate used in the simulation may well be an overestimate of the 'effective' rate. Nonetheless, the simulation serves to illustrate the cooling period option modelled by FIXBED. Furthermore, the graphs presented in Figures 12a-d exhibit the same qualitative behaviour as those presented by Boyce.

Figure 12b illustrates how, in the bottom half of the bed, nearest the air inlet, moisture from the relatively wetter ambient air (used over the cooling period 200-310 mins), is adsorbed by the grain. This causes the average m.c. to increase slightly over this period. In comparison with the experimental results, however, given in graphical form by Greig & Boyce (not presented here), the results shown in Figure 12 appear to indicate both over-drying and over-heating of the grain. In view of the uncertainty regarding ambient air temperature, no comparison of results obtained over the cooling period is made. After 200

* See discussion in section 7.2.

mins drying, however, the predicted average m.c. of 13.4% d.b. was 3.6% below the reported value of 17%. Temperatures at the bottom of the bed had both attained that of the inlet air, i.e. 82.2°C. Temperatures in the middle of the bed were approx. 75°C and 71°C respectively, for predicted and experimental values, while temperatures at the top of the bed were approximately 30°C and 41°C.

The observed differences, together with experience of experimental drying conditions, led to the suggestion† of a disparity between the 'effective' airflow rate and the reported rate. In view of this, a number of simulations were carried out with different airflow rates. Results obtained taking G_a = 5.0 kg/min/m², i.e. approx. 0.6 x (reported rate), were found to give closer agreement with the experimental values. In particular, a much higher average m.c. of 17.7% was predicted.

Case 3

The final test case is again taken from the series of experiments conducted by O'Callaghan et al (1971). In this case, actually the five drying runs B125,126,134,145 and 146, a deep bed of barley, of nominal depth 0.3050 m. at assumed uniform temperatures of 21°C, was ventilated by drying air at 68°C and at various flow rates in the range 10.58 - 10.72 kg/min/m². O'Callaghan et al reported the experimental drying times required to obtain a series of different average moisture contents. They also gave the times predicted by their model.

In view of the closeness of the reported airflow rates, it was decided to run FIXBED with a single airflow rate, and with the 'target moisture content' option, in order to obtain a set of predicted drying times which could be compared to those of O'Callaghan et al. However, in view of the foregoing comment on possible disparities between reported and effective airflow rates, (see Case 2), FIXBED was run with a variety of rates. The rate which gave predictions closest to the reported experimental drying times was found to be 6.5 kg/min/m², which again represents approximately 0.6 times the measured rate.

† Private communication - M.E.Nellist.

Bed conditions, as predicted by FIXBED, after attaining a final average moisture content of approximately 14% m.c.d.b., are given in Table 13a. Predicted times taken to attain various average moisture contents, during the course of this simulation, are presented, alongside those given by O'Callaghan et al, in Table 13b. It should be noted that each time predicted by FIXBED represents the centre of a 2 minute interval over which the corresponding average moisture content was attained.

The times predicted by FIXBED, taking a much lower airflow rate than that reported, agree, over the given set of moisture content values, with the experimental times, to within a maximum difference of 10%, while those predicted by O'Callaghan et al have a maximum error closer to 20%.

These validation cases illustrate some of the ways in which the qualitative behaviour of the air and grain states in a fixed bed drier may be approximately predicted. In view, however, of the present lack of suitably detailed experimental results, the accuracy of the quantitative predictions of FIXBED (or of other programs such as SIMUL and GERALD) remain to be proven.

FIXED BED SIMULATION
****

INITIAL GRAIN CONDITIONS INLET AIR CONDITIONS

(ASSUMED CONSTANT)

M.C. (%D.B.)=34.00
TEMP.DEG.C=21.00

SPEC.HUMIDITY=0.006
TEMP.DEG.C=68.30
MASS FLOW RATE=10.644
Kg/min/sq.m.

BED DEPTH=0.3048 m.

VELOCITY = 10.329 m./min.

CONDITIONS AT DIST.X FROM AIR INLET AFTER 5.00 mins
(VALUES COMPUTED TO APPROX 0.100 % LOCAL ACCURACY)
(USING EQUAL INTERVAL TIME STEPS OF 0.50)

	GRAIN			AIR			
X	M.C.%	EMC%	TEMP.	TEMP.	SP.HUM	R.H.%	DRYING RATE
0.000	29.100	6.909	46.302	68.300	0.0060	3.33	1.5E-4
0.015	32.123	8.628	39.036	52.857	0.0110	12.32	7.7E-5
0.030	32.982	10.422	32.714	42.735	0.0137	25.51	4.5E-5
0.046	33.388	12.619	28.133	35.466	0.0154	42.11	2.8E-5
0.061	33.585	15.483	25.049	30.290	0.0164	60.12	1.9E-5
0.076	33.714	19.553	23.085	26.667	0.0172	77.40	1.2E-5
0.091	33.837	25.910	22.134	24.332	0.0176	91.00	5.8E-6
0.107	33.992	37.168	22.148	23.097	0.0176	98.29	-2.2E-6
0.122	34.088	45.955	22.289	22.637	0.0173	99.53	-7.9E-6
0.137	34.073	44.312	21.979	22.349	0.0170	99.40	-6.7E-6
0.152	34.051	44.531	21.714	22.057	0.0167	99.42	-6.7E-6
0.168	34.044	42.416	21.566	21.819	0.0164	99.21	-5.3E-6
0.183	34.035	40.832	21.436	21.633	0.0162	98.99	-4.3E-6
0.198	34.025	39.707	21.319	21.487	0.0160	98.81	-3.5E-6
0.213	34.017	38.761	21.227	21.369	0.0159	98.63	-2.9E-6
0.229	34.012	37.923	21.160	21.272	0.0157	98.44	-2.4E-6
0.244	34.009	37.194	21.112	21.195	0.0156	98.26	-1.9E-6
0.259	34.007	36.573	21.076	21.134	0.0156	98.09	-1.6E-6
0.274	34.005	36.052	21.048	21.089	0.0155	97.94	-1.2E-6
0.290	34.003	35.617	21.029	21.058	0.0154	97.80	-9.8E-7
0.305	34.002	35.257	21.017	21.043	0.0154	97.68	-7.6E-7

AVERAGE M.C. ATTAINED =33.6861 % D.B.

Table 12. Simulation of the first 5 minutes in drying a deep bed of barley.

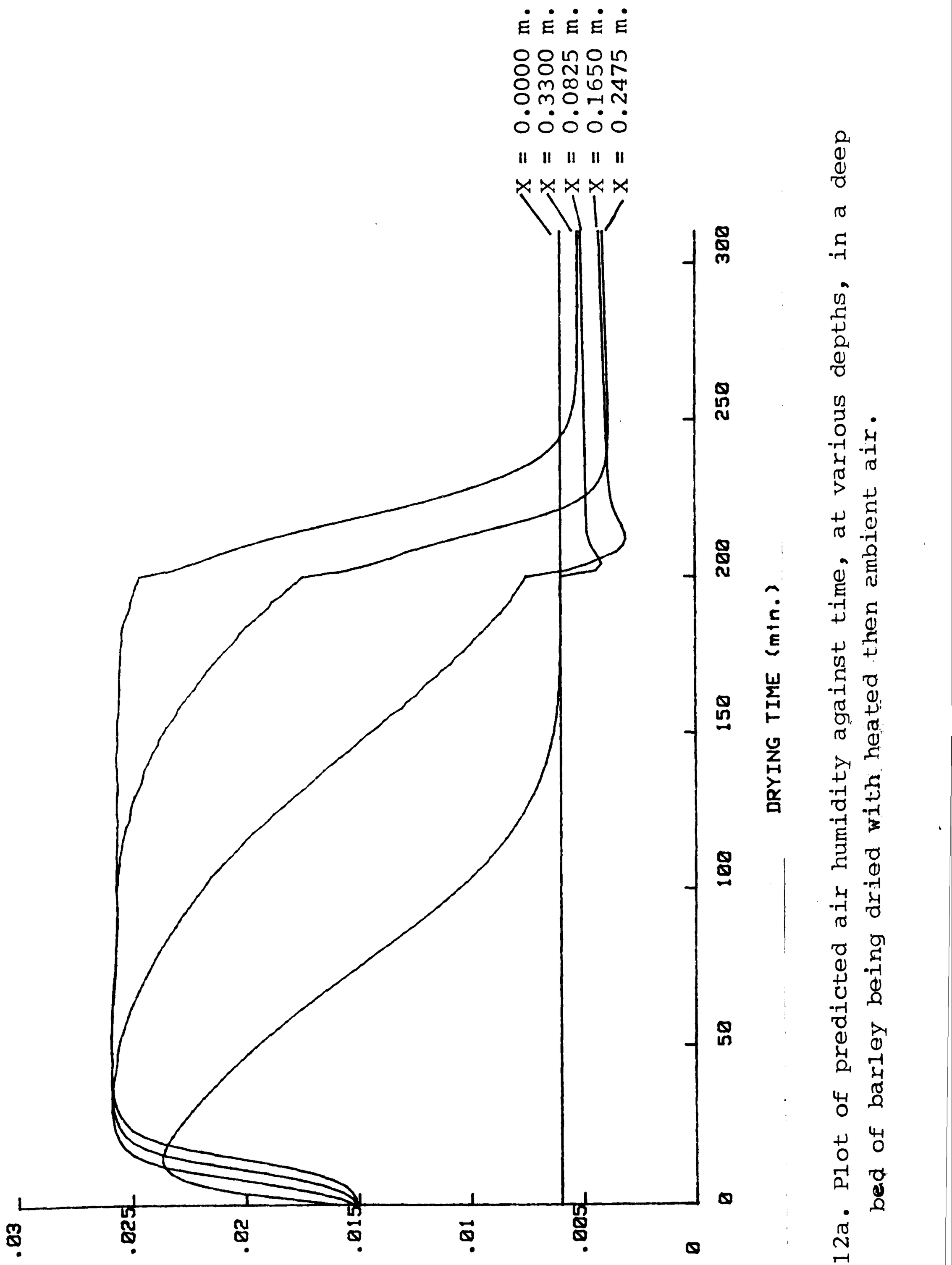

Figure 12a. Plot of predicted air humidity against time, at various depths, in a deep bed of barley being dried with heated then ambient air.

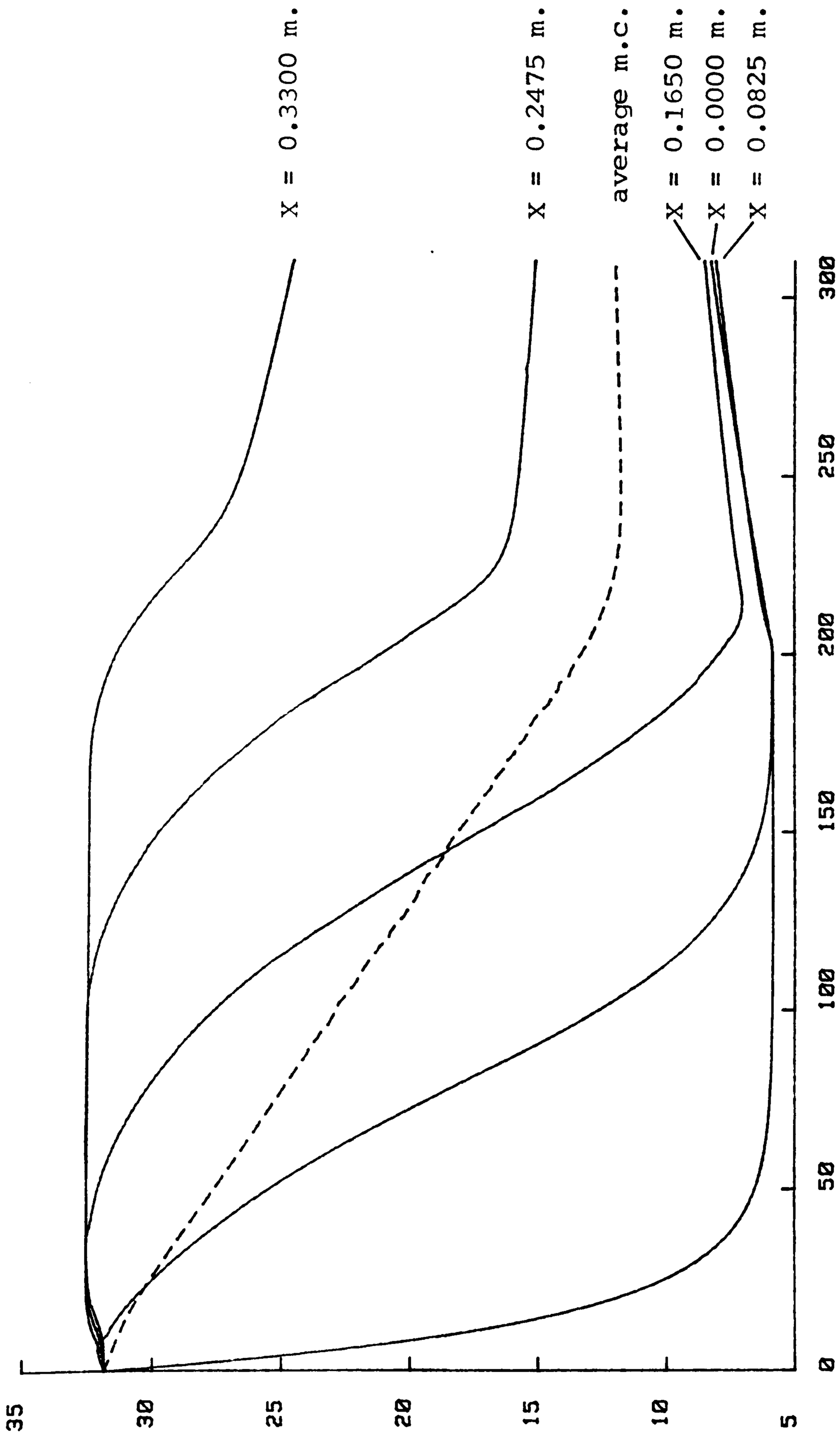

Figure 12b. Plot of predicted moisture content against time, at various depths, in a deep bed of barley being dried with heated then ambient air.

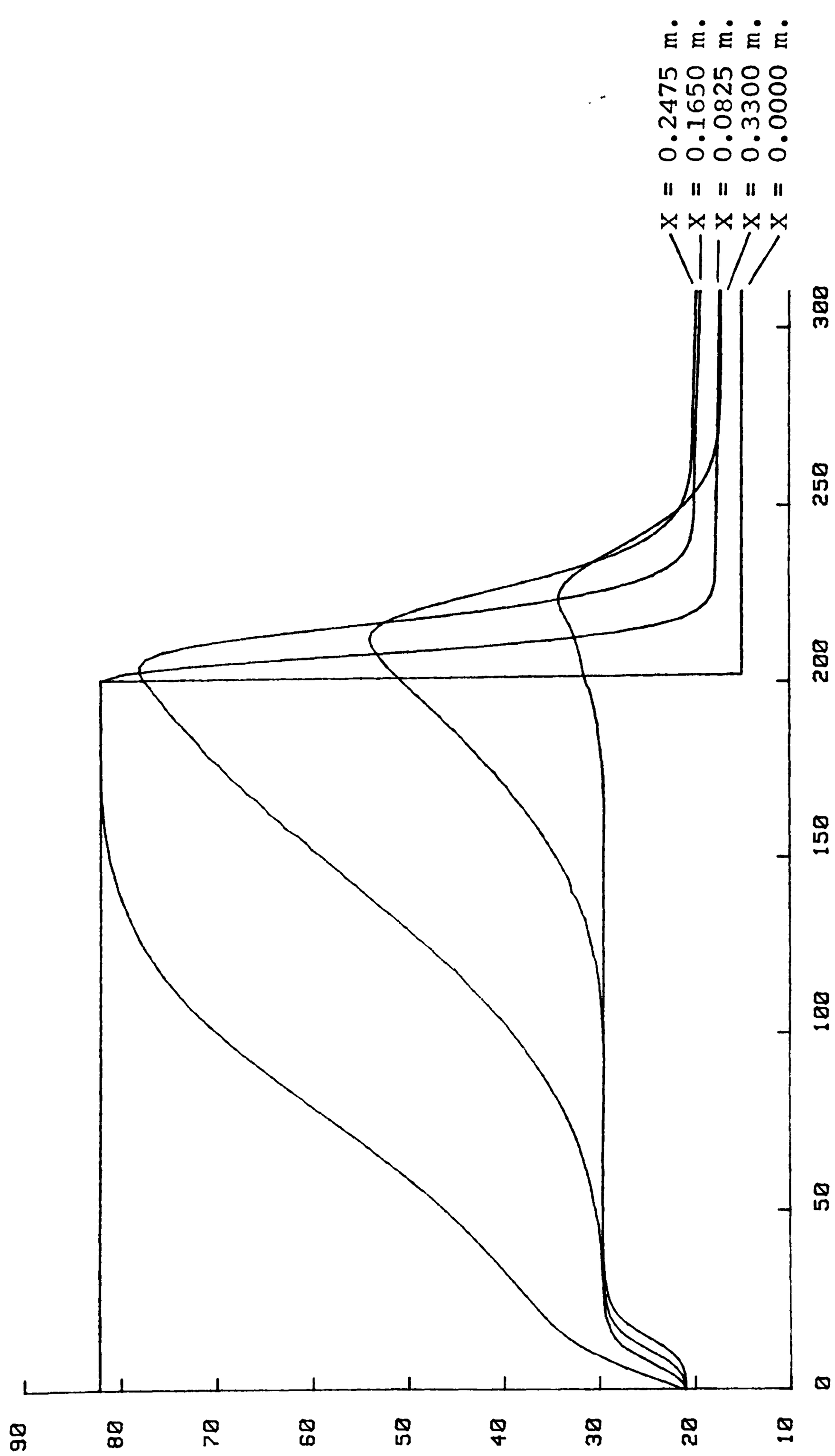

Figure 12c. Plot of predicted air temperature against time, at various depths, in a deep bed of barley being dried with heated then ambient air.

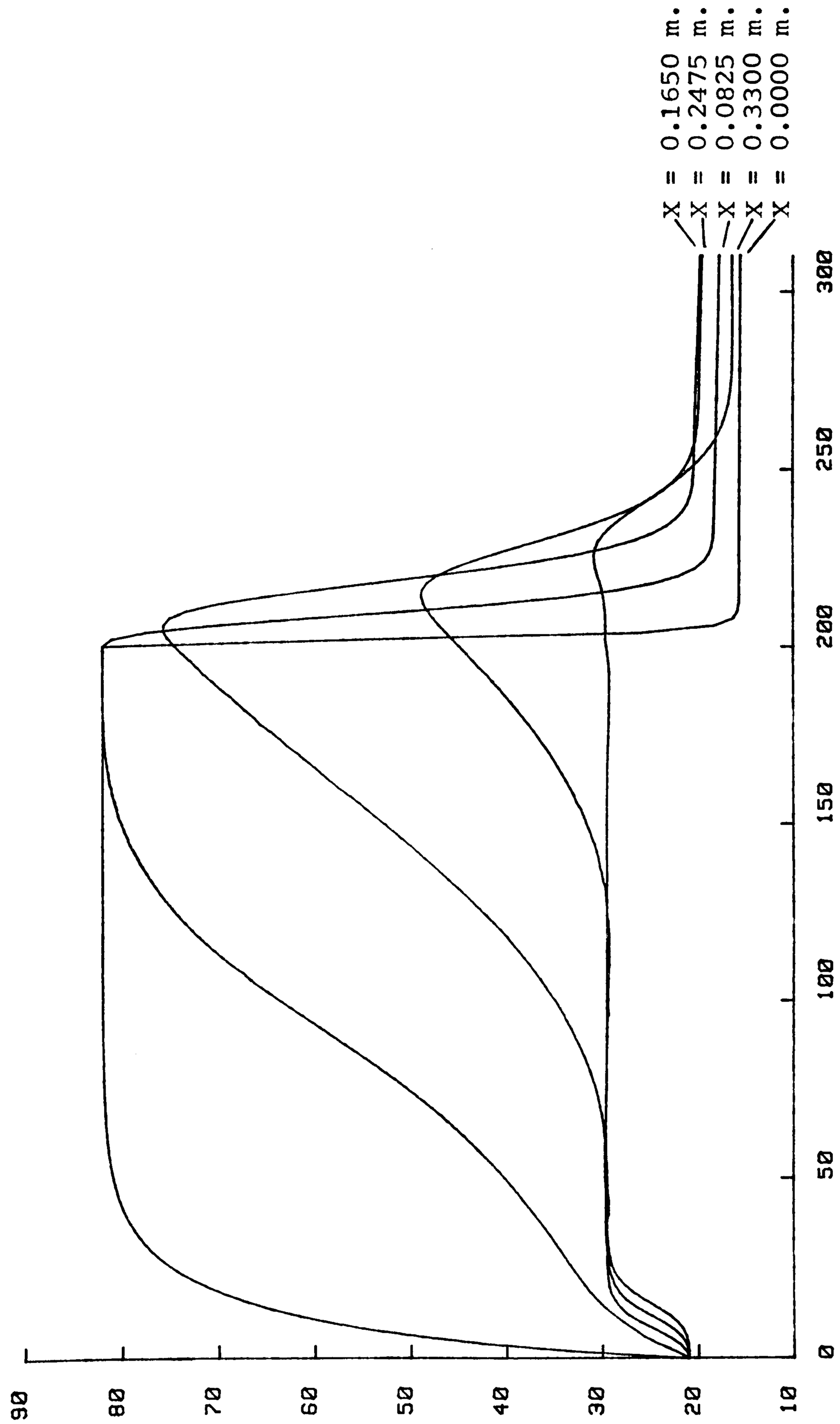

Figure 12d. Plot of predicted grain temperature against time, at various depths, in a deep bed of barley being dried with heated then ambient air.

FIXED BED SIMULATION
****

INITIAL GRAIN CONDITIONS

M.C.(%D.B.)=34.30
TEMP.DEG.C.=21.00
BED DEPTH =0.3050M.

AIR INLET CONDITIONS
(ASSUMED CONSTANT)

SPEC.HUMIDITY=0.006
TEMP.DEG.C.=68.00
MASS FLOW RATE KG./MIN./SQ.M.
= 6.500
VELOCITY = 6.3021 M./MIN.

CONDITIONS AT DIST.X FROM AIR INLET AFTER 278.00 MINS
(VALUES COMPUTED TO APPROX 1.000 % LOCAL ACCURACY)
(USING EQUAL TIME STEPS OF 2.00 MINS)

	GRAIN			AIR			
X	M.C.%	EMC%	TEMP.	TEMP.	SP.HUM	R.H.%	DRYING RATE
0.000	6.933	6.932	68.000	68.000	0.0060	3.37	0.26E-08
0.015	6.935	6.933	67.994	67.998	0.0060	3.37	0.18E-07
0.030	6.941	6.933	67.986	67.995	0.0060	3.37	0.56E-07
0.046	6.961	6.936	67.928	67.960	0.0060	3.39	0.16E-06
0.061	6.993	6.940	67.850	67.914	0.0060	3.40	0.34E-06
0.076	7.040	6.942	67.798	67.897	0.0060	3.41	0.64E-06
0.091	7.176	6.957	67.512	67.751	0.0061	3.47	0.14E-05
0.107	7.494	7.003	66.644	67.257	0.0063	3.65	0.31E-05
0.122	8.073	7.098	65.012	66.252	0.0066	4.02	0.59E-05
0.137	8.975	7.256	62.641	64.636	0.0072	4.68	0.97E-05
0.152	10.257	7.494	59.576	62.317	0.0080	5.79	0.14E-04
0.168	11.972	7.839	55.866	59.215	0.0092	7.61	0.18E-04
0.183	14.055	8.309	51.680	55.451	0.0106	10.47	0.21E-04
0.198	16.358	8.918	47.277	51.294	0.0121	14.67	0.23E-04
0.213	18.728	9.692	42.918	47.017	0.0138	20.53	0.22E-04
0.229	21.013	10.658	38.865	42.894	0.0153	28.20	0.21E-04
0.244	23.076	11.837	35.356	39.174	0.0167	37.40	0.19E-04
0.259	24.872	13.277	32.464	35.933	0.0179	47.75	0.16E-04
0.274	26.403	15.059	30.190	33.173	0.0190	58.76	0.14E-04
0.290	27.667	17.296	28.533	30.892	0.0198	69.73	0.11E-04
0.305	28.666	20.140	27.494	29.092	0.0205	79.79	0.82E-05

TARGET AVERAGE M.C. = 14.0000

AVERAGE M.C. ATTAINED = 13.9469 % D.B.

Table 13a. Predicted conditions in a bed of barley dried to an average moisture content (d.b.) of 14 % .

Target average m.c.	Drying times (mins)		
	experimental	predicted	
	O'Call.et al	O'Call.et al	FIXBED
30.2	57	45	51
26.2	105	85	101
22.5	160	127	145
18.2	211	168	211
14.0	255	230	277

Table 13b. Predicted and experimental drying times for various target moisture contents.

5.4 Factors affecting the Performance of the Algorithm

An overall analysis of the numerical technique devised for propagating the solution in FIXBED is not attempted in the present work. (see, however, the appropriate comments in section 5.2.2). Instead, some discussion is given of the various factors which appear to affect the accuracy and stability of the computed results.

The iterative nature of the scheme used for propagating M and θ along the C_2 characteristics (see section 5.2.2) allows for a certain degree of flexibility in selecting an appropriate time-step. This is particularly important when the equal-interval option is used. If too large a step is chosen then infeasible state points may be predicted and the scheme may then fail to converge. On the other hand, too small a step seems to lead to an unacceptable growth of rounding errors in 'unstable' regions, such as the first $\frac{1}{2}$ hour or so of the example illustrated in Figures 12a-d. The resultant behaviour of the computed solution also depends on the specified level of local accuracy. Similar comments apply to the (automatically determined) step-size used in SUBROUTINE SOLVEX, inasmuch as too high a specified accuracy would result in a possible growth of errors in any unstable region, whilst too low a value might cause the prediction of infeasible relative humidities, for example. Clearly some means of determining an optimal combination of the prescribed time-step and accuracy level should be sought. However, only general guidelines can be given here.

In view of the nature of the numerical integration scheme, a large number of derivative evaluations are reuqired in the course of a typical drier simulation. Table 14 gives the number of such evaluations after 10-minute intervals, over a drying period of 60 minutes, for the second validation case presented in section 5.3. The tabulated results are from simulations using equal-interval steps of $\frac{1}{2}$, 1 and 2 minutes. The first three columns of results were obtained with a prescribed relative accuracy of 1%, while for the last column this was changed to 0.1%. The entries in the table are the total number of calls to subroutines DERIVX and DERIVT. Thus the total number of scalar derivative evaluations is twice each entry. It is also noted

that the number of calls to DERIVT was between two and three times that to DERIVX. This is probably partly due to the (generally) higher order of the integration scheme used along the C_1 characteristics.

The bed conditions after 60 minutes (not presented here) were found to agree closely for each of the four simulations. For example, over the first three, the average moisture contents attained differed by less than 0.2% and the maximum difference in air or grain temperatures was below 0.2°C. For the final simulation these differences were only slightly greater. A graphical comparison (not presented here), of the form given in Figures 12a-d, does, however, indicate more significant variations in the predicted bed states over the first ½ hour of drying. (see the above comment). For a 'smooth' plot the extra accuracy of 0.1% was required (see Figures 12a-d).

The entries in Table 14 give some indication of the relative processing times required for different choices of time-step and accuracy. Obviously, the larger this step and the lower the requested accuracy, the shorter the processing time, although this advantage is, to some extent, offset by an increase in the number of iterations required to obtain values of M and θ for a given level of accuracy. The maximum number of such iterations is limited, within the program, to an arbitrary 25. This limit should not normally be attained unless too large a time-step has been chosen. In this case the simulation would terminate and would have to be re-run with a smaller step. In the cases represented in Table 14, only one or two iterations were sufficient over most of the latter part of the range of integration.

Use of the time-wise adaptive option of FIXBED, as currently implemented, does not appear to result in any significant computational economies. Over the set of cases simulated, the maximum permissible time-step was found to be approx. 2 min$. Since, however, results seem to indicate that, with the equal-interval option, a step of this size can produce results very close to those obtained with a step of ½ min., the greatest time-saving would appear to lie in choosing a larger step with the equal-interval option. For a more 'automatic' scheme, it would of course be desirable to make use of the variable time-step option. It is, however, suggested that the test for comparing solutions, as described in step 4 (section 5.2.2), might require revision.

Run time (mins)	Step-size (mins)			
	TOL = 1 %			TOL=0.1%
	0.5	1.0	2.0	2.0
10	21893	12405	7584	20056
20	46601	25439	15877	33939
30	70305	33726	24031	40377
40	85773	41201	28456	45927
50	99182	48798	31853	51127
60	111874	54958	35334	56370
max. its	2	3	5	7

Table 14. Number of derivative evaluations, taking various time-steps, for a fixed bed simulation, using the equal-interval option.

(max. its represent the maximum number of iterations required to obtain M and θ values).

CHAPTER SIX: STEADY STATE COUNTERFLOW DRIER SIMULATION

Equations representing the processes of heat and mass transfer in steady state counterflow drying were presented in section 3.1(d), where the problem of interest was shown to be a two-point boundary value problem.

In view of the difficulties encountered in searching for a semi-analytical solution to the drying equations for both the concurrent flow and fixed bed cases, and of the additional problems inherent in solving boundary value problems, no such approach is pursued here.

A general 'shooting and matching' technique for the solution of this problem is outlined in section 6.1. The computer implementation of such a scheme, incorporating NAG library subroutines, is described in section 6.2. Finally, a validation case for this program is presented in section 6.3. along with a cursory analysis of the sensitivity of the chosen technique to perturbations in estimates of the unknown boundary parameters i.e. outlet conditions of both grain and air.

6.1 A Technique for the Numerical Solution of the Model

Equations (3.1-27,28), together with the corresponding boundary conditions (3.1-25,26), assumed constant with respect to time, represent the problem of heat and mass transfer in steady state counterflow drying. The problem of interest is then to find $\underline{u} = [H,M,T,\theta]^T$, given

$$d\underline{v}/dx = \underline{f}(\underline{u}) \quad , \tag{1}$$

where $\underline{v} = [M,T,\theta]^T$,

together with

$$H = aM + b \quad , \tag{2}$$

where $a = G_p/G_a$, $b = G_a H_o - G_p p_2$,

subject to

$$\underline{u}(0) = [p_1, M_0, p_3, \theta_0]^T \quad , \tag{3}$$

$$\underline{u}(L) = [H_0, p_2, T_0, p_4]^T \quad , \tag{4}$$

and where $\underline{p} = [p_1, p_2, p_3, p_4]^T$ represents the vector of unknown boundary conditions $[H(0), M(L), T(0), \theta(L)]^T$.

To solve this two-point boundary problem numerically, a 'shooting and matching' technique of the following form is used.

1. Initial estimates are made of the unknown boundary parameters

$$\text{i.e.} \quad \underline{p} = \underline{p}^{(k)} \quad , \quad \text{where} \quad k=0.$$

2. A 'matching point', $x = X$, is chosen.

3a. System (1), subject to (2,3), is numerically integrated forwards, over the range $0 < x \leqq X$, to obtain an approximate solution $\underline{u}^{(k)}(x;0)$.

3b. System (1), subject to (2,4), is numerically integrated backwards, over the range $X \leqq x < L$, to obtain an approximate solution $\underline{u}^{(k)}(x;L)$.

4. The chosen 'matching function' $\underline{F}^{(k)}(x) = \underline{F}(x;\underline{p}^{(k)})$, say, is evaluated at $x = X$. If then

$$\| \underline{F}^{(k)}(X) \| < \varepsilon \qquad (5)$$

where ε is some specified tolerance and $\| \cdot \|$ is an appropriately defined norm*, the required solution is taken as

$$\underline{u}(x) = \begin{cases} \underline{u}^{(k)}(x;0) , & 0 \leq x < X , \\ \underline{u}^{(k)}(x;L) , & X \leq x \leq L. \end{cases}$$

5. If condition (5) is not satisfied, new estimates for the boundary parameters are computed from

$$\underline{p}^{(k+1)} = \underline{p}^{(k)} - \left[J_F(\underline{p}^{(k)})\right]^{-1} \underline{F}^{(k)}(X), \qquad (6)$$

where the Jacobian matrix J_F is defined by

$$J_F(\underline{p}) = \left\{\frac{\partial F_i}{\partial p_j}\right\} .$$

Steps 3a - 5 are then repeated until condition (5) is satisfied.

The above technique was implemented in a variety of ways as follows.

(i) Different matching points were chosen, namely X=0, X=L, X=L/2.

(ii) Different numerical integration schemes were used in step 3, including the modified midpoint rule used in CONFLO and the NAG routine D02QBF (both described in Chapter 4).

(iii) The elements of the matching function at X were taken as

$$F_j^{(k)}(X) = (u_j^{(k)}(X;0) - u_j^{(k)}(X;L))/U_j^{(k)}(X) , \qquad (7)$$

where $U_j^{(k)}(X)$ is the given boundary value, if known at X, or $(u_j^{(k)}(X;0) + u_j^{(k)}(X;L))/2$, if this is unknown.

* Both Euclidean and maximum norms were used for this test.

(iv) The elements of J_F were estimated using the forward difference approximation

$$\frac{\partial F_i^{(k)}}{\partial p_j^{(k)}} = \frac{F_i(p_j^{(k)} + \delta p_j^{(k)}) - F_i(p_j^{(k)})}{\delta p_j^{(k)}} , \quad (8)$$

where the $F_i(p_j^{(k)} + \delta p_j^{(k)})$ were obtained by solving system (1,2) with either of (3) and (4) perturbed by a small amount.

Limited success was, however, obtained using the above scheme. In particular, convergence appeared to be highly dependent on the initial estimate of the boundary parameters, $p_j^{(0)}$. This is probably due in part to the mere linear local convergence obtained using the approximation (8) and the difficulty of choosing appropriate perturbations $\delta p_j^{(k)}$.

In addition to the above scheme, a minimisation technique due to Powell (1964) was incorporated in a scheme, such as that described by Bakker-Arkema et al (1974), using an objective function of the form (1.3-1). Similar convergence problems were experienced here (see also note in section 1.3).

Since neither of the above schemes permitted an effective validation of the model, the NAG library subroutine D02ADF was incorporated in a program, CTRFLO, for the solution of this problem (described in section 6.2). The NAG routine employs a more sophisticated shooting and matching technique with Newton iteration than the scheme described in steps 1-5 but is similar in outline. The routine employs a 'mixed' error test of the form described in section 4.2.3.

6.2 Computer Implementation

The program CTRFLO comprises a MAIN segment together with six subroutines and the six inter-related function subprograms, determining the heat and moisture transfer rates and psychrometric properties, as used for programs CONFLO and FIXBED. The relationship between these is schematically indicated in Figure 13. In addition, this program invokes the NAG library subroutine NAGFLIB (1978).

The MAIN segment firstly calls SUBROUTINE IPDATA to read data from a user-supplied file. In SUBROUTINE SOLVDE, the input parameters required by the NAG subroutine D02ADF are set up. This subroutine is then called to solve the counterflow drying equations. The NAG routine calls SUBROUTINE DERIV, in which the derivatives of the dependent variables are computed at values of these quantities supplied by D02ADF.

SUBROUTINE STEP, called by D02ADF after each iteration, outputs the current values of the 'unknown' boundary parameters, i.e. outlet temperatures and moisture contents of both air and grain, together with the corresponding values of their 'matching functions' and their sum of squares, at the 'matching points' (see section 6.1.1), to an appropriately defined diagnostic output file. D02ADF, also calls the auxiliary subroutines D02ABF, F03AFF, F04AJF, P01AAF and X02AAF, whose functions are described in the NAGFLIB documentation. Finally, subroutines OPHEAD and OPSOLN perform the same functions as subroutines OPHEAD and OPFILE, respectively in CONFLO.

The NAG library, as implemented on the ARC 470/472 system is in DOUBLE PRECISION. For compatibility as well as for convenience, therefore, all computations within the program CTRFLO are carried out in double precision arithmetic.

The input data file must contain the specific and latent heats, atmospheric pressure, grain bulk density, airflow rates, bed depth and number of (equidistant) output intervals, as for CONFLO. In addition, the known inlet condition, together with an estimate for the corresponding outlet condition and required tolerance in the truncation error must be prescribed for each of the four state variables (see section 6.1.1). In its present implementation, the program also requires input of a matching point.

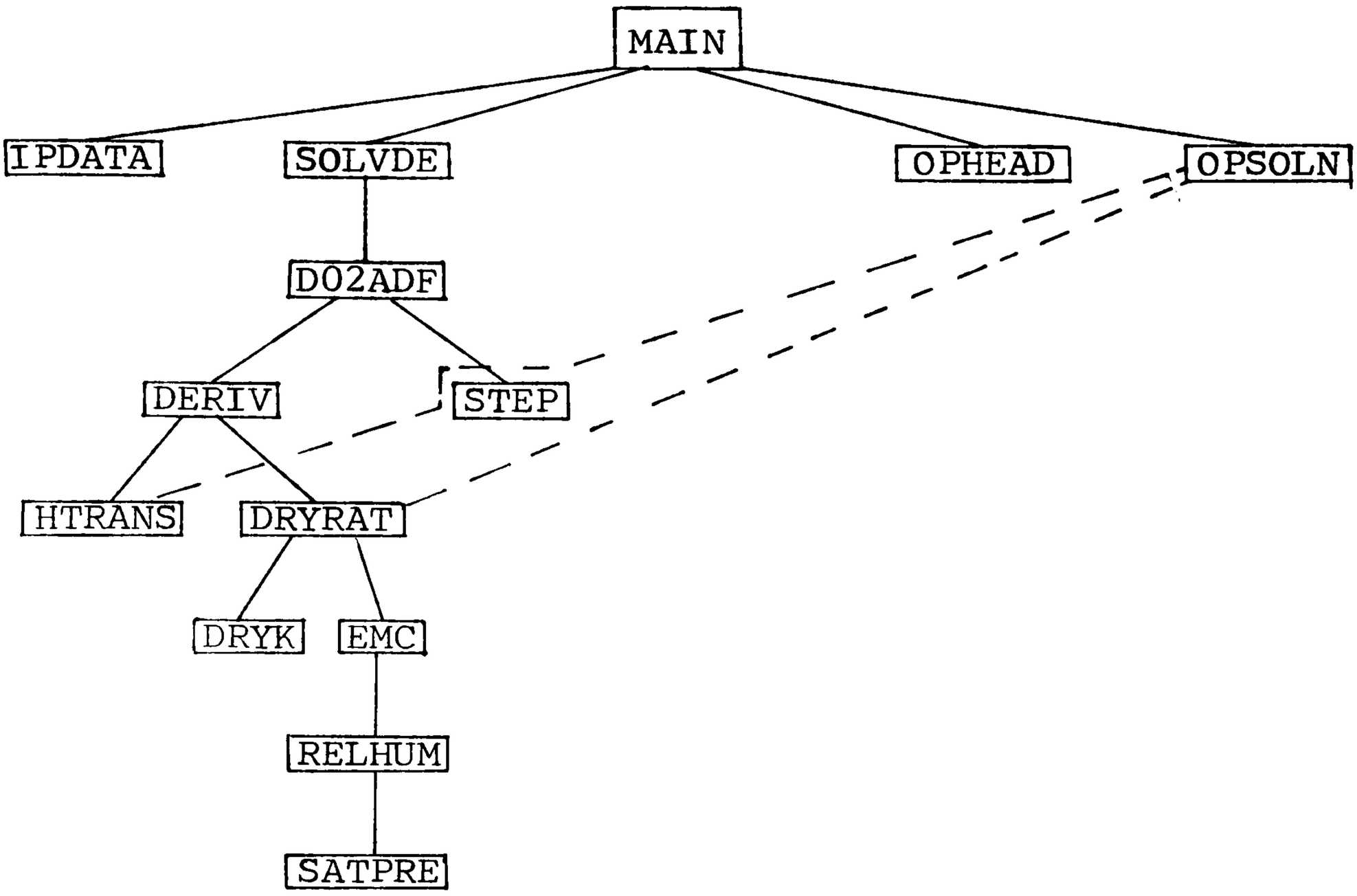

Figure 13. Flow diagram for the program CTRFLO.

6.3 Validation of the Model

Predicted results from the program CTRFLO were compared with those given by the general purpose NIAE program, SIMUL, described in Bruce (1983), over a number of simulations. The results presented in Table 15 and Figure 14 represent simulation of cooling in a 0.8 m. counterflow section of an experimental multistage drier*. Grain at initial temperature and moisture content of 46.41°C and 18.95% d.b. respectively was passed through this section with a throughput of approximately 12.2 kg (d.m.)/min./m^2. The cooling air temperature and mass flow rate were 15°C and 6.11 kg/min./m^2 respectively.

In order to provide 'realistic' estimates for the vector of unknown boundary parameters $\underline{p}$, use was made of the results obtained using the NIAE program. Firstly, CTRFLO was run taking as the vector $\underline{p}$, the outlet conditions predicted by SIMUL. The resulting new set of predicted outlet conditions were then 'perturbed' by varying amounts and the CTRFLO simulation repeated for each different set of perturbed boundary parameters. For each of these distinct sets of parameters, the results predicted by CTRFLO were found to be the same (to the given machine accuracy) and in good agreement with those obtained using SIMUL. Differences in temperatures were less than 0.3°C and in moisture contents much less than .1%. The number of iterations required for the NAG routine D02ADF to give convergence to a solution in each case is given in Table 16.

It may be seen from Table 16 that individual perturbations of ±20% in the parameters H(0), T(0) and M(L) gave convergence. For such a perturbation in $\theta(L)$, however, predictions of infeasible state points caused termination of the program with no convergence (indicated by the asterisk). Since, however, a perturbation of ±10% in this parameter gave convergence, all four boundary parameters were perturbed simultaneously by the amounts indicated (final row of Table 16) and the program was found to give satisfactory convergence. It is also suggested by these results that convergence is less sensitive to perturbations in the air conditions than to perturbations of the same relative magnitude in the grain conditions, particularly in grain temperature.

* Private communication - M.E.Nellist.

COUNTERFLOW SIMULATION
****

INLET CONDITIONS

GRAIN	AIR
M.C.(%DB)=18.95	SPEC.HUMIDITY=0.008
TEMP.DEG.C.=46.41	TEMP.DEG.C.= 15.00
THROUGHPUT= 12.198 KG(DM)/MIN./SQ.M.	MASS FLOW RATE= 6.110 KG/MIN./SQ.M.
BED DEPTH=0.8000 M.	

STEADY-STATE CONDITIONS AT DIST. X FROM INLET
RESIDENCE TIME OF GRAIN= 42.17 MINS

	GRAIN			AIR			
X	M.C.%	EMC%	TEMP.	TEMP.	SP.HUM	R.H.%	DRYING RATE
0.000	18.950	11.264	46.410	45.678	0.0342	52.91	0.10D-04
0.040	18.831	11.511	44.602	43.950	0.0318	54.00	0.89D-05
0.080	18.725	11.711	42.987	42.399	0.0297	54.83	0.79D-05
0.120	18.629	11.869	41.528	40.992	0.0278	55.42	0.72D-05
0.160	18.542	11.988	40.194	39.700	0.0260	55.80	0.66D-05
0.200	18.463	12.071	38.964	38.505	0.0244	55.99	0.61D-05
0.240	18.389	12.121	37.819	37.388	0.0230	56.01	0.57D-05
0.280	18.319	12.139	36.744	36.337	0.0216	55.86	0.53D-05
0.320	18.254	12.128	35.727	35.340	0.0203	55.55	0.50D-05
0.360	18.192	12.088	34.759	34.388	0.0190	55.09	0.48D-05
0.400	18.133	12.021	33.830	33.473	0.0179	54.46	0.46D-05
0.440	18.076	11.927	32.935	32.589	0.0167	53.68	0.44D-05
0.480	18.020	11.807	32.067	31.730	0.0156	52.72	0.43D-05
0.520	17.967	11.660	31.220	30.890	0.0145	51.59	0.42D-05
0.560	17.914	11.488	30.391	30.067	0.0135	50.26	0.41D-05
0.600	17.863	11.290	29.575	29.255	0.0125	48.73	0.40D-05
0.640	17.812	11.067	28.769	28.449	0.0115	46.98	0.40D-05
0.680	17.762	10.828	27.966	27.629	0.0105	45.04	0.39D-05
0.720	17.712	10.629	27.135	26.661	0.0095	43.25	0.38D-05
0.760	17.666	10.882	26.069	24.611	0.0085	44.15	0.33D-05
0.800	17.639	18.075	23.333	15.000	0.0080	75.07	-0.13D-06

Table 15. Simulation of a counterflow section of a mixed flow drier.

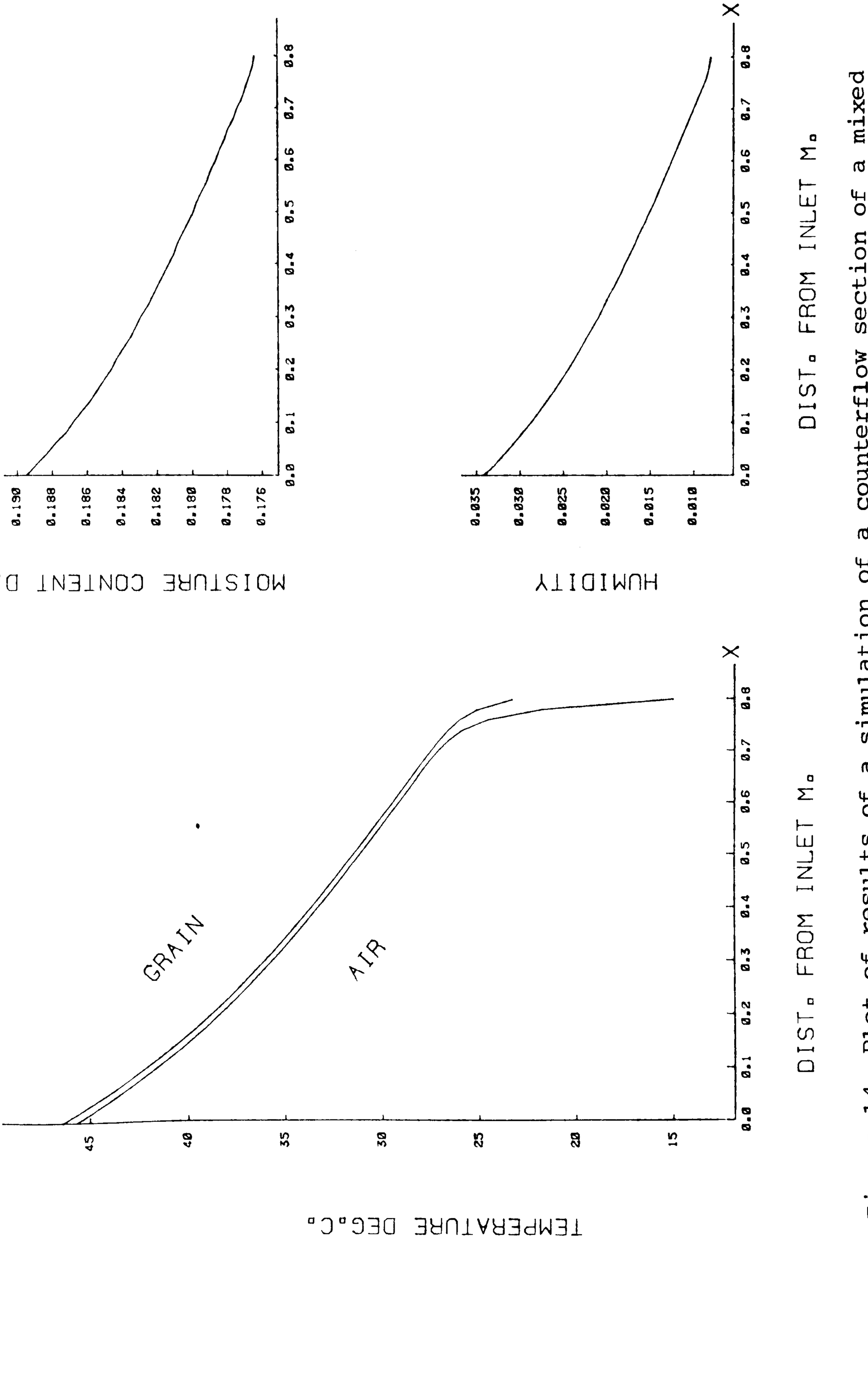

Figure 14. Plot of results of a simulation of a counterflow section of a mixed flow drier.

H(0)	T(0) deg.C	M(L) % d.b.	θ(L) deg.C	No. its
.0342	45.68	17.64	23.33	3
.0274 (-20%)				3
.0410 (+20%)				3
	36.54 (-20%)			3
	54.82 (+20%)			3
		14.11 (-20%)		7
		21.17 (+20%)		6
			21.00 (-10%)	8
			25.66 (+10%)	8
			18.67 (-20%)	*
			28.00 (+20%)	*
.0410 (+20%)	54.82 (+20%)	21.17 (+20%)	25.66 (+10%)	10

Table 16. Effect of perturbed boundary parameters on the convergence of results predicted by CTRFLO. (Figures in parentheses after each entry indicate size of perturbation.)

CHAPTER SEVEN : DISCUSSION AND CONCLUSIONS

7.1 Summary of Work Accomplished

A general framework for the derivation of mathematical models representing simultaneous heat and mass transfer in grain drying was presented in Chapter 2. This work, making use of the standard continuum theory of mixtures, constitutes a novel approach to the problem of modelling grain drying. It also provides a more rigorous derivation of the transfer equations than any presented in the available literature, particularly since the assumptions made are clearly stated.

The resultant general system of equations (2.2-15), together with the jump conditions, (2.1-13,14,15), holding across surfaces of discontinuity, represent, in compact form, the transfer equations for all the grain drying problems considered in the current work. The energy balance equations, as initially derived, contain kinetic energy terms and a diffusive force term which have no equivalent in any previous model. It is, however, acknowledged that the energetic contribution of these terms is generally very small, and this assumption is subsequently given cursory justification in section 4.5.

Systems of differential equations modelling drying in each of the four basic types of drier were deduced from (2.2-15), under appropriate simplifying assumptions, in Chapter 3. In the choice of constitutive equation (3.3-14) for the net energy transfer, ψ, an extra degree of freedom was introduced, namely the 'mean evaporation temperature', θ_v. In section 3.5 it is shown that in most of the well-known models in the literature the assumption is made, albeit implicitly, that evaporation takes place at the temperature of the drying air, T, and exceptionally at that of the grain, θ.

The fixed bed equations were reduced to two coupled systems of ordinary differential equations along given characteristic directions - families of straight lines in this case. Mathematically correct initial/boundary conditions were given for this problem. Such a formulation does not appear to have been given previously, perhaps partly because of the (noted) neglect of time-derivative terms in the air state variables.

General, i.e. time-dependent, equations were presented for the cases of crossflow, concurrent flow and counterflow drying. As far as can be determined, such equations do not appear anywhere in the available literature. Characteristics for the latter two cases (see Figures 4,5) are, again, shown to consist of two families of straight lines. In view, however, of the two independent space variables and one time variable in the general crossflow case, characteristics for this problem are surfaces.

In practice the modelling of steady state continuous flow drying can provide much of the design information sought by agricultural drier manufacturers. Furthermore, such models are clearly simpler in nature than their time-dependent counterparts. Finally, since the steady state crossflow equations are of the same nature as the fixed bed equations, and therefore numerically solvable using similar techniques, the solution of these equations was not considered in this work. Therefore, the only continuous flow cases investigated herein were those of steady state concurrent flow and steady state counter-flow drying. These were both shown to reduce to a system of three ordinary differential and one linear algebraic equation. The problems considered for these two cases, i.e. those of pracitcal interest, were shown to be a pure initial value problem and a two-point boundary value problem respectively.

Equations suitable for modelling equilibrium exchange in low airflow rate fixed bed applications were deduced from the fixed bed equations. In view of the differences between the basic fixed bed equations presented in Chapter 3 and those in the literature, corres-ponding differences were observed in the equilibrium equations. In view of their inclusion of the time derivative terms in the air prop-erties and no neglect of sensible heating terms, the equations in section 3.4 can only give a more accurate model than others. It was, however, acknowledged that for such a case, the differences might be considered negligible.

In view of the assumptions made in the derivation, particularly those of constant airflow rates and densities, the jump conditions presented in Chapter 2 were shown to imply simply that jump discont-

inuities in grain and air properties are propagated with the velocities of these 'constituents' i.e. can occur only across the characteristics associated with the corresponding equations. In the case of equilibrium exchange, however, it was noted that the characteristic directions are such that 'shock fronts' occur within the air-grain mixture. In this case the corresponding jump conditions are required in order to calculate the velocities of the 'singular surfaces'. Since, however, the main aim of this work was to examine detailed simulation, and more particularly of drying with higher airflow rates, investigation of the equilibrium case was not pursued further.

Overall, the equations derived in Chapter 3 were shown to represent a generalisation of some of the models presented in the literature. In addition, some of the implicit assumptions made in the derivation of these models were clarified with reference to the general equations. For example, among the fixed bed models considered, the neglect of time derivative terms in the air humidity and temperature, and of certain sensible heating terms were found to be most usual.

A linearised formulation of the steady state concurrent flow equations was presented in Chapter 4. A solution to this formulation was presented in 'spectral form' i.e. in terms of the eigenpairs of the Jacobian matrix of the derivatives of the state variables. Attempts made to 'evaluate' this solution as a means of providing an approximation to that of the non-linear problem were, however, largely unsuccessful. Two main problem areas were identified. Firstly, near to the inlet, in the region of high spatial temperature and moisture gradients, large variations were observed in the elements of the Jacobian matrix. In addition, its eigenvalue spectrum indicated instability of the drying equations. These factors resulted in severe restrictions on the useful range of applicability of the linearised form. Secondly, in the later, stable, region, over which increasingly larger 'steps' could be taken, matrix conditioning problems i.e. in the matrix of eigenvectors, were found to hamper evaluation of the solution. This would appear to be due, in some measure, to the near linear dependence of air and grain temperatures over this region.

A numerical solution to a concurrent flow problem was successfully obtained with the aid of a NAG library subroutine. It was, however, noted that a less sophisticated algorithm, with the attribute of 'portability', was required for present purposes. Attempts to obtain a numerical solution using an implicit (trapezoidal rule) integration technique were hampered by conditioning problems similar to those described above. Finally, a modified midpoint rule with polynomial extrapolation was utilised as the basis of an algorithm implemented in the FORTRAN program CONFLO.

A number of simulations were carried out at NIAE using CONFLO. These showed consistent results over the range of permissible accuracies. The results presented in section 4.3 indicate good agreement with other simulated and experimental results. It must, however, be claimed that CONFLO, partly in view of its adaptive nature, and hence its facility to cope with rapidly varying gradients can provide greater reliability in terms of overall accuracy than the program presently used at NIAE.

It would appear, from the cursory analysis of sensitivity to perturbations in the inlet conditions, that such perturbations are damped out towards the outlet. Clearly, this damping effect is consistent with the observed negativity of the eigenvalues of the Jacobian. It is, therefore, acknowledged that a more 'crude' method than that employed in CONFLO might produce similar predicted outlet conditions. The region of greatest interest in concurrent flow drying, however, is that in which consistently high grain temperatures, which might affect germination, are attained. An adaptive method is therefore certainly required for reliably accurate predictions over this region.

An analytical solution to a linearised formulation of the pure heat transfer problem, for grain heating/cooling in a fixed bed, was derived in Chapter 5, in terms of dimensionless independent and dependent variables. It was noted that this formulation encompassed a particular case for which the solution was given by Klapp (1963). This solution was then used in outlining a perturbation-type approach to finding a (semi-analytical) solution to the problem of simultaneous heat and mass transfer in a fixed bed.

Again, the semi-analytical approach was considered impracticable for detailed simulations. The need for the evaluation of integrals involving Bessel functions,together with restrictive simplifying assumptions led to the conclusion that a purely numerical algorithm might again provide a simpler and computationally more efficient means of obtaining an approximate solution.

A technique was devised which incorporates the numerical integration scheme used in CONFLO, and this was implemented in the FORTRAN program FIXBED. Simulated results obtained using the program with different time-steps were found to be very consistent, provided that the user-prescribed local relative accuracy to which the equations were solved was set to 0.1%. Differences in results obtained at lower accuracy levels were particularly noticeable in regions of rapidly varying gradients. Once again, this points to the need for any integration scheme to be adaptive.

The qualitative behavious of the numerical solutions obtained were observed to follow that of available experimental results very well. Owing, however, to possible disparities between experimentally measured airflow rates and effective rates, the results were found to be in closer quantitative agreement with experimental results if a somewhat lower airflow rate was assumed in simulations. This was also found to be the case with the NIAE model.

In view of differences in the basic models, comparison with other simulation programs, such as SIMUL and GERALD, are of limited significance. However, there does appear to be some evidence of differences due to neglect of the time-derivatives of the air properties. Such differences were observed in simulated results (not reported herein) carried out using a modified version of FIXBED.

In view of difficulties encountered in trying to implement a suitable numerical solution scheme for the counterflow case, a NAG library subroutine was incorporated into a FORTRAN program (CTRFLO) to provide a means of validating the model. This 'shooting and matching' technique was found to produce very similar results to those obtained using the corresponding option of the NIAE program, which in

turn appear to give a realistic profile of conditions inside an experimental mixed-flow drier at NIAE.

7.2 Suggestions for Further Work

The general 'grain drying' equations (2.2-15) were derived from the general 'mixture theory' framework, presented in Chapter 2, under a set of simplifying assumptions. Clearly a more accurate model might be obtained by replacing the basic assumption of a binary mixture of moist air and moist grain by one of a four phase model of dry air, dry grain, water vapour in the air and water/vapour in the grain. This model might be further enhanced by taking account of the diffusive forces and hence of the momentum balance equations. Such an approach is not pursued in this discussion, however, in view of the order of complexity inherent in any resulting model. A four equation model, derived under slightly different assumptions from those presented in section 2.2., can, however, provide some useful enhancements to the basic model.

Firstly, it was assumed that the densities of dry air and grain remain constant for a given problem. In FIXBED, for example, wherein it is necessary to provide a value for the air density independently of the mass airflow rate, this is computed, using an ideal gas type law, as a function of the inlet air temperature. As observed in section 5.3, however, significant shrinkage may occur in drying a bed of moist grain. Spencer (1972) incorporated a simple bed-shrinkage adjustment of the depth step in a revised version of his basic model. None of the models in the available literature, however, takes account of such shrinkage in the basic transfer equations.

To properly take account of bed shrinkage in the general equations, we must return to the basic differential balance equations (2.1-2,9). Suitable functional relationships must be assumed for ϱ_p and ε in terms of the four state variables and of the flow rates. This would then lead to extra derivative terms in the balance equations. Clearly, such additional terms would change the characteristic form of the transfer equations, which would then also become quasi-linear instead of semi-linear. There is no reason to suppose, however, that solution

techniques, similar to those used in the present work, could not be adapted to the solution of the resulting problems.

A second assumption made in deriving the basic model was that the latent heat of vaporisation, h_{fg}, is constant. A variable 'latent heat of desorption' has, however, been postulated by various authors. Nellist and Hughes (1973) presented plots of the 'net heat of desorption' (difference between the latent heats of vaporisation of moisture from the grain and of free water) against moisture content for maize and wheat, which summarised the results of other authors. They noted from these plots that above 30% m.c.d.b. this net heat is negligible and that there is a gradual increase with decreasing moisture content down to about 16%, below which the net heat increases rapidly.

In practice, grain in fixed beds tends to 'overdry' near the air inlet (see e.g. Table 13a), hence attaining a moisture content well below the average value for the bed. Particularly in view of this behaviour, it would seem justifiable to allow for the difference between desorptive and 'pure' latent heats in the basic model. Some workers have incorporated an allowance for this variation in the implementation of their models. In particular, Nellist's drying equations (Nellist (1974)) were derived with a term for the latent heat of desorption. Spencer (1972) makes use of an expression for this quantity which is a function of grain temperature and moisture content (due to Gallaher (1951)).

One possible means by which the extra heat energy required for desorption might be accounted for lies in the appropriate choice of a constitutive equation for θ_v (see e.g. (3.3-14)). This choice would be affected by the assumption made concerning the source of the extra energy i.e. whether derived from air or grain. Any such approach would, however, require work beyond the scope of this thesis.

For the purpose of validating the three basic models derived herein, expressions for the drying and heat transfer rates were taken from among existing models. In view of the importance of using suitable constitutive equations (see comment in section 4.3) some conclusions of a review of available models is presented in the following paragraphs (for further

detail see Parry (1983d)).

A number of theories of sorption and desorption in biological materials have appeared in the literature. Some of these would appear to be quite relevant to grain drying. Most of these theories, however, are only applicable with any degree of accuracy, over limited ranges of relative humidity and temperature. Furthermore, experimental errors represent a limiting factor in obtaining e.m.c. data.

In view of the above points, purely empirical models would seem to provide the best means currently available for the representation of e.m.c. data. In particular, piecewise polynomial functions, such as the cubic spline fit of Bakker-Arkema et al (1974) (see Appendix C) provide flexibility. In addition, experimental errors may be 'smoothed' by using a least-squares approach. Combination of two such approximation techniques might provide a computationally efficient and uniformly accurate representation for any range of e.m.c. data. 'Dynamic' e.m.c. models, such as that developed by Nellist (1974), would appear to be more suitable than 'static' models for deep bed simulations, particularly of high temperature, high airflow rate driers.

Thin layer drying models provide a means of estimating drying rates in deep bed simulations. Diffusion equation models can give a detailed profile of moisture content/temperature within the individual grain kernel. When incorporated into a deep bed model they are capable of yielding an accurate estimate of the drying rate, at a given point (x,t). However, such models require prior assumptions to be made concerning, for example, the geometry of a typical kernel and its mass diffusivity/thermal conductivity. Furthermore, the computation time required to solve such models is generally a large proportion of that required for the overall simulation. On the other hand, empirical models, such as variants of the Lewis model (1.2-1), are computationally inexpensive and may thus, for example, be more suitable for applications of control engineering to drying.

It would seem, in view of the comments made in section 1.2, that a thermal diffusion type model representing the 'convective' component of the net energy transfer (first term in (3.3-14)) is not generally

justified. The empirical cooling law, as used herein, and by most other workers, would seem to suffice. However, choice of volumetric heat transfer coefficient, h, in this work, was limited to the expression (3.3-15), due to Boyce (1966). Bakker-Arkema et al introduced an expression for h in terms of a particle Reynolds number and the surface to volume ratio for a typical grain kernel (see e.g. Bakker-Arkema et al 1967). Both expressions are functions of G_a. It was observed, however, by Nellist (1974) that the values given by these two expressions differed by as much as a factor of four.

Clearly, a completely non-dimensional formulation of the models presented herein would be of greater use in providing information on the operating characteristics and hence performance criteria for driers. Such an approach would, however, necessitate further experimental work to produce correlations for the heat and mass transfer rates in terms of selected non-dimensional parameters (see discussion, section 1.2). In view, therefore, of the limited scope of this work, established empirical expressions for these rates were incorporated into the models. Because of the nature of their functional dependences, these expressions were not amenable to non-dimensionalisation in the context of the general drying equations.

The semi-analytical approach to solving the concurrent flow equations, described in section 4.1, might be improved upon by expedient equilibration of the matrices involved in evaluating the spectral form (4.1-5). Some further analytical work might be carried out on the fixed bed equations. It would seem, however, that efforts might be more profitably directed towards finding a numerical solution to these problems by more efficient means. The algorithms presented herein would appear to give a suitably accurate and reliable means of solution. It is clear, however, that such accuracy is not always required. In particular, the drying equations are inherently stable over certain regions of space-time and any 'perturbations' due to initial differences in solution technique will tend to die out as bed conditions tend to the 'steady-state'.

In summary, it is hoped that this work has accomplished the following:

1. Provision of a general mathematical framework for the derivation of mathematical models for the simulation of simultaneous heat and mass transfer in agricultural grain drying.

2. Derivation of new models for the four basic types of convective grain drier.

3. Construction and implementation of algorithms for the accurate numerical solution of fixed bed, concurrent flow and counterflow equations.

4. Clarification of assumptions made in the derivation of other models.

5. Suggestions for further useful work.

ACKNOWLEDGEMENTS

I am greatly indebted to Prof. N.Laws for his supervision and encouragement throughout this work, but more particularly for his guidance on the derivation of the general model (Chapter 2). I should also like to acknowledge the value of discussions with Prof. D.R.Bland (also of CIT). I greatfully acknowledge the support of both an S.E.R.C. Case Award and Cranfield Study Award while carrying out this work.

I am indebted to the National Institute of Agricultural Engineering (NIAE) for facilities made available to me while carrying out this work and to many of the staff of NIAE for their assistance and encouragement. In particular, I am most indebted to Dr.M.E.Nellist, who provided the motivation for much of this work and whose contributions are too numerous to mention here. In addition, I am grateful for the patient assistance of Mr.D.Bruce on many occasions and for further encouragement and advice from Dr.D.S.Boyce.

Finally, I should like to acknowledge the undoubted endurance and support of my wife Christine and also the patience and skill of Mrs.E.McFall (School of Mathematics, Thames Polytechnic) who typed the thesis.

REFERENCES

AHLBERG, J.H., NILSON, E.N. & WALSH, J.L. 1967 The theory of splines and their applications. Academic Press.

AMUNDSON, N.R., ARIS, R. & SWANSON, R. 1965 On simple exchange waves in fixed beds. Proc. R. Soc. 286 (A), 129-139.

ATKIN, R.J. & CRAINE, R.E. 1976 Continuum theories of mixtures: Basic theory and historical development. Q. Jl Mech. Appl. Math. 29 (2), 209.

BAKKER-ARKEMA, F.W., BICKERT, W.G. & PATTERSON, R.J. 1967 Simultaneous heat and mass transfer during the cooling of a deep bed of biological products under varying inlet conditions. J. Agric. Engng Res. 12 (4), 297.

BAKKER-ARKEMA, F.W., LEREW, L.E. DE BOER, S.F. & ROTH, M.C. 1974 Grain dryer simulation. Res. rep. 224, Michigan State Univ.

BAKKER-ARKEMA, F.W., AHMADNIA-SOKHANSANJ, A. & GREEN, R. 1977 High temperature wheat drying. Amer. Soc. Agric. Engrs., paper No.77-3527.

BARRE, H.J., BAUGHMAN, G.R. & HAMDY, M.R. 1971 Application of the logarithmic model to cross-flow deep bed grain drying. Trans. Am. Soc. Agric. Engrs 14 (6), 1061-1064.

BOYCE, D.S. 1965 Grain moisture and temperature changes with position and time during through drying. J.Agric. Engng. Res. 10 (4), 333-341.

BOYCE, D.S. 1966 Heat and moisture transfer in ventilated grain. J.Agric. Engng. Res. 11 (4), 255-265.

BROOKER, D.B., BAKKER-ARKEMA, F.W. & HALL, C.W. 1974 Drying Cereal Grains. The AVI Publ.Co.Inc.

BRUCE, D. 1983 A simulation of multi-bed concurrent-flow and counter-flow grain driers. Part I. The Model. Div. Note 1171, Natn. Inst. Agric. Engng, Silsoe, March (unpubl.).

BUCKINGHAM, E. 1914 On physically similar systems; illustrations of the use of dimensional equations. The Physical Review Sec.II 4, 345-376.

BULIRSCH, R.E. & STOER, J. 1966 Numerical treatment of ordinary differential equations by extrapolation methods. Num. Math. 8, 1-13.

CHADWICK, P. 1976 Continuum Mechanics. London: George Allen & Unwin.

CHEN, C.S. & JOHNSON, W.H. 1969 Kinetics of moisture movement in hygroscopic materials. Trans. Amer. Soc. Agric. Engrs. 12 (1), 109-113.

CHIEN, K.S., MATTHES, R.K. & VERMA, B.P. 1969 Dimensional analysis of seed-moisture movement in deep-bed drying. Amer. Soc. Agric. Engrs., paper No.69-833.

COURANT, R. & FRIEDRICHS, K.O. 1952 Supersonic flow and shock waves. Interscience, New York.

CRANK, J. 1975 The mathematics of diffusion. Oxford Univ. Press, London.

DAVIS, P.J. 1963 Interpolation and approximation. Blaisdell Publ.Co.

ERDELYI, A., MAGNUS, W., OBERHETTINGER, F. & TRICOMI, F.G. 1954 Tables of Integral Transforms, Vol.I. McGraw-Hill Book Co. Inc.

FORSYTHE, G. & MOLER, C.B. 1967 Computer solution of linear algebraic systems. Prentice-Hall.

GALLAHER, G.L. 1951 A method of determining the latent heat of agricultural crops. Agric. Engng. 32 (1), 34.

GAMSON, B.W., THODOS, G. & HOUGEN, O.A. 1943 Trans. Am. Inst. Chem. Engrs. 39, 1.

GEAR, C.W. 1971a Numerical initial value problems in ordinary differential equations. Prentice-Hall, Englewood Cliffs, New Jersey.

GEAR, C.W. 1971b Algorithm 407, DIFSUB, for solution of ordinary differential equations. Comm. ACM 14, 185-190.

GRAGG, W. 1963 Repeated extrapolation to the limit in the numerical solution of ordinary differential equations. Thesis, UCLA.

GREIG, D.J. & BOYCE, D.S. 1967 Moisture temperature relationships during drying. Paper 1/C/5 pres. at the Agric. Engng Symp. of the Inst. Agric. Engrs at NCAE, Silsoe.

HACKBUSCH, W. 1977a Extrapolation applied to certain discretisation methods solving the initial value problem for hyperbolic differential equations. Num. Math. 28, 121-142.

HACKBUSCH, W. 1977b Extrapolation to the limit for numerical solutions of hyperbolic equations. Num. Math. 28, 455-474.

HENDERSON, S.M. & PABIS, S. 1961 Grain drying theory I. Temperature effect on drying coefficient. J.Agric. Engng. Res. 6 (3), 169-174.

HENDERSON, S.M. & PABIS, S. 1962 The effect of air flow-rate on the drying index. J.Agric. Engng. Res. 7, 85.

HENDERSON, J.M. & HENDERSON, S.M. 1968 A computational procedure for deep bed drying. J.Agric. Engng Res. 13 (2), 87-95.

HUANG, T-g. & GUNKEL, W.W. 1972 Theoretical and experimental studies of the heating front in a deep bed hygroscopic product. Am.Soc.Agric. Engrs., paper No.72-374.

HUKILL, W.V. 1954 Grain drying. In Storage of cereal grains and their products (ed. Anderson, J.A. & Alcock, A.W.). Amer. Ass. Cereal Chem., St. Paul, Minn.

HUSAIN, A., CHEN, C.S., CLAYTON, J.T. & WHITNEY, L.F. 1973 Mathematical simulation of mass and heat transfer in high moisture foods. Trans. Am. Soc.Agric. Engrs. 15, 732-736.

INGRAM, G.W. 1976a A general method for deep bed drier simulation with drying rates determined by the diffusion equation or empirical expressions. SIAE Dep. Note No. SIN/204 (unpubl.).

INGRAM, G.W. 1976b Deep bed drier simulation with intra-particle moisture diffusion. J. Agric. Engng. Res. 21 (3), 263.

INGRAM, G.W. 1979 Solution of grain cooling and drying problems by the method of characteristics in comparison with finite difference solutions. J.Agric.Engng.Res. 24 (3), 219-232.

JORDAN, D.W. & SMITH, P. 1979 Nonlinear Ordinary Differential Equations. Clarendon Press, Oxford.

KLAPP, E. 1963 Mathematical analysis of simultaneous heat and mass transfer processes in granular materials through which passes a gas. Translation 254, Harris, E., Scientific Information Dept., Nat. Inst. Agric. Engng., Silsoe, from Ingenieur-Archiv 32 (5), 360-372.

LAMBERT, J.D. 1973 Computational methods in ordinary differential equations. John Wiley & Sons.

LAWS, N.L. & PARRY, J.L. 1983 Mathematical modelling of heat and mass transfer in agricultural grain drying. Proc. R. Soc. Lond. A 385, 169-187.

LEIGHTON, W. 1976 An introduction to the theory of ordinary differential equations. Wadsworth Publ. Co. Inc., Belmont, California.

LEWIS, W.K. 1921 The rate of drying of solid materials. Industr. Engng.Chem. 13, 427.

LUIKOV, A.V. 1966 Heat and mass transfer in capillary porous bodies. Pergamon, New York.

MOREY, R.V., KEENER, H.M., THOMPSON, T.L., WHITE, G.M. & BAKKER-ARKEMA, F.W. 1978 The present status of grain drying simulation. Am.Soc. Agric.Engrs. Paper No.78-3009

NELLIST, M.E. & O'CALLAGHAN, J.R. 1971 The measurement of drying rates in thin layers of ryegrass seed. J.Agric.Engng.Res. 16 (3), 192-212.

NELLIST, M.E. & HUGHES, M. 1973 Physical and biological processes in the drying of seed. Seed Sci. & Tech. 1, 613.

NELLIST, M.E. 1974 The drying of ryegrass seeds in deep layers. PhD Thesis, Univ., Newcastle-upon-Tyne (unpubl.).

NELLIST, M.E. 1976 Exposed layer drying of ryegrass seeds. J.Agric. Engng.Res. 21, 49-66.

NELLIST, M.E. 1978 Safe temperatures for drying grain. Report No.29, Nat.Inst.Agric.Engng, Silsoe (unpubl.).

NELLIST, M.E. 1981 Predicting the viability of seeds dried with heated air. Seed Sci. & Tech. 9, 439-455.

NELSON, G.L. 1960 A new analysis of batch grain-drier performance. Trans.Amer.Soc.Agric.Engrs. 3 (2), 81-88.

NGODDY, P.O., BAKKER-ARKEMA, F.W. & BICKERT, W.G. 1966 Heat transfer in a deep bed of pea beans. Quart.Bull.Mich.Agric.Exp.Sta. 49 (2), 132-143.

NORDON, P. & BAINBRIDGE, N.W. 1972 Heat and moisture exchange in wool beds: Equilibrium theory in the hygroscopic range. J.Text.Inst.63, 429.

O'CALLAGHAN, J.R., MENZIES, D.J. & BAILEY, P.H. 1971 Digital simulation of agricultural drier performance. J.Agric.Engng.Res. 16 (3), 223-244.

PARRY, J.L. 1983a Mathematical modelling and computer simulation of steady state concurrent-flow grain drying. Part I. The Model.Div. Note DN/1178, Nat.Inst.Agric.Engng, Silsoe, May (unpubl.).

PARRY, J.L. 1983b Mathematical modelling and computer simulation of steady state concurrent-flow grain drying.Part II. The Computer Program. Div. Note DN/1179, Nat.Inst.Agric.Engng, Silsoe, May (unpubl.).

PARRY, J.L. 1983c Mathematical modelling and computer simulation of fixed bed grain drying. Part II. The Computer Program. To appear as Div. Note, Nat.Inst.Agric.Engng, Silsoe.

PARRY, J.L. 1983d Mathematical modelling and computer simulation of heat and mass transfer in agricultural grain drying: A review. Paper submitted to J.Agric.Engng.Res.

POWELL, M.J.D. 1964 An efficient method for finding the minimum of a functicn of several variables without calcualting derivatives. The Computer Journal 7, 155-162.

SABBAH, MA., KEENER, H.M. & MEYER, G.E. 1979 Simulation of solar drying of shelled corn using the logarithmic model. Trans. Am. Soc. Agric. Engrs. 22 (3), 637-643.

SHARAF-ELDEEN, Y.I., HAMDY, M.Y. & BLAISDELL, J.L. 1979 Mathematical Simulation of drying fully-exposed ear corn and its components. Amer. Soc.Agric.Engrs. Paper No.79-6523.

SHARP, J.R. 1982 A review of low temperature drying simulation models. J. Agric. Engng. Res. 27, 169-190.

SHERWOOD, T.K. 1936 Air drying of solids. Trans. Amer. Inst. Chem. Engrs. 32, 150-168.

SIMMONDS, W.H.C., WARD, G.T. & MCEWEN, E. 1953 The drying of wheat grain:

I The mechanism of drying.
II Through drying of deep beds.

Trans.Ins. Chem. Engrs. 31 (3), 265-288.

SMITH, G.D. 1978 Numerical Solution of Partial Differential Equations: Finite Difference Methods. Clarendon Press, Oxford.

SPENCER, H.B. 1969a A mathematical simulation of grain drying. J. Agric. Engng.Res. 14 (3), 226-235.

SPENCER, H.B. 1969b An examination of the accuracy of the finite difference technique for the solution of the drying equations. SIAE Dep. Note No.33 (unpubl.).

SPENCER, H.B. 1972 A revised model of the wheat drying process. J.AGric.Engng.Res. 17, 189-194.

SUTHERLAND, J.W., BANKS, P.J. & GRIFFITHS, M.J. 1971 Equilibrium heat and moisture transfer in air flow through grain, J.Agric.Engng.Res. 16 (4), 368.

THOMPSON, T.L., PEART, R.M. & FOSTER, G.H. 1968 Mathematical simulation of corn drying - a new model. Trans.Am.Soc.Agric.Engrs. 11 (14), 582-586.

VAN ARSDEL, W.B. 1955 Simultaneous heat and mass transfer in a nonisothermal system: Through-flow drying in the low-moisture range. Chem.Eng.Prog.Symp.Series 51 (16), 47-58.

VAN DER HOUWEN, P.J. 1977 Construction of integration formulas for initial value problems. N.Holland.

WHITHAM, G.B. 1974 Linear and nonlinear waves. New York: John Wiley.

YOUNG, J.H. & DICKENS, J.W. 1975 Evaluation of costs for drying grain in batch or crossflow systems. Amer.Soc.Agric.Engrs. 18, 734-739.

YOUNG, J.H. & NELSON, G.L. 1967 Research of hysteresis between sorption and desorption isotherms of wheat. Trans.Am.Soc.Agric.Engrs. 10 (2), 756-761.

APPENDIX A

Empirical relationships used in the validation of the model.

The assumed constitutive relation for the evaporation rate is

$$m = \rho_p k(M - M_e) \quad , \tag{1}$$

with drying coefficient of the (Arrhenius) form

$$k = a_1 \exp(b_1/T_k) \quad , \tag{2}$$

where $T_k = T + 273.2$ i.e. absolute temperature in °K.

In (1), the e.m.c. M_e is represented by alternative expressions of the form

$$M_e = \begin{cases} a_2 + b_2 T + c_2 \ln(1 - \phi) \\ \\ a_2' + b_2' \ln(T) + c_2' \ln(1 - \phi) \end{cases} , \tag{3}$$

where the relative humidity, ϕ , is given by

$$\left.\begin{aligned} \phi &= P_v/P_{sat} = HP_{atmos}/[(.622+H)P_{sat}] \\ \text{and where} \\ \ln\,(P_{sat}/100) &= a_3 + b_3 \ln(T_k) + c_3 T_k + d_3/T_k \end{aligned}\right\} (4) \ .$$

The second e.m.c. expression in (3) was developed by Nellist (see e.g. Nellist & Dumont (1979)) and fitted to data of McEwan & O'Callaghan for wheat. The first expression is a modification of this fit (also due to Nellist).

Assuming a constitutive relation of the form (3.3-14) for the net energy transfer, the volumetric heat transfer coefficient, h, is taken as

$$h = a_4 \left\{ \frac{G_a \ T_k}{P_{atmos}} \right\}^{b_4} \tag{5}$$

This expression was developed by Boyce (1966) for use in his simulations of the drying of barley.

The constants a_i, a_i', b_i, b_i', c_i, c_i', d_3 in the above expressions depend, in general, on the crop is simulated. In the simulations presented in this work, the following values were, however, used for these constants:

$a_1 = 139.3$, $b_1 = -4426$,

$a_2 = .1138$, $b_2 = -.000688$, $c_2 = -.0673$,

$a_2' = .11304$, $b_2' = -.01577$, $c_2' = -.07949$,

$a_3 = 72.73974$, $b_3 = -8.2$, $c_3 = .0057113$, $d_3 = -7235.4261$,

$a_4 = 856800$, $b_4 = .6011$.

APPENDIX B

Analytical expressions for the elements of the Jacobian matrix for the steady state concurrent flow drying equations.

Using empirical relationships for the air and grain properties of the form given in Appendix A and with the assumption of $\theta_v = \theta$, the elements of the Jacobian matrix $J(\underline{u}) = \{\partial f_i/\partial u_j\}$, where $\underline{u} = [M,T,\theta]^T$, are given by:

$$J_{11} = -(\rho_p/G_p)k\{ 1 - (G_p/G_a)(\partial M_e/\partial H)\} ,$$

where

$$\partial M_e/\partial H = \begin{cases} c_2 K_1 \\ c_2' K_1 \end{cases}$$

and where

$$K_1 = .622/[H(1 - \phi)(.622 + H)], \quad \text{for } \phi < 1.0.$$

$$J_{12} = (\rho_p/G_p)k\{(M - M_e)b /T_k^2 + (\partial M_e/\partial T)\} ,$$

where

$$\partial M_e/\partial T = \begin{cases} b_2 + c_2 K_2 \\ b_2'/T + c_2' K_2 \end{cases}$$

and where $K_2 = HP_{atmos}(b_3/T_k + c_3 - d_3/T_k^2)/[(.622+H)P_{sat} - HP_{atmos}]$.

$J_{13} = 0.0.$

$J_{21} = c_v G_p [(c_a + c_v H)G_a J_{11} - (h+mc_v)] (T-\theta)/[G_a^2(c_a + c_v H)^2].$

$J_{22} = -[(b_4 h/T_k - c_v G_p J_{12})(T-\theta) + (h+mc_v)]/[G_a(c_a + c_v H)].$

$J_{23} = (h + mc_v)/[G_a(c_a + c_v H)] .$

$J_{31} = [(h_{fg}+(c_v-c_w)\theta)(G_p(c_p+c_w M)J_{11}+c_w M) - c_w h(T-\theta)]/[G_p(c_p+c_w M)^2]$

$J_{32} = [b_4 h(T-\theta)/T_k + h + G_p J_{12}(h_{fg}+(c_v-c_w)\theta)]/[G_p(c_p+c_w M)] .$

$J_{33} = -[h + m(c_v-c_w)/[G_p(c_p+c_w M)] .$

APPENDIX C

Further empirical relationships used in validating the model

Thompson et al (1968), using a thin-layer approach, proposed a drying equation for 'yellow-dent shelled corn' (maize), over the approximate range of drying-air temperatures 120-340°F, of the form:

$$t = A\ \ln(MR) + B[\ln(MR)]^2 \ , \qquad (1)$$

where t is the drying time to attain a moisture ratio of MR. The coefficients A and B are given by expressions of the form

$$A = -a + bT_f \ , \quad B = c\ \exp(-dT_f),$$

where T_f is the drying air temperature in deg.F,

i.e. $T_f = 1.8*T + 32$, if T is in deg.C.

In Thompson's paper, expression (1) for the drying time was given in hours, while feet were used as length units. With these units, the constants a, b, c and d were given by

$$a = 1.862, \quad b = .00488, \quad c = 427.4, \quad d = .033.$$

Solving the quadratic (1) for MR gives

$$MR = \exp[(-A + \sqrt{(A^2 + 4Bt)})/(2B)].$$

Now since $B,t > 0$ and all quantities are real, taking $+\sqrt{(\text{discriminant})}$ would give $d(MR)/dt > 0$. Thus for drying we must take $-\sqrt{(\text{discriminant})}$, giving

$$M = M_e + (M_o - M_e)\exp[(-A - \sqrt{(A^2 + 4Bt)})/(2B)] \qquad (2).$$

Bakker-Arkema et al (1974) assumed the temperature of the product in the above expressions for A and B i.e. $T_f = 1.8*\theta + 32$, and made use of (2) in the following way:

Differentiating w.r.t. t these authors arrived at an expression which may be written in the form

$$dM/dt = -(A^2 + 4Bt)^{-\frac{1}{2}}\ (M - M_e) \qquad (3),$$

giving, for the drying coefficient

$$k = (A^2 + 4Bt)^{-\frac{1}{2}} \qquad (4).$$

Since $dM/dt = \partial M/\partial t + \partial M/\partial M_e (dM_e/dt)$,

the derivation of (3) implies the assumption that the second term in the above expression may be considered negligible.

N.B. for use in CONFLO the expression (4) for k must be multiplied by a conversion factor of (3.2808/3600).

Bakker-Arkema et al also fit separate cubic spline curves to the e.m.c. data of Rodriguez-Arias (1956) for shelled corn, over the two disjoint ranges

$$0.0 \leqq \phi \leqq 0.5 \quad \text{and} \quad 0.5 < \phi \leqq 1.0.$$

The cubic spline for M_e may be expressed in terms of its second derivatives, M_i say, as

$$M_e(\phi) = \frac{M_i(\phi_{i+1} - \phi)^3}{6h} + \frac{M_{i+1}(\phi - \phi_i)^3}{6h}$$

$$+ \left(\frac{f_{i+1}}{h} - \frac{hM_{i+1}}{6}\right)(\phi - \phi_i) + \left(\frac{f_i}{h} - \frac{hM_i}{6}\right)(\phi_{i+1} - \phi) \quad (5),$$

over the interval $\phi_i \leqq \phi \leqq \phi_{i+1}$, where $\phi_i = ih$, $f_i = M_e(\phi_i)$, and

where the parameters M_i are obtained by solving the system of linear equations

$$M_{i+1} + 4M_i + M_{i-1} = (6/h^2)(f_{i+1} - 2f_i + f_{i-1}), \quad (6)$$

$$\text{for } i=1,2,\ldots,N-1.$$

These equations express the conditions for second derivative continuity of M_e at the interior knots, ϕ_i, $i=1,2,\ldots,N-1$.

Bakker-Arkema et al divided each of their two intervals into a further three equal intervals, giving $h=1/6$. In addition, they assumed a zero value of e.m.c. at $\phi=0$, and zero values of the second derivatives of e.m.c. at the ends of each of the two ranges. The resulting approximation to $M_e(\phi)$ is then given by (5) with M_i values determined from two systems which may be written in the form

$$M_0 = M_3 = M_6 = 0, \quad f_0 = 0,$$

$$\begin{bmatrix} M_1 \\ M_2 \end{bmatrix} = \begin{bmatrix} -9 & 6 & -1 \\ 6 & -9 & 4 \end{bmatrix} \begin{bmatrix} f_1 \\ f_2 \\ f_3 \end{bmatrix}$$

$$\begin{bmatrix} M_4 \\ M_5 \end{bmatrix} = \begin{bmatrix} 4 & -9 & 6 & -1 \\ -1 & 6 & -9 & 4 \end{bmatrix} \begin{bmatrix} f_4 \\ f_5 \\ f_6 \\ f_7 \end{bmatrix}$$

where $\underline{f} = [f_1, f_2, \ldots f_7]^T = \underline{a} - 10^{-3}\ \underline{b}\ T_f$,

with $\underline{a}^T = [.1000, .1328, .1646, .1624, .2075, .2532, .3931]$,

$\underline{b}^T = [.3922, .4353, .5359, .5375, .7075, .7449, .1071]$,

and where T_f is the drying air temperature in °F.

The authors claimed that, over the range of drying air temperatures 40-140°F, these equations gave maximum and average deviations between experimental and interpolated moisture content of 2.0% and 0.5% respectively.